



UNIVERSITY *of the*
WESTERN CAPE

***In vitro* investigation of the ubiquitination and
degradation of p53 by Murine Double Minute 2 (MDM2)
and Retinoblastoma Binding Protein 6 (RBBP6)**



Lauren Sarah Jooste
WESTERN CAPE

A thesis submitted in partial fulfilment of the requirements for the degree
Magister Scientiae in the Department of Biotechnology, University of the
Western Cape.

Supervisor: David J. R. Pugh (D.Phil Oxon)

November 2015

Abstract

***In vitro* investigation of the ubiquitination and degradation of p53 by Murine Double Minute 2 (MDM2) and Retinoblastoma Binding Protein 6 (RBBP6)**

L. S. Jooste, MSc (Biotechnology) thesis, Department of Biotechnology, Faculty of Natural Sciences, University of the Western Cape.

p53 is one of the most important tumour suppressor proteins in the body which protects the cell against the tumourigenic effects of DNA damage by initiating processes such as apoptosis, senescence and cell cycle arrest. Regulation of p53 is key — so that the abovementioned processes are not initiated inappropriately. The principle negative regulator of p53 is Murine Double Minute 2 (MDM2), a RING finger-containing protein which catalyses the attachment of lysine48-linked poly-ubiquitin chains, targeting it for degradation by the 26S proteasome. It has been found to work in conjunction with the MDM2 homologue MDMX.

Retinoblastoma Binding Protein 6 (RBBP6) is a RING finger-containing protein known to play a role in mRNA 3'-end processing, as well as interacting with p53 and another crucial tumour suppressor, pRb. It has previously been shown to cooperate with MDM2 in the ubiquitination and degradation of p53 *in vivo* and acts as a scaffold.

The objectives of this project are to investigate the proposed role of RBBP6 in the MDM2-catalysed ubiquitination of p53 using a fully *in vitro* ubiquitination system. Due to the difficulty of expressing full length RBBP6 in bacteria, a shortened version, dubbed “R3” was used which includes the RING finger domain but excludes the domain identified in earlier studies as the p53-binding domain. Proteins required to set up the fully *in vitro* p53 ubiquitination assays – including E1 and E2 enzymes, MDM2, R3, p53 and ubiquitin - were all successfully expressed in bacteria. The active 26S proteasome was successfully purified out of human cell lysates using antibodies targeting the α_2 -subunit.

Cloning, expression and purification results showed that p53, MDM2 and R3 were not very stable proteins to work with — with degradation being initiated almost immediately after expression and purification which progressed during the downstream processing of the proteins. Although levels of intact protein were not always high, they were sufficient for *in vitro* assays.

MDM2 and GST-R3 were both capable of poly-ubiquitinating p53 independently in “partially *in vitro*” assays using human cell lysate. The fully *in vitro* ubiquitination of p53 using MDM2 and R3 was established based on the well-known MDM2/MDMX system. When acting together R3 and MDM2 was shown to produce poly-ubiquitination which is lysine-48 linked and recognised by the 26S proteasome leading to degradation. When the proteasome inhibitor MG132 was added, the poly-ubiquitinated p53 was rescued from degradation. R3 was also shown to successfully poly-ubiquitinate p53 independently of MDM2 and also interact with

p53 *in vitro*. These results suggest R3 to be of the same order of importance as that of MDM2 — which is known to be the most important regulator of p53. It would also rule out the proposed model of RBBP6 functioning as a scaffold as it is able to poly-ubiquitinate p53 independent of MDM2.

These results allow us to better understand the mechanism in which p53 is down-regulated by E3s.

Keywords: cancer, p53, tumour suppressor, ubiquitination, degradation, MDM2, RBBP6, R3, *in vitro*, protein



Declaration

I declare that “*In vitro investigation of the ubiquitination and degradation of p53 by Murine Double Minute 2 (MDM2) and Retinoblastoma Binding Protein 6 (RBBP6)*” is my own work that has not been submitted for any degree or examination in any other university, and that all the sources I have used or quoted have been indicated or acknowledged by complete references.

Lauren Jooste

November 2015

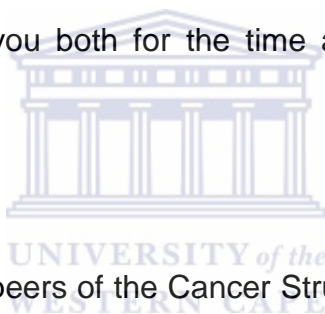


Signed:.....

Acknowledgements

The highest praise goes out to my Lord and Saviour Jesus Christ who had equipped me for this challenge. I could not have completed this chapter of my life without Him.

I wish to sincerely thank my supervisor, Dr David Pugh for his guidance and assistance during the course of my MSc. I also wish to extend my gratitude to Dr Andrew Faro who has offered me invaluable guidance in the laboratory and for all the moral support. Thank you both for the time and effort you have offered to assist me!



I would like to thank all my peers of the Cancer Structural Biology Research group and the Biotechnology Department at UWC for all the support, friendship and fellowship.

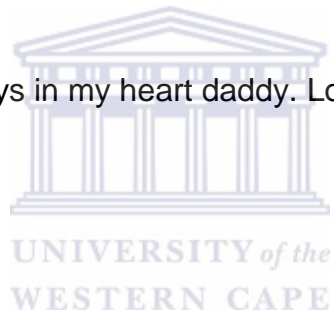
I would like to give a heartfelt thank you to my family and friends! A special thank you is owed to my grandmother Sarah, my mother Valerie, my brother Wayne, my sister Erin and my fiancé Chad for their continuous support and patience during my studies. The level of support they have shown me has helped me tremendously.

I would like to thank the NRF for financial support.

Dedication

I wish to dedicate my thesis to my late father and role-model Keith Jooste, who motivated me to start my MSc but sadly was not with me to see me finish it.

You're always in my heart daddy. Love you always.



List of Abbreviations

Amp	Ampicillin
APS	Ammonium persulphate
ATP	Adenosine tri-phosphate
bp	base pair
C-terminus	Carboxyl terminus
CV	Column volume
Cys or C	Cysteine
DNA	Deoxyribonucleic acid
dNTP	2'-deoxynucleoside 5'-triphosphate
DTT	1,4-dithio-D-threitol
E1	E1 ubiquitin-activating enzyme
E2	E2 ubiquitin conjugating enzyme/Ubc
E3	E3 ubiquitin ligase.
EDTA	Ethylenediaminetetra acetic acid
ESI	Electrospray ionization
Fig	Figure
GST	Glutathione S-Transferase
HDM2	Human Double Minute 2
His or H	Histidine
<i>Hs</i>	<i>Homo sapiens</i>
Hsp70	Heat shock protein 70
IPTG	Isopropyl-1-thio-D-galactoside

kb	kilo base
kDa	kilo Dalton
LB	Luria broth
Lys or K	Lysine
MALDI	Matrix assisted laser desorption/ionization
MDM2	Mouse double minute 2
Mpe1	mutant PCFII extrogenic suppressor 1
mRNA	messenger RNA
MS	Mass spectrometry
N-terminus	Amino terminal
p53	protein 53 kDa
P2P-R	proliferation potential protein-related
PACT	p53-Associated Cellular protein-Testes derived
PAGE	Polyacrylamide Gel Electrophoresis
PBS	Phosphate buffer saline
PCR	Polymerase chain reaction
PDB	Protein Data Bank
PVDF	Polyvinylidifluoride
Rb	Retinoblastoma
RBBP6	Retinoblastoma binding protein 6
RBQ-1	RB-binding Q-protein
RING	Really interesting new gene
RNA	Ribonucleic acid
s	seconds

SDS	Sodium dodecyl sulphate
TEMED	<i>N, N, N', N'</i> -tetramethylethylenediamine
TBE	Tris Borate EDTA
TE	Tris EDTA
Ubc	Ubiquitin conjugating enzymes
UV	Ultra Violet
Y2H	Yeast-2-Hybrid
YB-1	Y-box binding protein 1



Table of Contents

Abstract	i
Declaration	iv
Acknowledgements	v
Dedication	vi
Abbreviations	vii
List of Figures	xiii
List of Tables	xvi

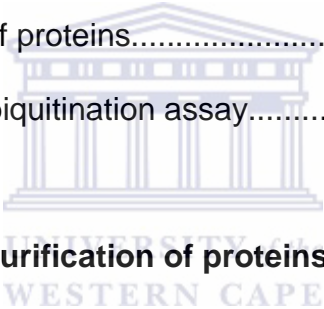
1. Literature Review

1.1. Introduction.....	1
1.2. The Ubiquitin Proteasome System.....	3
1.3. Retinoblastoma Binding Protein 6.....	13
1.4. p53.....	22
1.5. Objectives of this MSc.....	34

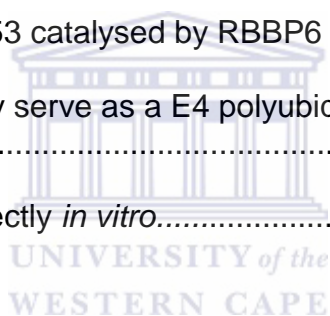


2. Materials and methods

2.1. Bacterial strains.....	37
2.2. Antibodies.....	38
2.3. Selection.....	38
2.4. Bacterial transformation.....	38
2.5. Preparation and manipulation of DNA.....	39
2.5.1. Plasmid isolation.....	39
2.5.2. PCR amplification.....	39
2.5.3. Restriction enzyme digests.....	40
2.5.4. Agarose gel electrophoresis.....	41
2.5.5. Cloning of DNA fragments.....	42
2.6. Large scale expression of recombinant proteins.....	43

2.7. Protein extraction and preparation of crude cell lysate.....	44
2.8. Protein purification.....	44
2.8.1. GST-glutathione affinity chromatography.....	44
2.8.2. Nickel ion affinity chromatography.....	45
2.8.3. Cation exchange chromatography.....	46
2.9. SDS-PAGE analysis of proteins.....	46
2.10. Western blotting of proteins.....	47
2.11. Purification of proteasome from human cell lysate.....	48
2.12. Ubiquitination assays.....	49
2.13. Immunoprecipitation of proteins.....	50
2.14. <i>In vitro</i> two-step E4 ubiquitination assay.....	50
	
3. Cloning, expression and purification of proteins for <i>in vitro</i> assays	
3.1. Introduction.....	53
3.2. Generation of pmEGFP-DWNN13 construct for immunofluorescence microscopy.....	55
3.3. Generation of an expression construct for the E2 Ubch1.....	59
3.4. Generation of expression construct for stabilised p53 quadruple mutant.....	62
3.5. Expression and purification of three different p53 constructs: GST-p53 (wild type), His ₆ -p53 (wild type) and His ₆ -p53 (quadruple mutant).....	64
3.6. Expression and purification of the ubiquitin-ligating enzymes MDM2 and R3.....	68
3.7. Expression and purification of various ubiquitin-conjugating enzymes (E2s) and ubiquitin.....	70
3.8. Purification of intact proteasomes from human cell lysate.....	77

4. <i>In vitro</i> investigation of the ubiquitination of p53 by RBBP6 and MDM2	
4.1. Introduction.....	79
4.2. R3 is able to ubiquitinate p53 in a partially <i>in vitro</i> system.....	80
4.3. Optimisation of <i>in vitro</i> ubiquitination assays.....	85
4.4. Ubch5a is the preferred E2 for p53 <i>in vitro</i> poly-ubiquitination by GST-MDM2 and GST-R3.....	87
4.5. Ubiquitination by a combination of R3 and MDM2 leads to enhanced ubiquitination of p53 and proteasomal degradation <i>in vitro</i>	93
4.6. The DWNN domain is not required for the ubiquitination of p53.....	98
4.7. Poly-ubiquitination of p53 catalysed by RBBP6 is Lys-48 linked.....	102
4.8. RBBP6 could potentially serve as a E4 polyubiquitination chain extension factor for p53.....	105
4.9. p53 and R3 interact directly <i>in vitro</i>	107
5. Discussion and Conclusion.....	110
Bibliography.....	121
Appendix.....	128



List of Figures

Chapter 1

Figure 1.1:	The ubiquitin proteasome system.....	5
Figure 1.2:	The various fates of the different ubiquitin chains on a substrate.....	9
Figure 1.3:	Using mass spectrometry to detect ubiquitinated substrates..	14
Figure 1.4:	Domain organisation of RBBP6 orthologues in and various eukaryotic genomes.....	15
Figure 1.5:	Full length human RBBP6 and partial human and mouse proteins identified in various studies.....	17
Figure 1.6:	Activators and effectors of p53 function.....	23
Figure 1.7:	Schematic representation of the p53 protein.....	24
Figure 1.8:	Mis-sense mutations of p53.....	25
Figure 1.9:	Tetramerization of p53 explains the frequency of mis-sense mutations in the clinic.....	25
Figure 1.10:	Cell cycle checkpoints ensure quality control as the cell progresses through the cycle.....	27
Figure 1.11:	Figure showing some of the "hotspots" for point mutations within the <i>p53</i> gene.....	28
Figure 1.12:	Sites on p53 which gets modified by neddylation (Ne), sumoylation (Su) and ubiquitination (Ub)	31

Chapter 3

Figure 3.1:	Plasmid map of pmEGFP-C1.....	57
Figure 3.2:	Cloning of DWNN13 into pmEGFP-C1.....	58
Figure 3.3:	Plasmid map of pGEX-6P-2.....	59
Figure 3.4:	Amplification and PCR-colony screening of Ubch1.....	61
Figure 3.5:	Subcloning of the quadruple mutant p53 (p53-QM) from a pUC57 vector into the expression vector pET28a.....	63

Figure 3.6:	Western blot showing cleavage and purification of GST-p53...	65
Figure 3.7:	SDS-PAGE gel showing expression and purification of wild-type His ₆ -p53 using nickel ion affinity chromatography.....	67
Figure 3.8:	SDS-PAGE gel showing small-scale expression and purification of the quadruple mutant p53-QM.....	68
Figure 3.9:	SDS-PAGE gel showing expression and purification of GST-MDM2.....	69
Figure 3.10:	SDS-PAGE gel showing expression and purification of GST-R3.....	70
Figure 3.11:	SDS-PAGE gels showing expression, purification and cleavage of GST-UbcH1.....	72
Figure 3.12:	Removal of residual GST from UbcH1 using three 5 ml GSTrap™ columns connected in series.....	73
Figure 3.13:	Expression and purification of the E2 His ₆ -UbcH13 using a nickel ion affinity chromatography column.....	74
Figure 3.14:	SDS-PAGE gel showing the purification of the ubiquitin-K(0) mutant.....	76
Figure 3.15:	Immuno-blot showing purification of the 20S α ₂ -subunit of the 26S proteasome from HeLa cell lysate.....	78

Chapter 4

Figure 4.1:	R3 and MDM2 promote the poly-ubiquitination of p53 in the presence of human HepG2 lysate.....	82
Figure 4.2:	MDM2 and MDMX titration to find the optimal conditions for p53 ubiquitination.....	86
Figure 4.3:	GST-MDM2 and GST-R3 titration to find the optimal conditions for p53 ubiquitination.....	88
Figure 4.4:	<i>In vitro</i> E2 screen using His ₆ -p53 confirms that UbcH5a act as E2s with E3s GST-MDM2 and GST-R3 to poly-ubiquitinate p53.....	90
Figure 4.5:	R3 is able to ubiquitinate p53 independently of MDM2 using UbcH5a in an <i>in vitro</i> assay.....	92

Figure 4.6:	Enhanced degradation using both GST-R3 and GST-MDM2 <i>in vitro</i>	94
Figure 4.7:	Ubiquitination of p53-QM using a combination of R3 (no GST tag) and GST-MDM2 leads to enhanced ubiquitination and results in proteasomal degradation.....	97
Figure 4.8:	The DWNN domain is not required for the ubiquitination of p53.....	101
Figure 4.9:	Poly-ubiquitination of p53 by GST-MDM2/GST-R3 is lysine48-linked.....	104
Figure 4.10:	“Two-step” assay to determine if R3 functions as an E4.....	107
Figure 4.11:	Far Western blot showing interaction between p53 and GST-R3.....	109



List of Tables

Table 2.1: Example of set-up for restriction enzyme digestion of the pmEGFP vector and DWNN13 PCR product for ligation.....	41
Table 2.2: Expression conditions for proteins used in this work.....	44
Table 2.3: Reagents used in the <i>in vitro</i> ubiquitination assay.....	51
Table 2.4: Setup for 2-step ubiquitination assay: Step 1.....	51
Table 2.5: Setup for 2-step ubiquitination assay: Step 2.....	52



CHAPTER 1

Literature Review

1.1. Introduction

The importance of functional p53 in suppression of human cancer has been demonstrated in numerous studies since its first identification during the 1970s. Up to 2013 it was the subject of more than 65 000 research papers (Hoe *et al.*, 2014) and has been honoured with titles as grand as “Guardian of the genome” (Efeyan & Serrano, 2007), “Cellular Gatekeeper” (Levine, A, 1997), “Policeman of Oncogenes” (Efeyan & Serrano, 2007) and “Death Star” (Vousden, K, 2000), amongst others. Functional loss of p53 can be due to mutation of the gene, denoted *TP53*, itself or to inactivation of the p53 signal transduction pathway. The *TP53* gene has been found to be mutated in 30-50% of frequently-occurring human cancers (Weinberg, R. 2007). Gain-of-function and dominant negative mutants of p53 have long been recognised as significant causes of tumourigenicity; a recent study has shown that mutant p53 is the main driver of breast cancer, prompting the authors to give it the less complimentary title of “Rebel Angel” (Walerych *et al.*, 2012). The rare Li-Fraumeni syndrome is an autosomal dominant hereditary disorder in which the patient suffers early onset of several types of cancer, all caused by a mutant p53 loss-of-function allele (Hoe *et al.*, 2014).

However in many cases the p53 gene is not mutated, but p53 is nevertheless inactivated due to over-expression of negative regulators such as the human

orthologue of Murine Double Minute 2 (MDM2), also called HDM2, or its co-regulator MDMX (Lee & Gu, 2010; Lee & Moore, 2014; Weinberg. R, 2007). (In the remainder of this thesis the term MDM2 will be used rather than HDM2, which is common practice in the literature).

The primary function of p53 is as a transcription factor, transducing expression of genes initiating cell cycle arrest, DNA repair and apoptosis, among others. Since initiation of apoptosis in the wrong context can be catastrophic for an organism, p53 levels are kept low through the actions of E3 ubiquitin ligases, also known as E3s, catalysing the attachment of chains of ubiquitin moieties which serve to recruit p53 to the 26S proteasome, where it is degraded. The first and still the best characterised of these p53 targeting E3s is MDM2. Genotoxic stresses such as DNA damage catalyse the activation of kinases which phosphorylate the N-terminus of p53, abolishing ubiquitination by MDM2 and causing p53 levels to rise (Brown *et al.*, 2009, Lai *et al.*, 2001).

MDM2 is only one of a number of E3s known to target p53 in this manner (Honda *et al.*, 1997; Schloush *et al.*, 2011; Lee *et al.*, 2012); and a full understanding of more of these E3s and their modes of action is therefore critical to ongoing efforts to design inhibitors to re-activate p53 by rescuing it from degradation (Lee *et al.*, 2012). A hallmark of many E3s is the presence of a RING finger domain, whose function is to bind to the ubiquitin conjugating enzyme, also known as an E2. A 2007 study by Li and co-workers showed that Retinoblastoma Binding Protein 6, a RING finger-containing protein known to be

associated with mRNA 3'-end processing (RBBP6), may play such a role, either by directly ubiquitinating p53 or by assisting MDM2 to do so. The study was carried out in mice, and showed that knock-out of the *RBBP6* gene led to embryonic death due to overexpression of p53 and widespread ectopic apoptosis. The study also demonstrated direct interaction between the MDM2 and RBBP6 proteins (Li *et al.*, 2007). The study concluded that RBBP6 functions by activating the ubiquitination activity of MDM2 rather than having activity of its own. The aim of this thesis is to set up a fully *in vitro* ubiquitination assay to investigate the role of RBBP6 in ubiquitination of p53. The questions of particular interest will be (i) whether RBBP6 has E3 ligase activity of its own for p53 or acts only by enhancing the activity of MDM2 and (ii) whether the putative ubiquitination produced by RBBP6 leads to proteasomal degradation *in vitro*.



1.2. The Ubiquitin Proteasome System

The Ubiquitin Proteasome System (UPS) is a highly regulated system for rapid and efficient removal of specific proteins from the cell. Through the action of a number of dedicated enzymes, target proteins are tagged with polymers of ubiquitin moieties which act as recognition motifs for the 26S proteasome complex, causing them to be fed into the proteasome and digested into small peptides for re-use by the cell. The enzymes in question are the ubiquitin activating enzyme, also known as E1, ubiquitin conjugating enzymes, also known as E2s and ubiquitin-ligating enzymes, also known as E3s. In addition, certain ubiquitination systems require the use of an ubiquitin chain extension factor, also known as an E4 (Pant & Loranzo, 2014; Koegl *et al.*, 1999).

Ubiquitin is an 8.5 kDa protein containing 76 amino acids, which is highly conserved across all eukaryotes but not present in either bacteria or Archaea (Sorokin *et al.*, 2009). It contains a di-glycine motif at positions 76, which plays a crucial role in its conjugation to side-chain amino groups of lysine residues on target proteins, a process known as ubiquitination or mono-ubiquitination. Ubiquitin itself contains 7 lysine residues, at positions 6, 11, 27, 29, 33, 48 and 63 respectively, which can form the attachment points for additional ubiquitin moieties, leading to the assembly of poly-ubiquitin chains. Typically, linkage is through only one of the internal lysines, giving rise to the concept of lysine48-linked poly-ubiquitin chains, lysine63-linked chains and so on. Ubiquitination has been reported to give rise to a number of different results in addition to signalling degradation in the proteasome, including endocytosis of receptors and sorting into specific cellular compartments (Woelk *et al.*, 2007). Ubiquitination is a reversible reaction; a number of iso-peptidases, known as de-ubiquitination enzymes, or DUBs, are present in cells which regulate the level of ubiquitination as well as removing ubiquitin tags from proteins for recycling before they are degraded in the proteasome (Woelk *et al.*, 2007). The ubiquitin proteasome system (UPS) is illustrated schematically in the Figure 1.1.

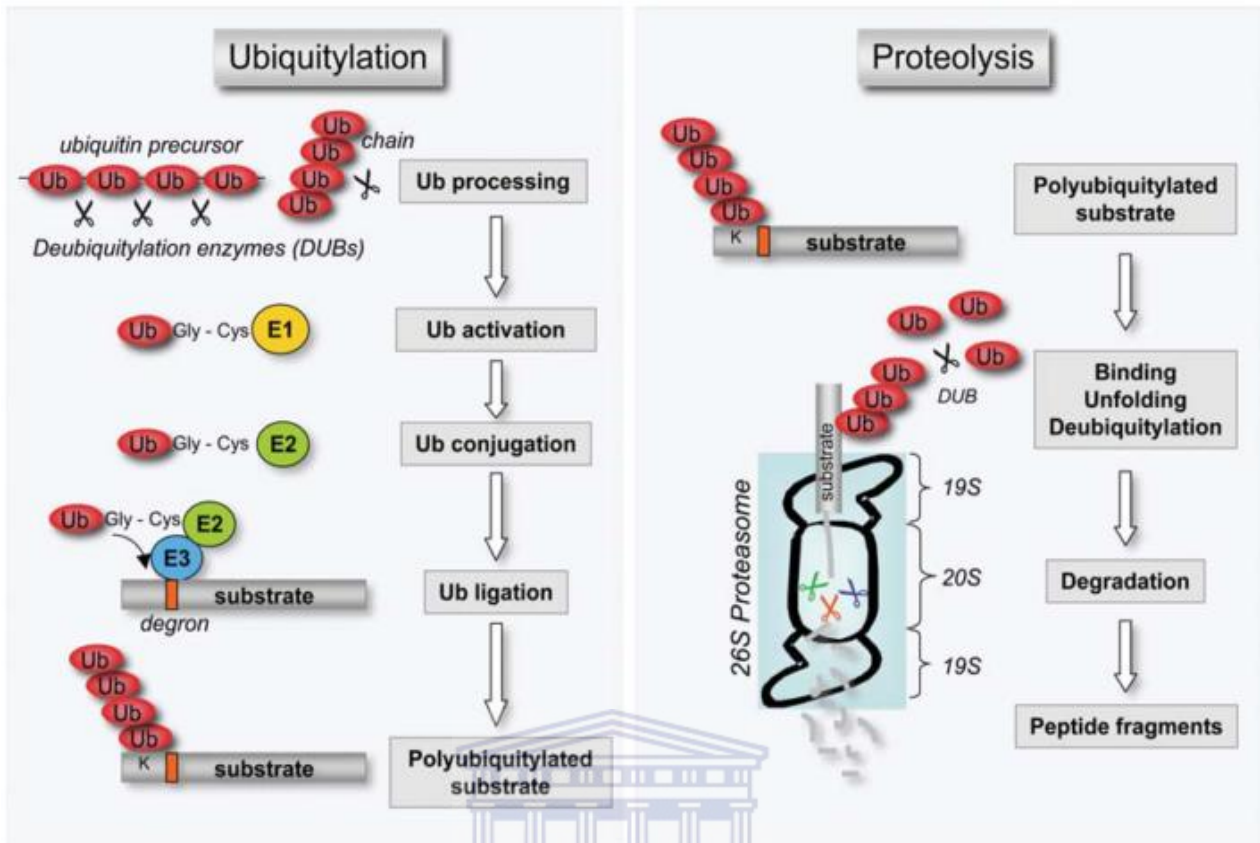


Figure 1.1. The ubiquitin proteasome system as depicted in Datura & Lindsten (2010). Ubiquitin (Ub) is indicated in red and the substrate in grey. The ubiquitin activating enzyme (E1) is depicted in yellow, the ubiquitin conjugating enzyme (E2) in green and the ubiquitin-ligating enzyme (E3) in blue.

UNIVERSITY of the
WESTERN CAPE

In the first step, the E1 activates ubiquitin by hydrolysing ATP to ADP and using the liberated energy to create a high-energy thioester bond between the C-terminus of ubiquitin and the side-chain SH group of the catalytic cysteine of the E1. In the second step ubiquitin is transferred from the E1 to the E2, where it again forms a thioester bond with the side-chain SH group of the catalytic cysteine of the E2. In the third step the ubiquitin-conjugated E2 is recruited to the substrate by the E3, where it is transferred to the side-chain amino group of a lysine on the substrate. The C-terminal carboxyl of ubiquitin forms a bond with the lysine amino group which is chemically identical to the peptide bonds found

on the backbone of peptides; however to distinguish them from backbone peptide bonds they are referred to as isopeptide bonds, which means “peptide-like” (Metzger *et al.*, 2014).

The role of the E3 is to recognise and recruit the substrate to the ubiquitin-conjugated E2, and hence it must contain a substrate binding domain as well as an E2-binding domain. E3s are therefore specific for one or a small number of substrates, and hence there must be approximately the same number of them as there are substrates requiring to be modified. In humans the number of E3s is more than 600. The E1, in contrast, needs to recognise only ubiquitin and the E2 and there are consequently fewer of them; in humans there are two – Uba 6 and Ube1. The E2 needs to recognise the small number of E1s and a subset of the large number of E3s, and we may therefore expect there to be an intermediate number of them; in humans there are approximately 35 (van Wijk & Timmers, 2010; Metzger *et al.*, 2014)

The role of E2-binding domain is played by one of two different domains: the HECT (Homologous to E6-AP Carboxy Terminus) domain or the RING (Really Interesting New Gene) domain (Woelk *et al.*, 2007; Windheim *et al.*, 2008; Metzger *et al.*, 2014). HECT-type E3s transfer the ubiquitin from the E2 to the substrate via a catalytic cysteine on the HECT domain and hence becomes covalently attached to ubiquitin during the reaction. An important consequence of this mechanism is that the substrate and the E2 do not have to interact simultaneously with the E3. RING-type E3s, on the other hand, act purely as

adaptor molecules, binding the substrate and E2 simultaneously in order to facilitate transfer of the ubiquitin from the E2 to the substrate (Metzger *et al.*, 2014).

RING fingers are small 70-residue domains that coordinate a pair of Zn²⁺ ions in a cross-braced arrangement. U-boxes adopt essentially the same structure as RING fingers, but manage to do so without requiring the assistance of any bound zinc ions. The similarity of the structures of U-boxes and RING has raised the question of whether U-box-containing E3s are specific for any particular type of substrate or biological outcome. Soon after their first identification U-boxes were proposed to be specific to ubiquitin chain extension factors (E4s), which means that they are capable of extending existing ubiquitin chains but not adding the first one to the substrate. However a number of U-box-containing proteins have since been shown to be able to catalyse ubiquitin of substrate molecules without the aid of other E3s (Kappo *et al.*, 2011). Some, such as CHIP (C-terminus of Hsp70-associated protein), are known to associate with chaperones such as Hsp70, which has led to the current hypothesis that they are specific for chaperone-mediated degradation of misfolded proteins (Metzger *et al.*, 2014; Kappo *et al.*, 2011).

A distinction is drawn in the literature between “poly-ubiquitination”, “mono-ubiquitination” and “multiple mono-ubiquitination”. Mono-ubiquitination, in which a single ubiquitin moiety is attached to the substrate, has been linked with non-proteolytic processes such as endocytosis, DNA repair, nuclear export,

endosomal sorting, cytoplasmic translocation and histone regulation as shown in Figure 1.2 (Brooks *et al.*, 2004, Woelk *et al.*, 2007). The attachment of a single ubiquitin to more than one lysine residue on the protein is called multiple mono-ubiquitination, and sometimes “multi-ubiquitination”. Multiple mono-ubiquitination may represent the signal for degradation of the protein by endocytosis in the lysosomes of the cell (Sorokin *et al.*, 2009). Poly-ubiquitination refers to the attachment of four or more ubiquitin moieties to a single lysine residue on a protein (Windheim *et al.*, 2008), and involves internal isopeptide bonds between the C-terminus of each ubiquitin moiety and the side-chain amino group of one of the seven lysines present on the next ubiquitin. The use of different internal lysines gives rise to differently-shaped chains, which is expected to account for the differing specificities of particular linkages. For example, a lysine48-linked chain is expected to bind specifically to part of the 19S cap of the proteasome in order to be degraded (Ciehanover & Stanhill, 2014). Shi and co-workers (Shi *et al.*, 2009) showed that multiple mono-ubiquitination results in export of p53 from the nucleus, leading to poly-ubiquitination and degraded in the cytoplasm.

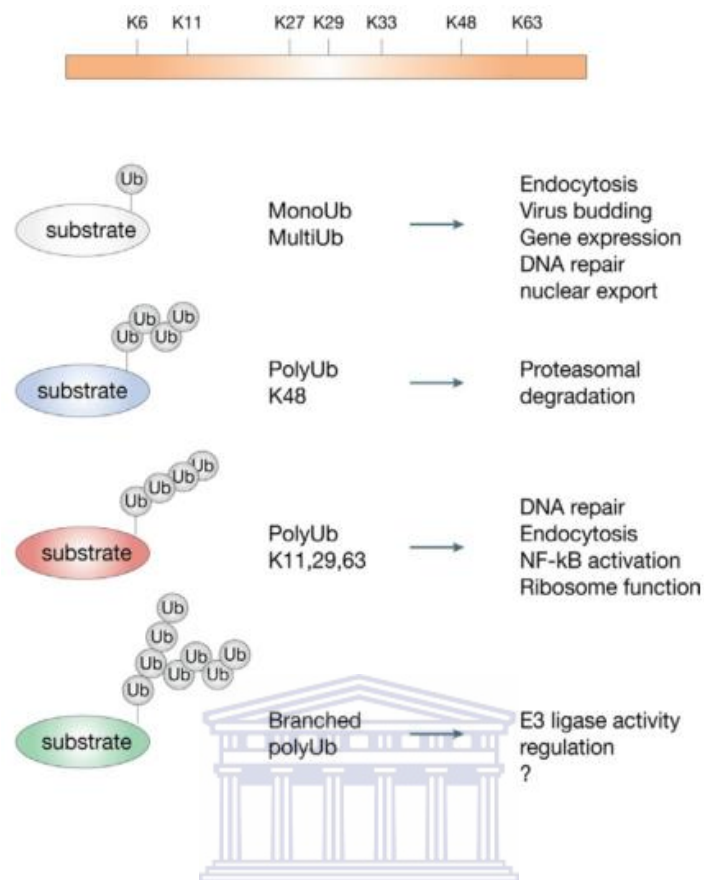


Figure 1.2 The various fates of the different ubiquitin chains on a substrate. Lysine48-linked chains are associated with degradation in the 26S proteasome. Adapted from Woelk *et al.*, 2007.

The 26S proteasome mediates degradation of lysine48 linked poly-ubiquitinated proteins. It is made up of a two parts: the 19S regulatory particle and the 20S core particle. The 20S core particle is a barrel-shaped structure made up of 14 α - and 14 β -subunits, arranged in 4 rings of 7 subunits in a $\alpha_7\beta_7\beta_7\alpha_7$ configuration and contains all the proteolytic activity. The masses of the α - and β -subunits are between 21 and 31 kDa each. The 19S regulatory particle is made up of 19 subunits, which include six related ATP-ase subunits and four non-ATPase subunits and the lid which contains nine non-ATPases subunits, which is responsible for recognising lysine48-linked adducts, unfolding the

conjugated protein and feeding it into the 20S barrel (Hayter *et al.*, 2005, Kao *et al.*, 2012).

Once a protein has been recognised for degradation by the 26S proteasome, it undergoes de-ubiquitination. De-ubiquitination is the removal of ubiquitin molecules from a ubiquitinated protein to restore it to its original state as depicted in Figure 1.1. For example the de-ubiquitinating protein HAUSP is able to restore ubiquitinated p53 to its unmodified form through the removal of the ubiquitin molecule from the protein. It is also able to de-ubiquitinate MDM2 and MDMX. Regulation of this de-ubiquitination process is still not well understood, but has important implications in stabilising p53 (Brooks & Gu, 2011).

Methods for investigation of ubiquitination

SDS-PAGE and Western blot

The standard method of investigating ubiquitination involves separation on SDS-PAGE followed by a Western blot using an antibody targeting either the substrate or ubiquitin. A common method involves the use of HA-tagged ubiquitin, facilitating detection with anti-HA antibodies. However, difficulties can arise when probing for ubiquitin since both the E2 and the E3 may become ubiquitinated in addition to the substrate. Immunoprecipitation of the substrate prior to detection can be used to overcome this problem (Wu *et al.*, 2011; Shi *et al.*, 2009).

Another issue is the difficulty, using the SDS-PAGE method, of distinguishing between poly-ubiquitination at single substrate lysines and mono-ubiquitination at different substrate lysines, since both would lead to ladders of higher molecular weight species. In the present context, p53 contains 7 lysines on its C-terminus alone, and therefore mono-ubiquitination of each lysine would result in the protein with an effective molecular weight of at least 110 kDa. In the literature, the presence of bands under 140 kDa has been taken as evidence of multiple mono-ubiquitination, and bands above 140 kDa as evidence of poly-ubiquitination (Wang *et al.*, 2011).

An alternative method of distinguishing between mono- and poly-ubiquitination is through the use of antibodies which bind specifically to poly-ubiquitin chains. These antibodies also have the capacity to distinguish between the different linkages. For example Newton and co-workers have developed antibodies which specifically detect K-48 and K-63 poly-ubiquitin chains (Newton *et al.*, 2008).

Investigation of poly-ubiquitination *in vivo* or in cell lysates is further complicated by the action of de-ubiquitinating enzymes (DUBs), which remove ubiquitin moieties through hydrolysis of the isopeptide bond. A number of chemical inhibitors, including cysteine protease inhibitors such as iodoacetamide (IAA) and N-ethylmaleimide (NEM) have been used in order to overcome this problem (Hjerpe *et al.*, 2009). However they have been found to be only partially effective due to their non-specificity. They were also not able to function for

extended periods of time in aqueous solutions, they only managed to partially inhibit ubiquitin proteases and they also caused aberrant covalent modifications which rendered them effectively useless in the study of poly-ubiquitination (Wilson *et al.*, 2012; Hjerpe *et al.*, 2009).

In an attempt to improve the detection of poly-ubiquitination, Tandem Ubiquitin Binding Entities (TUBEs) were designed to bind to and protect poly-ubiquitinated substrates from the action of DUBs and degradation by the proteasome. TUBEs are synthetic proteins comprising of four ubiquitin-associated (UBA) domains linked in tandem (Hjerpe *et al.*, 2009) and are available commercially from LifeSensors (Pennsylvania, USA). Different TUBEs are available that bind lysine48-linked and lysine63-linked chains respectively. An alternative to TUBEs is MultiDsk, which is a polymer of five repeats of the ubiquitin-associated domain from the yeast Dsk2 protein (Wilson *et al.*, 2011). MultiDsk has been shown to protect poly-ubiquitinated proteins from the action of the DUBs and has been used as a mechanism to precipitate poly-ubiquitinated proteins or to enrich for poly-ubiquitinated proteins. Unlike TUBEs, MultiDsk has been reported to bind equally to K48-and K63-linked poly-ubiquitin chains (Hjerpe *et al.*, 2009; Wilson *et al.*, 2012).

Mass spectrometry

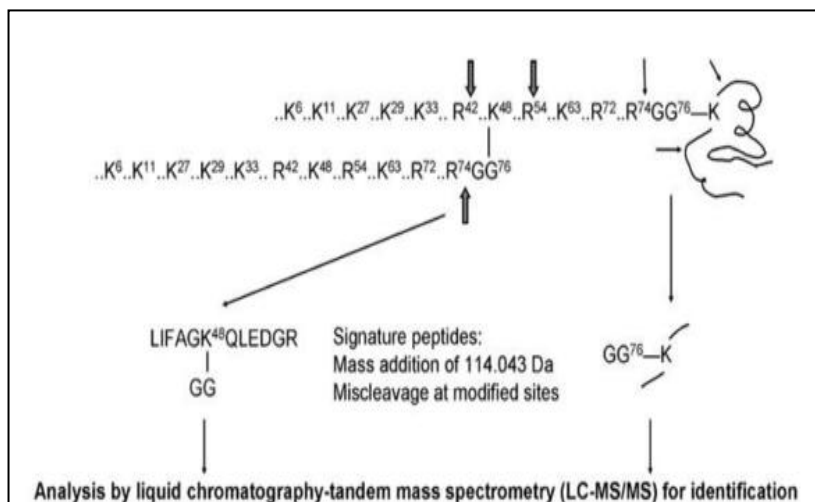
During ubiquitination the carboxyl group of the glycine at the C-terminus of the ubiquitin molecule forms an isopeptide bond with the ϵ -amino group of a lysine residue on the substrate. Ubiquitination of target proteins can be detected by

mass spectrometry using the tryptic digest method. Following separation on SDS-PAGE, potential ubiquitinated protein species are excised from the gel and subjected to in-gel tryptic digest and the resulting peptide fragments analysed by mass spectrometry. The sequence of ubiquitin ends -Arg-Gly-Gly, so tryptic digest following the Arg (trypsin cuts immediately after positively-charged residues) will leave di-glycine adducts, with a mass of 114.042 Da) attached to lysine residues on the substrates, as shown in Figure 1.3 (A). The dipeptide adds a mass of 114.042 Da onto the affected lysine residue of the protein which can be identified by matching fragment masses against the protein database, allowing for the addition of 114.042 Da per lysine residues (Figure 1.3 (A)). Mass spectrometry has the advantage that it can identify the precise site of modification (Xu & Peng., 2007; Xu *et al.*, 2010). Antibodies specifically recognising Lys-iso-Gly-Gly adducts are available commercially which can be used to enrich peptides prior to the mass spectrometry step (Figure 1.3 (B)).

1.3. Retinoblastoma Binding Protein 6

Retinoblastoma Binding Protein 6 (RBBP6) is a 200 kDa protein which has been shown to interact directly with both the tumour suppressor proteins p53 and pRb. It is known to form part of the mRNA 3'-end processing complex in humans (Shi *et al.*, 2009) and to play a role in 3'-end processing in humans (Di Giammartino *et al.*, 2014) and in yeast (Lee & Moore, 2014). Studies show that it is essential for viability in a number of organisms, including yeast (Vo *et al.*, 2001), the worm *C. elegans* (Huang *et al.*, 2013), the fruit fly *D. melanogaster* (Mather *et al.*, 2005) and mouse (Li *et al.*, 2007).

(A)



(B)

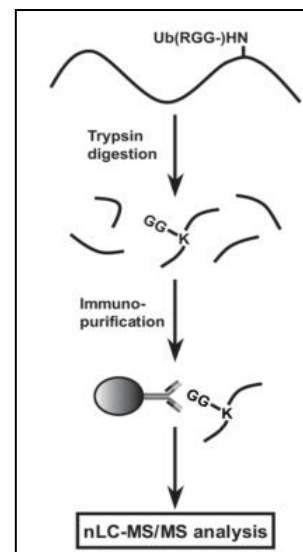


Figure 1.3. Using mass spectrometry to detect ubiquitinated substrates. (A) Tryptic digest of ubiquitinated substrates gives rise to Lys-iso-Gly-Gly adducts on substrate fragments, which can be identified by mass spectrometry. (B) Immunoprecipitation with antibodies specific for the Lys-iso-Gly-Gly adduct can be used to enrich tryptic fragments for those containing adducts (Xu *et al.*, 2010).

RBBP6 orthologues appear to be present in all eukaryotic genomes, in many cases at single copy number, but not at all in prokaryotes. Bioinformatic analysis of orthologues from a number of eukaryotic genomes has revealed the presence of a number of previously-characterised domains as shown in Figure 1.4. All eukaryotic genomes appear to contain at least the DWNN domain, zinc finger domain and RING finger domain, but higher eukaryotes also contain longer C-terminal extensions, as shown in Figure 1.4.

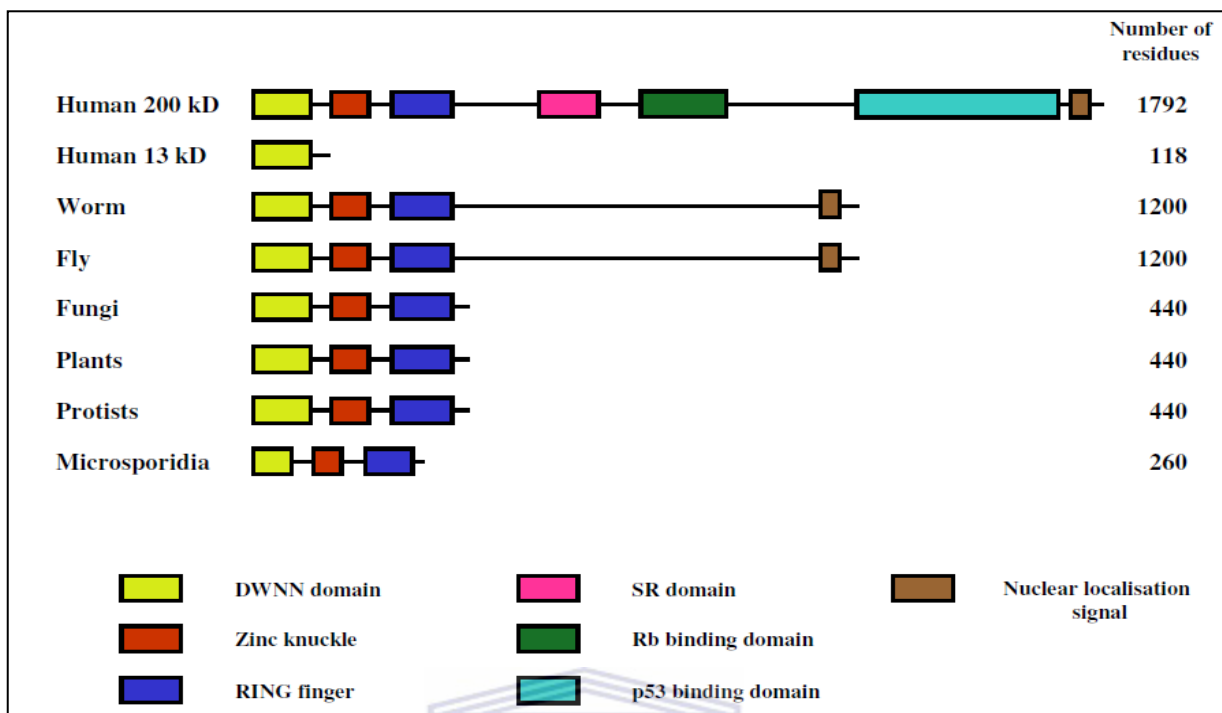
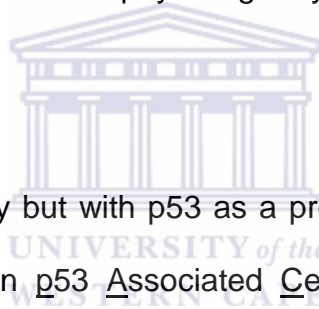


Figure 1.4 Domain organisation of RBBP6 orthologues in and various eukaryotic genomes. All eukaryotes contain at least the DWNN domain, zinc knuckle domain and RING finger domains. Higher eukaryotes contain C-terminal extensions, including p53- and pRb-binding domains as well as an SR domain similar to those found in splicing factors (Adapted from Pugh *et al.*, 2006).

UNIVERSITY of the
WESTERN CAPE

In many organisms more than one protein isoform is expected to be generated from each RBBP6 gene by alternative splicing or the use of alternative promoters. In humans, for example, four different isoforms have been identified: isoform 1 consists of 1792 amino acids and has a molecular weight of 201,6 kDa, isoform 2 consists of 1758 amino acids and has a molecular weight of 197,3 kDa and isoform 4 contains 952 amino acids and has a molecular weight of 106,0 kDa. Isoform 3, which consists of 118 amino acids and has a molecular weight of 13.2 kDa, is expressed from an alternate promoter and consists of the first 100 residues of full length RBBP6, including the DWNN domain, followed by an unique 18 residue tail which is not present in any of the other isoforms (Genbank: NP_008841, Genbank: NP_061173, Genbank: NP_116015).

RBBP6 was originally identified on the basis of its binding to pRb by Sakai and co-workers (Sakai *et al.*, 1995) who screened a Lambda ZAPII cDNA expression library using pRb as a probe. A protein which was later found to correspond to residues 150-1146 of RBBP6 was isolated and called RBQ-1 (Rb-binding Q-protein-1). This protein was found to bind to hypophosphorylated pRb but not to hyper-phosphorylated pRb, leading the authors to suggest that it may function as an oncogene by opposing the tumour suppressive effects of hypophosphorylated pRb. They also showed that the binding of RBQ-1 was disrupted by E1A (Adenovirus Early Region 1A), which suggests that RBQ-1 binds to the physiologically important pocket region of pRb.



Using a similar methodology but with p53 as a probe, Simons and co-workers identified the mouse protein p53 Associated Cellular protein-Testes derived (PACT), which was subsequently found to correspond to residues 207-1792 of RBBP6. In addition to interacting with p53, it was also found to interact with pRb. PACT was found to bind to wild-type p53, but not to transcriptionally-inactive mutants such as R273H. PACT was also shown to localise in nuclear speckles where splicing factors and splicing-associated Sm proteins are known to localise (Simons *et al.*, 1997).

An independent study by Witte and Scott (1997) screened a 3T3 cDNA λ gt11 library using an AC88 monoclonal antibody which specifically detects both proliferation-related proteins (P2Ps) and Hsp90. They identified a protein

subsequently shown to correspond to residues 199-1772 of RBBP6 (see Figure 1.5), which they named Proliferation Potential Related Protein (P2P-R). Witte and Scott showed that expression of P2P-R is significantly repressed during terminal differentiation of cells (Witte & Scott, 1997).

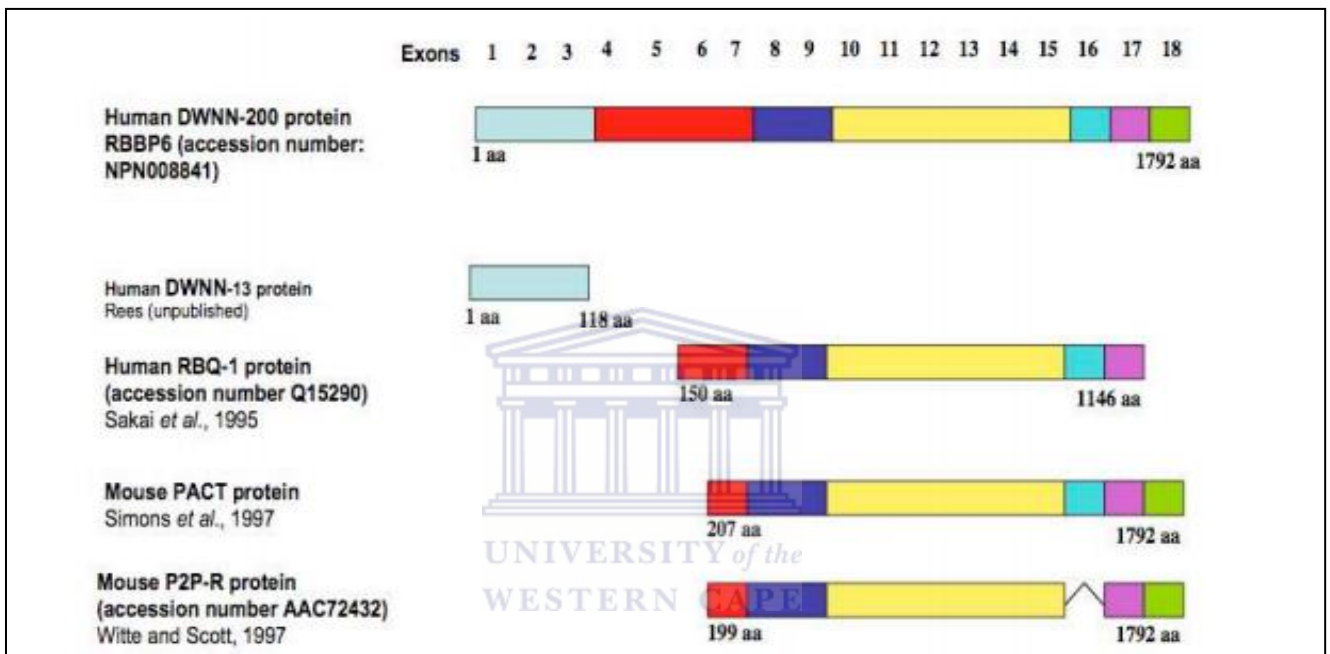


Figure 1.5 Full length human RBBP6 and partial human and mouse proteins identified in various studies. DWNN13 is the 13 kDa form, also known as isoform 3, which is translated from an alternative transcript transcribed from an alternate promoter. The C-terminal 18-amino acid residues of DWNN13 are not present in the other three isoforms, all of which are generated from the same transcript by alternative splicing. (Adapted from Pretorius *et al.*, 2011)

A study by Vo and co-workers in 2001 identified Mpel as the yeast homologue of human RBBP6, and showed that it was closely involved in 3'-processing in yeast (Vo *et al.*, 2001). Mpel was found to form part of the Cleavage and Polyadenylation Factor (CPF) of *Saccharomyces cerevisiae* and to be necessary for 3'-end cleavage and polyadenylation processing of mRNA transcripts in yeast. Lee and More subsequently showed that the first three domains of Mpel (DWNN, zinc knuckle and RING finger domains) are essential

for correct 3'-end polyadenylation in yeast (Lee & Moore, 2014). Manley and co-workers have demonstrated that RBBP6 forms part of the 3'-end processing complex in humans, which closely mirrors its role in the CPF in yeast. They showed that knockdown of RBBP6 directly influences 3'-end processing of human mRNA transcripts and that isoform 3 modulates the activity of the full length RBBP6 by competing with the DWNN domain of full length RBBP6 (di Giammartino *et al.*, 2014).

RBBP6 plays a role in tumourigenesis

Reports in the literature link RBBP6 to a number of different cancers, including colon, breast, prostate, colorectal, pancreatic, bladder, cervical and gastric cancers (Khan *et al.*, 2014). RBBP6 is reported to be over-expressed in patients with oesophageal (Yotishake *et al.*, 2004), breast (Moela *et al.*, 2014), cervical (Mbita *et al.*, 2012), gastric (Morisake *et al.*, 2014), colon (Chen *et al.*, 2013) and lung cancer (Motadi *et al.*, 2011) and has been linked to low survival rates in all of these. Motadi and co-workers demonstrated in 2011 that RBBP6 suppresses apoptosis and upregulates cellular proliferation in the context of lung cancer (Motadi *et al.*, 2011). Miotto and co-workers reported that depletion of RBBP6 leads to DNA damage, cell cycle arrest and slowing down of replication forks during DNA replication (Miotto *et al.*, 2014).

RBBP6 forms part of the pre-mRNA splicing machinery due to its localisation in nuclear speckles which are the main sites of pre-mRNA processing. Although this may suggest a primary role for RBBP6 in mRNA processing, the presence

of a RING finger domain and the ubiquitin-like DWNN domain suggested it may also play a role in the process of ubiquitination. Using a yeast two-hybrid screen with the RING finger domain as bait, Chibi and co-workers identified Y-Box Binding Protein-1 (YB-1) and zBTB38 as interactors of RBBP6 and showed that RBBP6 had E3 ubiquitin ligase activity against both (Chibi *et al.*, 2008; Miotto *et al.*, 2014). Using the DWNN domain as bait, Kappo and co-workers identified heat shock protein HSPA14 and the splicing associated protein Sm-G as interactors (Kappo *et al.*, 2011).

Y-box binding protein (YB-1) is a transcription factor that transduces the expression of a number of tumour-promoting genes, including MDR1 which codes for the multidrug resistance protein P-glycoprotein (Braithwaite *et al.*, 2006). Nuclear localisation of YB-1 is tightly correlated with aggressiveness and poor patient prognosis in a number of cancers (Homer *et al.*, 2005). It is also closely associated with mRNA maturation, to the extent that it has been identified as an mRNA chaperone (Chen *et al.*, 2000). Chibi and co-workers found that RBBP6 interacted with the extreme C-terminus of YB-1 through its RING-finger domain and ubiquitinated it both *in vivo* and *in vitro*. Overexpression of the RING finger domain in HEK293T cells led to dose-dependent and proteasome-specific suppression of YB-1 levels, suggesting that RBBP6 negatively is a suppressor of YB-1 (Chibi *et al.*, 2008). RBBP6 has subsequently been shown to ubiquitinate YB-1 in fully *in vitro* ubiquitination assay, using UbcH1 as E2 (Faro, A and Pugh, D.J.R., manuscript in preparation).

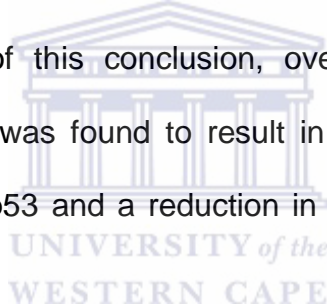
zBTB38 is a transcriptional repressor which represses the replication protein MCM10. A study by Miotto and co-workers demonstrated that RBBP6 catalyses the ubiquitination and proteasomal degradation of zBTB38 *in vivo*, independent of both p53 and MDM2 (Miotto *et al.*, 2014). Knock-down of RBBP6 in HeLa cells using RNA interference led to over-expression of zBTB38, leading to suppression of MCM10 and consequent accumulation of DNA damage.

Parkin is an E3 ligase protein implicated in Parkinson's disease which has structural similarities to RBBP6. In addition to a RING finger domain, it contains an N-terminal ubiquitin-like domain. Chaugule and co-workers demonstrated that the ubiquitin-like domain regulates the ubiquitination activity of Parkin by folding over and blocking access to the RING finger domain. In pathogenic mutations of Parkin this autoinhibition is disrupted, leading to over-activation of Parkin's activity (Chaugule *et al.*, 2011).

RBBP6 is a negative regulator of p53

In 2007 Li and co-workers reported that the RING finger-containing protein PACT, which is an alternative name for RBBP6, plays an essential role in embryonic growth and development in mice (Li *et al.*, 2007). Following knock-out of the RBBP6/PACT gene by the insertion of a neomycin resistance gene at exons 11-12, heterozygous knock-out (PACT^{+/-}) mice were found to be healthy and fertile. However, crosses between PACT^{+/-} and PACT^{+/-} mice gave no viable PACT^{-/-} offspring, compared to the expected 25%.

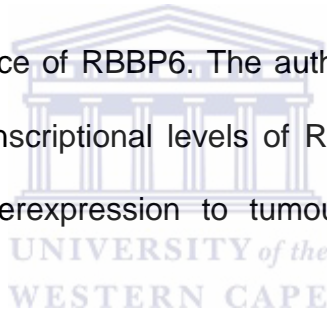
On further investigation it was found that PACT^{-/-} embryos died after 7.5 days (E7.5) and the embryos were developmentally retarded and smaller in size as compared to their wild type counterparts. They were also found to possess elevated levels of p53 and a large number of apoptotic cells. Suspecting a role for p53 in the death of the homozygous mice, Li and co-workers performed the same RBBP6/PACT knock-out in p53 null mice (p53^{-/-}). The p53^{-/-}/PACT^{-/-} offspring survived slightly longer (up to embryonic day 11.5) although they were still smaller in size compared to wild type mice. They concluded from this that RBBP6/PACT plays an essential role in suppression of p53 during development. In support of this conclusion, over-expression of exogenous PACT in mammalian cells was found to result in increased levels of MDM2-mediated ubiquitination of p53 and a reduction in the transcriptional activity of p53.



Li and co-workers went on to show that endogenous PACT interacts with MDM2 in U2OS and MCF7 human cell lysates. Over-expression of endogenous PACT enhanced the interaction between p53 and MDM2. However over-expression of PACT on its own did not lead to reduced levels of p53, whereas it did when MDM2 was simultaneously over-expressed. However p53 degradation was abolished when PACT was over-expressed without the RING finger, even in the presence of over-expressed MDM2. Li and co-workers concluded that PACT facilitates ubiquitination of p53 by MDM2 but is incapable of ubiquitinating it on its own. They hypothesised that RBBP6 may act as a scaffold protein bringing

MDM2 and p53 together to facilitate ubiquitination, possibly playing the role of an E4 ligase (Li *et al.*, 2007).

In a study by Chen and co-workers, p53 expression levels were found to be negatively influenced by upregulation of RBBP6 in advanced colon cancer and metastasis (Chen *et al.*, 2013). This was found to be due to its being more susceptible to ubiquitination by MDM2 than mis-sense mutated p53. Mutated p53 was therefore found to be more stable than wild type p53, possibly due to an altered conformation of the protein due to the mis-sense mutation. This mutant p53 was said to therefore be unable to be ubiquitinated and degraded by MDM2 with the assistance of RBBP6. The authors concluded that both the transcriptional and post-transcriptional levels of RBBP6 are elevated in colon cancer, linking RBBP6 overexpression to tumour invasion and metastasis (Chen *et al.*, 2013).



1.4. p53

p53 has been dubbed “The Guardian of the Genome” due to its key role in coordinating the response of the cell to genotoxic stresses. Figure 1.6 depicts the broad range of stress signals impinging on p53 and some of the mechanisms through which it responds.

The p53 protein is made up of 393 amino acids, as depicted in Figure 1.7. The N-terminus is comprised of a transactivation domain (residues 1-42), which is the site of extensive post-translational modification, and a proline-rich region

(residues 61-94). The central domain (residues 102-292), also known as the “core” domain or the DNA binding domain, binds to a consensus DNA sequence within the promoters of target genes. Most clinically-important mutations of p53 occur within this region and it has consequently been the focus of studies aimed at understanding the role of mutations in inactivating p53 activity. The C-terminus comprises the tetramerization domain (residues 324-355) and the regulatory domain (residues 363-393), which is heavily post-translationally modified by ubiquitination, acetylation and phosphorylation (Rodriguez *et al.*, 2000; Bai & Zhu, 2006).

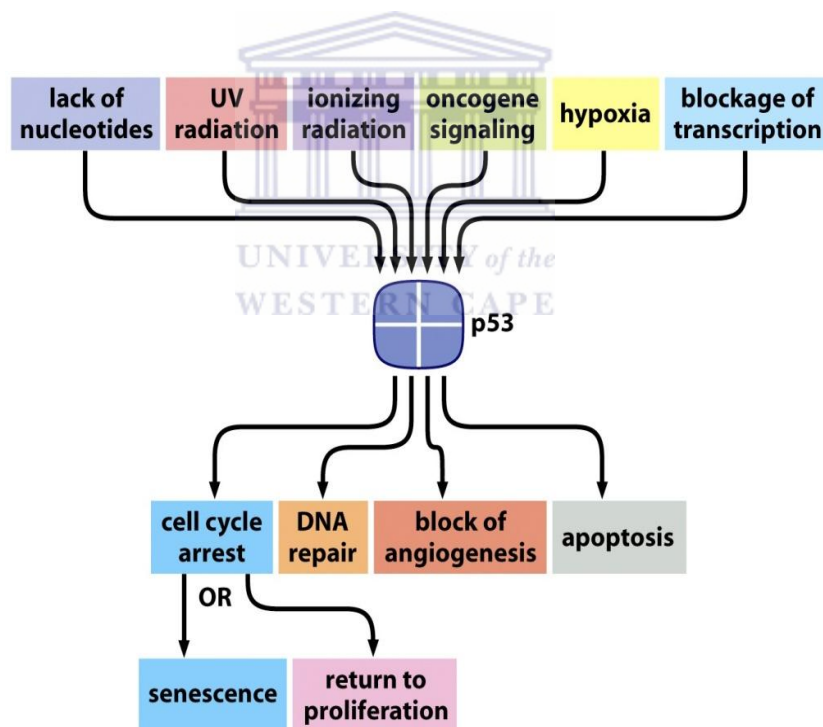


Figure 1.6 Activators and effectors of p53 function. A broad range of genotoxic stress signals impinge on p53, which responds by initiating signals aimed at halting the cell cycle, initiating DNA repair, inhibiting angiogenesis or initiating apoptosis (adapted from Weinberg, R. 2007).

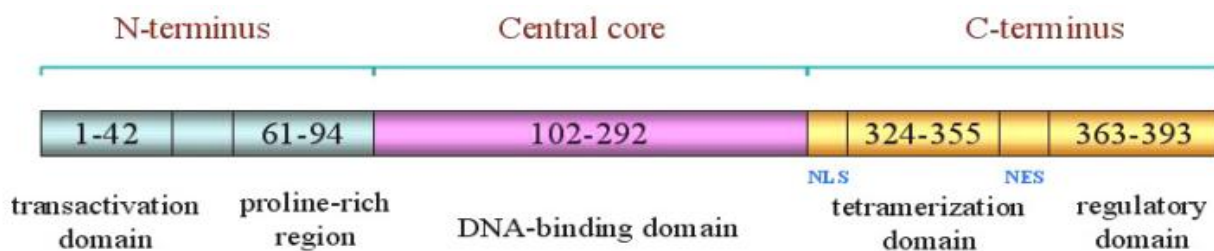


Figure 1.7 Schematic representation of the p53 protein depicting the transactivation domain, proline-rich domain, DNA-binding domain, tetramerization domain and the regulatory domain. NLS is the nuclear localisation signal and NES is the nuclear export signal (Adapted from Bai & Zhu, 2006).

p53 functions as a tetramer. This provides an explanation for the observation, illustrated schematically in Figure 1.8, that mis-sense mutations of p53 — those that change one or two amino acids rather than truncating or deleting the entire protein — make up a large fraction of all p53 mutations than in similar proteins such as APC, ATM or BRCA1. According to the simple model illustrated in Figure 1.9, mutant alleles which abolish the activity of any tetramer in which they are incorporated will reduce the overall activity of p53 by a factor of $15/16 = 93\%$ (Weinberg, R. 2007). While this represents an extreme case, the model shows how even mild suppression of the activity of the tetramer by mis-sense mutants can reduce the activity of p53 by more than the 50% expected for a monomeric protein. Hence, mis-sense mutants of p53 are more potent suppressors of p53 function than knock-out mutations, which explains why they are encountered so frequently in the clinic (Weinberg, R. 2007).

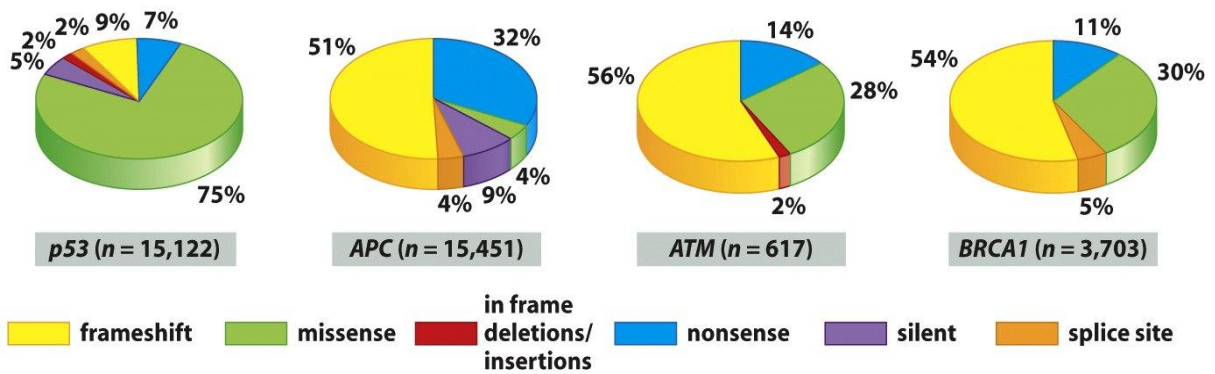


Figure 1.8 Mis-sense mutations of p53 make up 75% of all p53 mutations, compared to 4% for APC, 28% for ATM and 30% for BRCA1 Weinberg, R. 2007

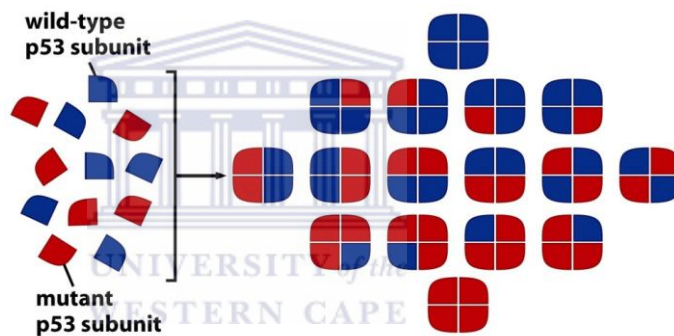


Figure 1.9 Tetramerization explains the frequency of mis-sense mutations of p53 in the clinic. If one of the two alleles is able to form part of a tetramer but abolishes its activity it will reduce the overall activity of p53 by $15/16 = 93\%$, compared to the 50% expected if p53 were monomeric. (Adapted from Weinberg, R. 2007).

p53 affects many pathways within the cell, but one of the most significant is cell cycle arrest, largely through its activation of the cell cycle inhibitor p21. Division of a cell into its two daughter cells, a process known as mitosis, takes place according to a strict sequence of events called the cell cycle, which are depicted schematically in Figure 1.10. Duplication of the genome occurs in the S phase ('Synthesis') and division during the M phase ('Mitosis'), which are separated by resting ('Gap') periods denoted G₁ and G₂ respectively. During G₁ the cell

makes critical decisions about whether to replicate or differentiate, based in part on external inputs such as levels of growth factors and nutrients outside the cell. During G_2 the cell prepares itself for division into two daughter cells during the M phase, making use of various checkpoints to check that everything has proceeded correctly during DNA synthesis (Weinberg, R., 2007).

For example DNA damage caused by exposure to radiation results in delays during both the G_1 and G_2 phases of the cell cycle. p53 plays a key role in arresting the cell cycle during G_1 , allowing the DNA repair machinery within the cell to initiate repair. The cell cycle then resumes normally once this damaged DNA has been repaired. However if the DNA damage is too extensive, the cell will undergo apoptosis, which is initiated directly by p53 (Weinberg, R., 2007). This happens primarily as a result of p53-driven expression of the cyclin-dependant kinase inhibitor p21^{CIP1} which blocks phosphorylation of pRb by cyclin-dependent kinases, leading to suppression of the activity of E2F by hypophosphorylated pRb.

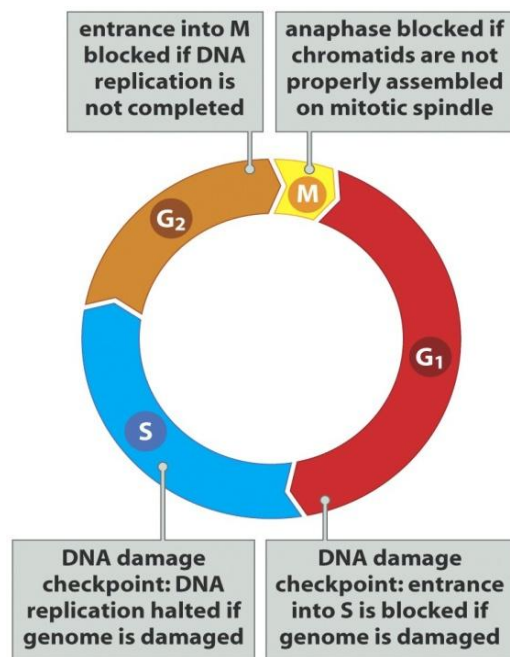
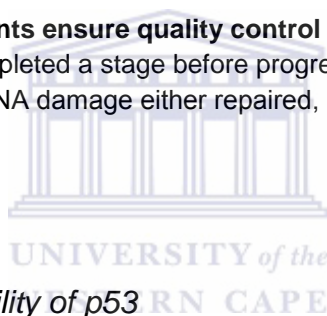


Figure 1.10 Cell cycle checkpoints ensure quality control as the cell progresses through the cycle. A cell has to have completed a stage before progressing to the next stage. If not, the cell's progression is halted and DNA damage either repaired, or cell is degraded if damage is too severe (Weinberg, R., 2007).



Mutations affecting the stability of p53

More than 95% of all clinically-occurring p53 mutations lie within the core DNA-binding domain, as shown in Figure 1.11 (Brown *et al.*, 2009). This impacts the function of p53's transcriptional activation activity. Of these, 75% are mis-sense mutations. These mis-sense mutations can be further divided into DNA contact mutations, which interfere directly with the binding of p53 to the DNA and therefore affect its transcriptional activity, and structural contact mutations, which affect the stability of the entire p53 protein. Structural contact mutations typically exert a dominant negative effect due to the quaternary nature of the functional complex, as described earlier (see Figure 1.9) (Brown *et al.*, 2009; Weinberg, R., 2007; Liu *et al.*, 2010).

Addition of zinc has also been shown to be important in the proper folding of the core domain of p53, so mutations which affect the zinc binding, such as C242S, H179R, C176F and R175H, are often found in human cancers (reviewed by Hoe *et al.*, 2014). In addition, a number of mutations, especially in the N-terminal domain, affect the stability of p53 by modulating the effect of post-translational modification such as phosphorylation and ubiquitination. These are discussed at more length below.

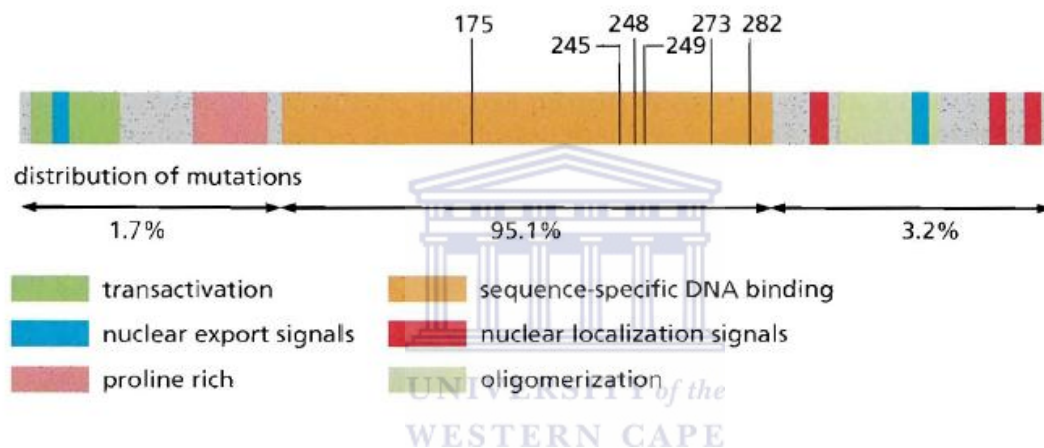


Figure 1.11 Hotspots for point mutations within the human p53 gene. 95% of mutations affect the core DNA-binding domain. The amino acid numbers which are frequently mutated are indicated above the DNA-binding domain (adapted from Weinberg, R. 2007).

The difference in free energy between the folded and the unfolded state of a protein is known as the free energy of folding. The wild-type p53 core domain has a free energy of folding of only 7.5-8.5 kcal/mol at 25 °C and no more than 2-3 kcal/mol at physiological temperature, with the result that it is only marginally stable under physiological conditions. A number of single amino acid substitutions are therefore sufficient to lower its stability sufficiently to unfold a significant fraction of the protein at 25 °C (Bullock *et al.*, 2001).

In order to increase the stability of p53 for the purpose of delivering it into cells as part of gene therapy, Nikolova and co-workers compared the amino acid sequences of p53 homologues from 23 species. By means of four separate mutations — M133L, V203A, N239Y and N268D — they managed to increase the stability of human p53 from 8.5 to 11.3 kcal/mol at 25 °C without compromising its ability to bind DNA (Nikolova *et al.*, 1998). When the crystal structure was determined in 2004 the overall structure of the so-called “quadruple mutant p53” was found to be unchanged from that of wild type p53 (Joergher *et al.*, 2004). Due to the poor stability of wild type p53, the quadruple mutant was used as a proxy for wild type p53 in some of the investigations reported later in this thesis. Since the reported interactions between p53 and MDM2 involve primarily the N-terminus of p53, and ubiquitination is reported to take place on the C-terminus (see below), the four mutations are not expected to affect the ubiquitination behaviour of p53.

Ubiquitination of p53 by MDM2 and MDMX

Regulation of p53 level is very important; levels which are too high may result in ectopic apoptosis and levels which are too low may result in failure to avoid the consequences of genotoxic stress. Post-translational modifications are covalent additions of certain groups to a protein which alter its conformation or its activity, but are not coded for by the gene. Common post-translational modifications include addition of a phosphate group (phosphorylation), of an acetyl group (acetylation), of a methyl group (methylation), of a carbohydrate chain (glycosylation) or one of a number of small proteins, of which the most

important is ubiquitin (ubiquitination). Ubiquitination of p53 by MDM2 leads to its targeting to the proteasome and subsequent degradation. Phosphorylation of the N-terminal transactivation domain by stress-induced kinases such as ATM and Chk2 leads to protection of p53 from ubiquitination by MDM2, leading to a rapid rise of p53 levels and induction of the anti-genotoxic response (Hock & Vousden, 2013; Pant & Loranzo, 2014).

The major target for p53 ubiquitination is the C-terminus. Of the last 30 amino acids on the C-terminus of p53, six — K370, K372, K373, K381, K382 and K386 — are lysine residues and potential sites for ubiquitination (see Figure 1.12). In a study by Rodriguez and co-workers single and multiple substitutions of lysine for arginine were generated (Rodriguez *et al.*, 2000). When the lysines were individually mutated to arginine no effect on the stability of p53 was observed, but when all six were substituted, degradation of p53 catalysed by MDM2 did not occur (Rodriguez *et al.*, 2000). It has subsequently been found that other lysines elsewhere in p53 are also able to target p53 for degradation, since even a truncated form of p53 without its C-terminus is still able to be ubiquitinated by MDM2 (Pant & Loranzo, 2014).

MDM2 was the first E3 ligase shown to catalyse degradation of p53 *in vitro* (Honda *et al.*, 1997). However it was subsequently questioned whether MDM2 was able to catalyse poly-ubiquitination of p53 in fully *in vitro* ubiquitination assays, or whether it was restricted to multiple mono-ubiquitination (Lai *et al.*,

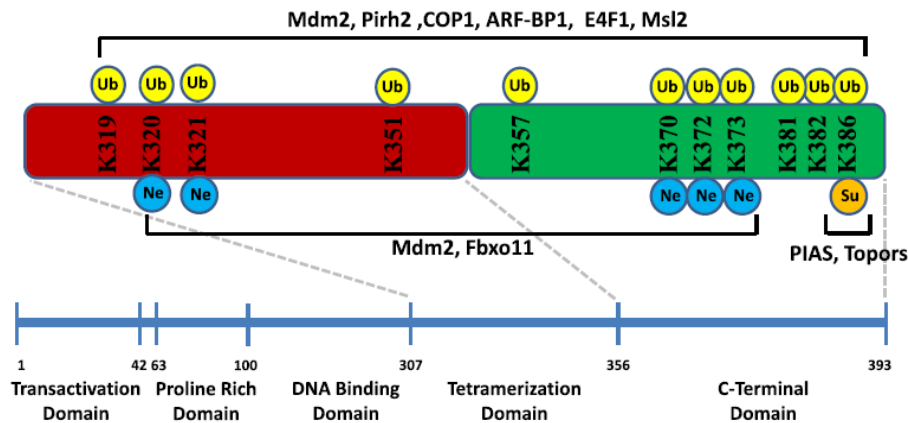


Figure 1.12 Sites on p53 modified by neddylation (Ne), sumoylation (Su) and ubiquitination (Ub) and the corresponding E3 enzymes catalysing which elicit these modifications (Adapted from Brookes & Gu, 2011).

2001). MDMX was subsequently identified as a partner for MDM2 that could potentially activate MDM2 to poly-ubiquitinate p53.

MDMX is a close structural homologue of MDM2 which nevertheless lacks the E3 ligase activity of MDM2. Both MDM2 and MDMX form homodimers in solution through their respective RING finger domains; MDM2 and MDMX were subsequently shown to also form heterodimers, again through their RING finger domains, and the heterodimer complex was shown to have more poly-ubiquitination activity than the MDM2 homodimer (Wang *et al.*, 2011).

Although poly-ubiquitination of p53 by GST-MDM2 had been previously reported in the literature (Lai *et al.*, 2001) in 2011 Wang and co-workers showed that His₆-MDM2 could only mono-ubiquitinate p53 (Wang *et al.*, 2011). Wang and co-workers concluded that since GST is well known to form homodimers in

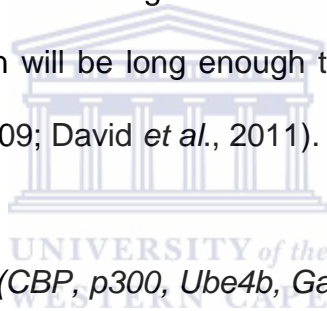
solution; GST was therefore artificially enhancing the poly-ubiquitination activity of GST-MDM2 by promoting its dimerisation (Wang *et al.*, 2011).

The combination of MDM2/MDMX has subsequently been shown to also catalyse poly-ubiquitination of p53 with the ubiquitin-like protein Nedd8, in a process called Neddylation. Neddylation occurs on three C-terminal residues of p53, resulting in loss of its transcriptional activity and nuclear export ability as shown in Figure 1.11 (Hock & Vousden, 2013).

E2 ligases known to be responsible for p53 ubiquitination

As described above, E2 acts as an adaptor between the activating enzyme E1 and the substrate-specific E3. The first E2 enzymes identified for p53 ubiquitination were the Ubch5 family by Honda and co-workers in 1997 (Honda *et al.*, 1997). Saville and co-workers established that Ubch5a, b and c together with E2-25K (also known as Ubch1 or Hip2) are capable of ubiquitinating p53 together with MDM2 *in vitro* (Saville *et al.*, 2004). Ubch1 is widely known to be expressed in mammalian tissues and is has been shown to synthesize unanchored poly-ubiquitin chains leading to protein degradation *in vitro*. The core domain of this protein was shown to be crucial in its activity and its specificity (Haldeman *et al.*, 1997). Ubch5b and Ubch5c have been well studied and shown to share 88-89% homology in their amino acid sequence with Ubch5a (Jensen *et al.*, 1995).

E2s were always thought of as simple “ubiquitin-carriers”, but have recently been shown to play an important role on determining the length and topology of the growing ubiquitin chain. These E2s are crucial in chain elongation as they determine whether a lysine residue in the ubiquitin or the substrate will receive the next ubiquitin molecule. They are therefore also responsible for determining the linkage of the growing ubiquitin chain, ultimately deciding the fate of the target protein. E2s are also responsible for controlling the processivity of the growing ubiquitin chain. The processivity is the number of ubiquitin molecules which can be transferred to the growing chain of ubiquitins in one round of association with the substrate. The higher this rate of processivity, the greater the likelihood that this chain will be long enough to be recognised by the 26S proteasome (Ye & Rape, 2009; David *et al.*, 2011).



E4 ubiquitin ligases for p53 (CBP, p300, Ube4b, Gankyrin)

The existence of an E4 was first proposed by Koegl and co-workers (Koegl *et al.*, 1999) as a fourth enzyme involved in poly-ubiquitin chain formation; they are proposed to catalyse the attachment of the C-terminus of a ubiquitin moiety to a lysine on another ubiquitin, but not to a substrate lysine. Consequently a defining characteristic of an E4 is that it can only catalyse poly-ubiquitination of already mono-ubiquitinated substrates.

A number of proteins have been reported to act as E4s for p53. Shi and co-workers showed that CREBS Binding Protein (CBP) and its paralogue p300 were able to extend chains initiated by MDM2. The N-termini of p300 and CBP

have been shown to harbour the E3 and E4 activities of these proteins (Shi *et al.*, 2009). Wu and co-workers showed that Ube4b was also able to extend chains initiated by MDM2 (Wu *et al.*, 2011). Wu *et al.*, (2011) investigated Ube4b as an E4 in the regulation of p53. Ube4b was identified in this study to be a U-box containing protein which enabled degradation of p53. They discovered that both MDM2 and Ube4b were only capable of mono-ubiquitinating p53 when either of these proteins were knocked-down in H283 cells respectively. They performed two-step assays in which p53 was firstly mono-ubiquitinated with MDM2 and then allowed to be poly-ubiquitinated with Ube4b. Ube4b was found to not be a molecular clamp in the interaction of HDM2 and p53 like that of the E4 Yin-Yang 1 (Wu *et al.*, 2011). Yin Yang 1 was found to enhance the poly-ubiquitination of p53 by MDM2 and also increase the affinity of MDM2 towards p53. It also binds to p300 and recruits it in its campaign to poly-ubiquitinate p53 (Hock & Vousden, 2014). Gankyrin is an E4 known to associate directly with a subunit of the 26S proteasome and control the ubiquitin ligase activity of MDM2 (Hock & Vousden, 2014).

1.5. Objectives of this project

Li and co-workers have established that RBBP6 plays a central role in suppression of p53 during development, activating MDM2 to poly-ubiquitinate it and causing its degradation in the proteasome (Li *et al.*, 2007). The first objective of this project was therefore to use *in vitro* ubiquitination assays to investigate the role of RBBP6 in the ubiquitination of p53 in more detail. This involved recombinant expression and purification of all of the required proteins,

including E1, a number of E2s, various forms of ubiquitin, different fragments of RBBP6, MDM2 and a number of forms of p53, and using them to set up fully *in vitro* ubiquitination assays with p53 as substrate and MDM2 or RBBP6 as E3. Because full length RBBP6 is not suitable for heterologous expression in bacteria, an N-terminal fragment denoted R3 was used as a proxy for RBBP6 in these assays.

The second objective was to establish if RBBP6 enhances the ubiquitination activity of MDM2 or whether RBBP6 is capable of poly-ubiquitinating p53 on its own. The third, and related, objective was to establish whether poly-ubiquitination of p53, produced either by RBBP6 acting alone or in cooperation with MDM2 was able to cause degradation of p53 in the proteasome, and whether it corresponds to lysine48-linked poly-ubiquitination or some other form of linkage.

The fourth objective was to assess whether the ubiquitin-like DWNN domain of RBBP6 plays any role, either stimulatory or suppressive, in ubiquitination of p53. This was carried out by replacing R3 in ubiquitination assays with a shorter fragment excluding the DWNN domain and denoted R2.

The presentation of results begins by describing a sub-project whose aim was to generate a DNA plasmid for expressing isoform 3 of RBBP6, also called DWNN13, fused to the C-terminus of the monomeric enhanced Green

Fluorescent Protein, (mEGFP) for use by co-workers in immunofluorescence microscopy studies.



CHAPTER 2

Materials and Methods

A list of suppliers, general stock solutions and buffer preparations can be found in the Appendix

2.1. Bacterial strains

Escherichia coli strain MC1061

F⁻ araD139 D(ara-leu) 7696 galE15 galK16 D(lac)X74 rpsL (Str^r) hsdR2 (rK₋ mK⁺) mcrA mcrB1. This strain was used to produce plasmid DNA.

Escherichia coli strain BL21 (DE3)pLysS

F⁻ ompT gal dcm lon hsdS_B(r_B⁻ m_B⁻) λ(DE3) pLysS(cm^R). This strain was used to express recombinant proteins. It contains a chromosomal copy of the lambda DE3 sequence (λ(DE3)) encoding RNA polymerase from phage T7, and is therefore suitable for use with the pET family of protein expression plasmids.

Escherichia coli strain Codon Plus

B F⁻ ompT hsdS(rB⁻ mB⁻) dcm⁺ Tetr gal λ (DE3) endA Hte [argU proL Cam^r] [argU ileY leuW Strep/Spec^r]. This strain also contains λ(DE3) and is therefore a suitable host for pET vectors.

2.2. *Antibodies used*

- Anti-p53 primary sc-6243 (Santa Cruz Biotechnology, Inc., CA, USA, Rabbit polyclonal raised against full length human p53.
- Anti-rabbit secondary (HRP-conjugated) sc-2313 (Santa Cruz Biotechnology, Inc., CA, USA)
Donkey anti-rabbit secondary (HRP-conjugated)

2.3. *Antibiotic selection*

For experiments with *E. coli* containing ampicillin- or kanamycin-resistant plasmids, transformed cells were plated on nutrient agar (Merck, Darmstadt, Germany) containing 100 µg/ml ampicillin (Sigma Aldrich, Missouri, USA) or 25 µg/ml kanamycin (Sigma Aldrich, Missouri, USA). Selection was maintained during growth in liquid culture by the inclusion of the appropriate antibiotic at the same concentration.

2.4. *Bacterial transformation*

Competent cells were first thawed on ice for 15 minutes. Then 50-500 ng of the plasmid DNA solution was added to 100 µl of the competent cells, gently mixed and incubated on ice for a further 30 min. The cells were then heat shocked by transfer to a 42 °C heating block for 90 seconds whereafter, 500 µl of pre-warmed Luria Bertani (LB) broth (Merck, Darmstadt, Germany) was added and the mixture incubated at 37 °C for an hour to allow for the expression of the antibiotic resistance marker. 50-100 µl of the transformed cell suspension was

then plated onto LB nutrient agar plates containing the appropriate antibiotic which were then incubated overnight at 37 °C.

2.5. Preparation and manipulation of plasmid DNA

2.5.1. Plasmid isolation

A single colony of transformed *E. coli* was inoculated into 5-10 ml of LB containing the appropriate antibiotic. The broth was then incubated at 37 °C with vigorous shaking overnight after which the cells were pelleted by centrifugation at 16000 *g* for 10 minutes in a fixed angle JA-14 rotor in a Beckman bench top centrifuge (Brea, California, USA). Plasmid DNA was isolated using the GeneJet Miniprep kit (ThermoFischer Scientific, Waltham, Massachusetts, USA), according to the manufacturer's instructions. DNA sequencing was carried out at Inqaba Biotechnical Industries (Hatfield, South Africa) and were compared with the expected sequences using the bl2seq tool in the BLAST suite (<http://www.ncbi.nlm.nih.gov/BLAST/bl2seq/wblast2.cgi>).

2.5.2. PCR amplification

Reactions consisted of 50 ng template DNA, 1x High Fidelity PCR buffer (ThermoFischer Scientific, Waltham, Massachusetts, USA), 0.25 mM of each dNTP, 2U Phusion™ HF DNA polymerase (ThermoFischer Scientific, Waltham, Massachusetts, USA) and 10 pmol of forward and reverse gene-specific oligonucleotides, made up to a final volume of 50 µl with deionised water.

The reaction mixture was cycled through the following parameters:

96 °C for 4 minutes (Initial denaturation)

94 °C for 1 minute (Denaturation)	} 30 cycles
60 °C 1 minute (Annealing)	
72 °C for 2 minutes (Extension)	

72 °C for 10 min (Final extension)

PCR reaction products were analysed by electrophoresis in 0.8-1% agarose gels in 1x TAE. The amplified product was purified away from contaminating fragments using the GeneJet Gel Purification kit (ThermoFischer Scientific, Waltham, Massachusetts, USA).



2.5.3. Restriction enzyme digests

Restriction enzyme (ThermoFischer Scientific, Waltham, Massachusetts, USA) digests were performed according to the manufacturer's instructions and using the reagents set out in Table 2.1. Table 2.1 shows an example of the set up performed for each ligation reaction set up in this thesis.

Table 2.1 Example of set-up for restriction enzyme digestion of the pmEGFP vector and DWNN13 PCR product for ligation

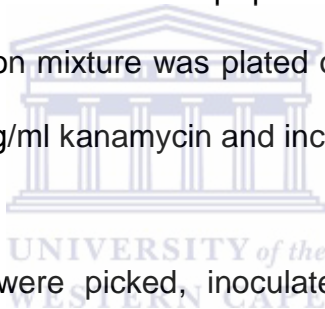
Reagent	Final Concentration	Vector pmEGFP	DWNN13 PCR amplicon
10x buffer	1x	10 µl	10 µl
DNA	1 ug	3.14 µl	10 µl
Restriction enzyme 1	1 U	5 µl	5 µl
Restriction enzyme 2	1 U	5 µl	5 µl
Nuclease free water	-	76.86 µl	70.5 µl
Total	100 µl	100 µl	100 µl

2.5.4. Agarose gel electrophoresis of DNA

DNA fragments were analyzed by electrophoresis on 0.8-1% agarose gels and visualised under UV light using GR Green stain (Inqaba Biotechnological Industries, South Africa). Gels were prepared by adding the required volume of 1x TAE to the appropriate mass of electrophoresis grade agarose. The agarose was boiled and then cooled to 55 °C followed by the addition of GR Green to a final concentration of 0.5 µg/ml after which it was poured onto a gel-casting tray. The appropriate molecular weight marker (Solis biodyne 1 kb marker (Tartu, Estonia) or O'GeneRuler 1 kb marker (ThermoFischer Scientific, Waltham, Massachusetts, USA) was loaded in the first lane to show the sizes of the bands. The DNA was visualized at 300 nM using the UVP BioSpectrum Imaging System (Upland, California).

2.5.5. Cloning of DNA fragments

PCR amplifications were designed to incorporate flanking restriction sites to facilitate directional cloning into plasmids digested with the same enzymes. Generally 20-25 ng of cloning vector was used for the ligation with 4-8 ng of PCR product. Ligations were set up in 20 μ l reaction volumes containing 1x buffer and 1.0 Weiss unit of T4 ligase (ThermoFischer Scientific, Waltham, Massachusetts, USA). The ligation reactions were incubated at room temperature for 1 hour after which T4 ligase was inactivated at 70 °C for 5 minutes. 10 μ l of the ligation mixture was used to transform 50 μ l of *E. coli* MC1061 competent cells after which 900 μ l pre-warmed LB both was added. 25-50 μ l of the transformation mixture was plated on LB agar plates containing 100 μ g/ml ampicillin or 25 μ g/ml kanamycin and incubated overnight at 37 °C.



Several isolated colonies were picked, inoculated into 25 ml of LB broth containing 100 μ g/ml ampicillin or 25 μ g/ml kanamycin and grown overnight at 37 °C. The cells were harvested and plasmid DNA isolated using a Genejet plasmid isolation kit (ThermoFischer Scientific, Waltham, Massachusetts, USA) according to the manufacturer's instruction. Putative transformants were then validated using double restriction digest as described in Section 2.5.3 to release the cloned insert. In certain cases colony-PCR was used to detect the presence of cloned insert, using the same PCR primers used to amplify the insert out of the template.

2.6. Large scale expression of recombinant proteins

E. coli cells transformed with the appropriate expression plasmid were grown overnight at 37 °C on LB nutrient agar plates containing the appropriate antibiotic. In the morning a single *E. coli* colony was picked and inoculated into 25 ml of LB and allowed to grow overnight with the appropriate antibiotic at 37 °C on a rotary shaker.

The culture was scaled up to 1 L with LB containing the appropriate antibiotic and allowed to grow until the OD₆₀₀ was between 0.4-0.6. 30 minutes prior to induction, 100 µM ZnSO₄ was added to the culture to ensure proper folding of zinc-binding proteins. Induction of protein expression was carried out by adding isopropyl β-D-1-thiogalactopyranoside (IPTG) (Inqaba Biotechnical Industries, Hatfield, South Africa) and incubating the culture overnight using the conditions set out in Table 2.2.

Following induction, bacterial cells were harvested and pelleted at 4 °C for 15 minutes at 4000 g. The supernatant was discarded and the cell pellet re-suspended in 30 ml extraction buffer containing protease inhibitor cocktail tablets without EDTA. Cells were lysed immediately or else frozen at -20 °C for later processing.

Table 2.2 Expression conditions for proteins used in this work

Expression construct	Protein expressed	Temperature after induction	IPTG concentration for expression
pGEX-6P2-p53	GST-p53	25 °C	1 mM IPTG
pGEX-4T3-MDM2	GST-MDM2	25 °C	0.5 mM IPTG
pET15b-p53	His-p53 WT	25 °C	1 mM IPTG
pET28a-p53-QM	His-p53 QM	25 °C	1 mM IPTG
pGEX-6P2-R3	GST-R3	25 °C	1 mM IPTG
pET15a-ubiquitin	HA-Ubiquitin	30 °C	0.5 mM IPTG
pGEX-6-P2-UbcH1	GST-UbcH1	25 °C	1 mM IPTG

2.7. Protein extraction and preparation of crude cell lysate

Frozen cell pellets were thawed on ice and cells were lysed by sonication in 20-30 ml protein extraction buffer. Cells were sonicated in 30 second intervals followed by 30 seconds incubation on ice, repeated for a total of 5 minutes. Following sonication, the cells were pelleted at 4300 g for 30 minutes at 4 °C.

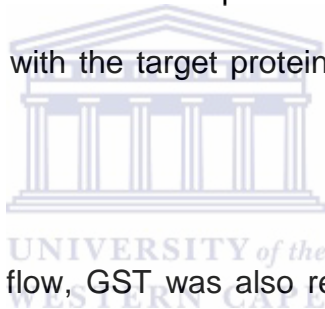
2.8. Protein purification

2.8.1. GST-glutathione affinity chromatography

The column was prepared by addition of 5-15 ml of glutathione agarose slurry (ABT Bead Technologies, Madrid, Spain) into an empty gravity flow columns (Bio-Rad, Hercules, California). The column was washed with 3 column volumes (CV) of 1 M NaCl and then equilibrated with 5 CV of wash buffer. Crude lysate was added to the column and the flow-through collected after which the column was washed with 3 CV of wash buffer. Bound proteins were eluted with elution buffer containing 20 mM reduced glutathione (Sigma Aldrich,

Missouri, USA). Fractions were analysed by SDS-PAGE, as described in Section 2.11.

Fractions containing fusion proteins were pooled and transferred to SnakeSkin[®] Pleated Dialysis Tubing (MWCO 3500Da) (Thermo Scientific, Massachusetts, USA). After addition of 3C protease, produced in-house as a GST fusion protein, the dialysis tube was placed in 2 litres of 1x PBS with 1 mM DTT and cleavage allowed to proceed overnight at 4 °C. In the morning the contents of the dialysis bag was returned to the glutathione agarose column in order to remove the cleaved GST, uncleaved fusion protein and GST-3C protease which was retained by the beads, with the target protein being collected in the flow-through.



As an alternative to gravity flow, GST was also removed using three GSTrap columns (GE Healthcare, Little Chalfont, UK) connected in series, operated under control of a ÄKTA FPLC Purification System (GE Healthcare, Little Chalfont, UK).

2.8.2. Nickel ion affinity chromatography

Empty gravity flow columns were packed with Ni-NTA affinity beads (Sigma-Aldrich, Missouri, USA) according to the manufacturer's instructions. The column was washed with 3 column volumes (CV) of 1 M NaCl and then equilibrated with 5 CV of wash buffer. The crude lysate was then added to the column and the flow through collected. The column was washed with 3 CV of

wash buffer, before the bound proteins were eluted with the appropriate buffer. 300-400 mM imidazole was used to elute the His₆-tagged proteins. Fractions were analysed by SDS-PAGE, as described in Section 2.11.

2.8.3. Cation exchange chromatography

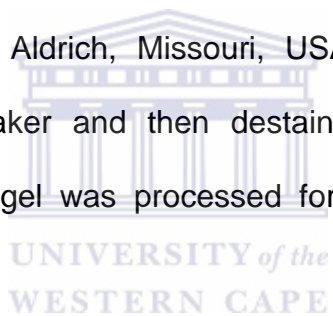
Wild type ubiquitin, which was expressed without an affinity tag, was purified using a method which takes advantage of its high stability at low pH, returning to neutral pH using cation exchange chromatography. Glacial acetic acid (Merck, Darmstadt, Germany) was added to clarified lysate until it turned cloudy (approximately pH 4.5) indicating denaturation of most of the accompanying proteins. Denatured proteins were pelleted by centrifugation and the supernatant transferred to SnakeSkin[®] Pleated Dialysis Tubing. The solution was dialysed against 2 litres of 20 mM sodium acetate, pH 4.5, overnight and subsequently transferred to a 3 ml self-packed POROS S20 cation exchange column, following pre-equilibration of the column with sodium acetate, pH 4.5. The flow through was collected and the column washed with 2 column volumes of sodium acetate, pH 4.5. Bound proteins were eluted from the column using PBS (pH7.4) containing increasing concentrations of NaCl.

2.9. SDS-PAGE analysis of proteins

Protein samples were separated on SDS-polyacrylamide gels (SDS-PAGE) according to Laemmli's method (Laemmli, 1970). 16% separating gels were prepared using 4 ml 40% acrylamide: bis-acrylamide stock (Merck, Darmstadt, Germany), 2.63 ml separating buffer, 40 µl 10% ammonium persulphate (Merck,

Darmstadt, Germany), 105 µl 10% SDS, 7.5 µl TEMED (Sigma Aldrich, Missouri, USA) and 3.2 ml distilled water. The stacking gel was prepared from 0.75 ml 40% 37:5:1 polyacrylamide, 25 µl 10% APS, 50 µl 10% SDS, 1.25 ml stacking buffer, 5 µl TEMED and 3.05 ml distilled water.

Protein samples were prepared by adding an equal volume of 2x SDS sample buffer to the samples, followed by boiling (placing in a dry heating block at 95 °C) for 5 minutes. 12-20 µl of each sample was loaded on the SDS-PAGE gel and the samples were separated by electrophoresis using the Bio-Rad Mini-Protean system operated at 150 V. Proteins were visualised by incubating the gel in Coomassie (Sigma Aldrich, Missouri, USA) staining solution for 30 minutes on an orbital shaker and then destained overnight in destaining solution. Alternatively, the gel was processed for Western blot analysis, as described below.



2.10. Western blotting of proteins

Proteins separated on SDS-PAGE were incubated for 5 minutes in 1x ProSieve Ex transfer buffer (Lonza, Basel, Switzerland). Pall Biotrace PVDF membrane (New York City, USA) was activated in 50 ml Absolute Ethanol (Merck, Darmstadt, Germany) and proteins were then transferred to it by semi-dry transfer using the Bio-Rad Transblot[®] Turbo[™] transfer system (Bio-Rad, Hercules, California) for 10-12 minutes. Following transfer, the membrane was blocked with 1% casein in PBS-T (1x PBS containing 0.1% Tween 20) and then incubated with the appropriate antibodies for 1-2 hours. The membrane was washed three times for 5 minutes each with PBS-T and then incubated with the

appropriate HRP-conjugated secondary antibody. The membrane was again washed three times for 5 each minutes with PBS-T and then incubated in 5 ml Clarity Western ECL Substrate (Bio-Rad) and viewed using a UVP BioSpectrum Imaging System (UVP, Upland, California).

2.11. Purification of proteasome out of human cell lysate

MCP21 hybridoma cells expressing antibodies targeting the α_2 -subunit of the human proteasome were purchased from Sigma-Aldrich (Missouri, USA) and serum was produced from them by Ms Ania Szmyd-Potapczuk, a co-worker in the laboratory. The antibody was coupled to Affi-Gel[®] beads (Bio-Rad, Hercules, California) as follows: 500 μ l of Affi-Gel[®] beads were washed with an equal volume of cold distilled water, centrifuged at 4300 g and the supernatant discarded. The beads were then incubated with 2.5 ml of HEPES (pH 7.5) for 1 hour at 4 °C with rolling after which 100 μ g of anti-proteasome antibody was added and allowed to incubate at 4 °C overnight. In the morning the beads were centrifuged at 4 °C at 4300 g at 4 °C and the supernatant discarded. The beads were quenched with 1 M Tris pH 8.0 (to prevent the binding of any additional proteins to the beads) and allowed to incubate for a further 30 minutes at 4 °C before being washed with 3 CV of 10 mM citric acid pH 8.0 and 3 CV of 1x PBS. The beads were then stored in 2 ml 1x PBS containing 0.02% NaN₃.

Lysates from cultured human A549, HepG2 or HeLa cells were kindly provided by Ms Andronica Ramaila, a co-worker in the laboratory. 2.5 mM Mg-ATP was mixed with 100 μ g cell lysate which was then incubated with 100 μ l Affi-Gel[®]

beads coupled to the anti- α_2 antibody as described above, overnight at 4 °C with rolling. The following day the beads were pelleted for 5 minutes at 5000 g at 4 °C and then washed three times with binding buffer as above before being resuspended in 200 μ l binding buffer with 5 mM Mg-ATP and stored at 4 °C.

2.12. Ubiquitination assays

Lysate-based ubiquitination assays were set up by adding HepG2 or HeLa cell lysates to purified recombinant proteins. Fully *in vitro* assays were set up by omitting the cell lysates. Reaction mixtures were made up as set out in Table 2.3 or as otherwise stated (following a modified protocol established by Honda *et al.*, 1997). Briefly, reactions were performed using buffer containing 1x PBS, 5 mM Mg-ATP, 10% glycerol, 0.5 mM ZnSO₄ unless otherwise stated. Reaction mixtures were briefly vortexed, centrifuged and then incubated overnight at 37 °C with shaking. Reactions were stopped by acetone precipitation, as follows: 400-800 μ l acetone was added to each tube and incubated at -20 °C for 30 minutes following which the precipitate was pelleted at 5000 g at 4 °C for 10 minutes. The pellets were dried at 37 °C and 2x SDS-PAGE sample buffer added. The proteins were separated on SDS-PAGE and visualised by Western blotting using the appropriate antibodies.

2.13. Immunoprecipitation of proteins

1 μ g anti-p53 antibody (sc-6243, Santa Cruz Biotechnologies, Inc., CA, USA) was added to each reaction tube and allowed to incubate at 4 °C with rolling for 15 minutes. During this time, 100 μ l of Protein A/G PLUS agarose beads (sc-

2003, Santa Cruz Biotechnology, Inc., CA, USA) was washed three times at 13 000 rpm with 500 μ l IP buffer. Beads were resuspended in 150 μ l IP buffer and 20 μ l beads added per assay tube and allowed to incubate for 1 hour at 4 °C with rolling. The beads were then washed three times with IP buffer as before.

2.14. *In vitro* two-step E4 ubiquitination assay

The assay was carried out following the protocol of Wu and co-workers (Wu *et al.*, 2011). It requires an E3 (MDM2 in this case) to mono-ubiquitinate the substrate (p53 in this case), and a putative E4 (R3 in this case) to poly-ubiquitinate the mono-ubiquitinated substrate.

The assay was performed by setting up an initial ubiquitination reaction (Step 1) using MDM2 as E3 and p53 as the substrate. Exact quantities for each reaction in Step 1 are set out in Table 2.4. After 1 hour p53 was immunoprecipitated using the protocol described in Section 2.14, incubating the reaction with anti-p53 antibodies for 1 hour at 4 °C. Step 2 was a ubiquitination reaction using R3 as E3/E4 and the Protein A/G beads containing the 'monoubiquitinated p53' as substrate. Exact quantities for each reaction in Step 2 are set out in Table 2.5. The ubiquitination reaction was incubated at 37 °C overnight. Note that while reaction 5 corresponds to the assay as described (MDM2 in Step 1 and R3 in Step 2), reaction 6 corresponds to the reverse order (R3 in Step 1 and MDM2 in Step 2). Following completion of the reaction, the

beads were washed with 1x PBS, SDS sample buffer was added and the results visualised by Western blot analysis as before.

Table 2.3 Reagents used in the *in vitro* ubiquitination assay

Reagent	Experimental reaction	Control reaction(s)
Cell lysate	50-100 µg	50-100 µg
E1	0.35 µM	0.35 µM
E2 (UbcH5a)	2 µM	2 µM
E3 (MDM2 & R3 &/or R2)	1- 10 µM	-
Substrate (p53)	1-5 µM	1-5 µM
MG132 (proteasome inhibitor)	1 mM	1 mM
HA-Ubiquitin	1 mM	1 mM
Buffer	50-70 µl	50-70 µl
1x PBS	Made up to 150-200 µl	Made up to 150-200 µl

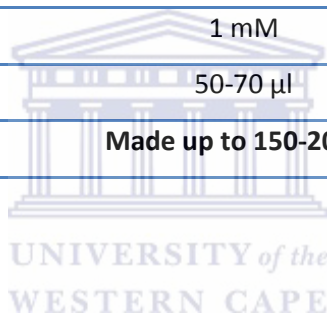


Table 2.4 Setup for 2-step ubiquitination assay: Step 1

Components	1	2	3	4	5	6
p53	+	+	+	+	+	+
MDM2	-	-	-	+	+	-
R3	-	-	-	-	-	+
E1, E2, Ubiquitin, ATP, 1x PBS buffer	-	+	+	+	+	+
PBS	+	+	+	+	+	+
Reaction volume	100 µl	100 µl	100 µl	100 µl	100 µl	100 µl

Table 2.5 Setup for 2-step ubiquitination assay: Step 2

Components	1	2	3	4	5	6
Protein A/G beads (p53~Ub)	+	+	+	+	+	+
MDM2	-	-	-	-	-	+
R3	-	-	+	-	+	-
E1, E2, Ubiquitin, ATP, 1x PBS buffer	-	+	+	+	+	+
PBS	+	+	+	+	+	+
Reaction volume	100 μl	100 μl	100 μl	100 μl	100 μl	100 μl



CHAPTER 3

Cloning, expression and purification of proteins for *in vitro* ubiquitination assays

3.1. Introduction

In order to establish if RBBP6 is capable of ubiquitinating p53 alone or if it only enhances MDM2-mediated p53 ubiquitination, *in vitro* ubiquitination assays were carried out using proteins produced recombinantly in bacteria. This chapter documents the expression and purification of these proteins, as well as generation of a number of expression constructs by molecular cloning.

Assays were designed to detect ubiquitination of p53 directly as higher molecular weight bands on SDS-PAGE gels, visualised by Western blotting with anti-p53 antibodies. An alternative approach, directly detecting ubiquitin using anti-ubiquitin antibodies, although potentially more sensitive, was not used since molecules other than the substrate, including the E3s, are known to be poly-ubiquitinated and could therefore lead to false results.

p53 is a notoriously unstable protein that is highly sensitive to proteolysis when expressed in bacteria. Three different constructs were used for expression of full-length p53 in an attempt to overcome this problem: GST-tagged wild type p53 expressed from a pGEX-6P-2 vector, N-terminally His₆-tagged wild type p53 expressed from a pET15b vector and the M133L/V203A/N239Y/N268D

quadruple mutant reported by Fersht and co-workers (Nicklova *et al.*, 1998). The latter construct was codon-optimised for expression in bacteria and expressed from a pET28a vector with an N-terminal His₆ tag.

MDM2, a well-established E3 ligase and the putative E3 ligase RBBP6 were investigated in the study. Since full length RBBP6 is over 200 kDa in size and unlikely to express stably in bacteria, a shortened fragment containing the first 3 domains — the DWNN domain, the zinc knuckle domain and the RING finger domain — and named R3, was expressed and used in this study. An even shorter fragment containing only the second and third domains — the zinc knuckle and RING finger domain — and named R2, was also used.

Bacterial expression of other proteins documented in this chapter include the E2 enzymes Ubch1 and Ubch13 as well as ubiquitin and the ubiquitin-K0 mutant, in which all lysines have been replaced by arginines. Expressed samples of a number of other proteins were kindly donated by co-workers in the laboratory; these include the E1 enzyme, the ubiquitin-K48R mutant, His₆-MDMX and the E2 Ubch5a from Dr Andrew Faro, E2s Ubch5b and Ubch5c from Dr Mautin Kappo, E2s Mms2 and Ubch7, as well as the MultiDSK protein, from Ms Tephney Hutchinson and R2 from Ms A'tieyah Salie.

An important issue raised in the literature concerned whether attached GST can artificially enhance the ubiquitination activity of MDM2 against p53 by artificially enhancing homo-dimerisation (Wang *et al.*, 2011). Samples of R3 and MDM2

were therefore produced with and without attached GST in order to test whether there was any significant enhancement in their ubiquitination potential.

The first section of this chapter describes subcloning of isoform 3 of RBBP6 into the mammalian expression construct pmEGFP. This sub-project was conducted on behalf of a co-worker in the laboratory and does not form part of the *in vitro* ubiquitination studies. It nevertheless represents an important reagent for the broader understanding of the localisation of RBBP6 within mammalian cells and it is therefore appropriate that its construction is documented in this thesis.

3.2. Generation of pmEGFP-DWNN13 construct for immunofluorescence microscopy

RBBP6 is known to be independently expressed *in vivo* in at least two isoforms: the 200 kDa full length protein, also known as isoform 1, and a 13 kDa isoform known as isoform 3 which consists almost entirely of the ubiquitin-like DWNN domain found at the N-terminus of isoform 1. Due to its molecular weight we will also refer to isoform 3 as DWNN13. Sequencing of a previous pEGFP-DWNN13 construct revealed that the DWNN domain had been inserted in the negative orientation, rendering it useless; we therefore set out to amplify it from the incorrect construct and clone it into pmEGFP-C1 in the correct orientation. pmEGFP-C1, which was a gift from Dr. Benjamin Glick (Addgene plasmid No. 36412), encodes a monomeric form of Enhanced Green Fluorescent Protein (EGFP), obtained by introduction of the monomerising A206K mutation into the EGFP gene. The map of pmEGFP-C1 is shown in Figure 3.1 with the Multiple

Cloning Cassette (MCC) indicated by a yellow box. Target proteins are fused to the C-terminus of mEGFP.

Oligonucleotide primers were designed incorporating XhoI and KpnI restriction sites in the forward and reverse primers, respectively, as shown in Figure 3.2. 5'-TAA and 5'-TGA stop codons were introduced into the reverse primer immediately preceding the KpnI site. Since the XhoI site is not “in frame with the promoter”—the frame is C|TCG|AG, rather than |CTC|GAG|—two additional nucleotides (CT) were incorporated into the forward primer between the XhoI site and the first codon (TCC) of DWNN13. The initial methionine was omitted from DWNN13, yielding an amino acid sequence beginning with SCVHYK...

DWNN13 was successfully amplified, as shown in Figure 3.2(b), and cloned between the XhoI and KpnI sites of pmEGFP-C1. Nine putative positive colonies were screened by colony-PCR using the primers shown in Figure 3.2(a) and all found to be positive, as shown in Figure 3.2(c). Colonies 8 and 9 were investigated further by double digestion with XhoI and KpnI, releasing inserts of the expected sizes (Figure 3.2 (d)). The sequence was verified by direct sequencing (Inqaba Biotechnical Industries, Hatfield, South Africa) and found to be 100% in agreement with the expected sequence (see Appendix).

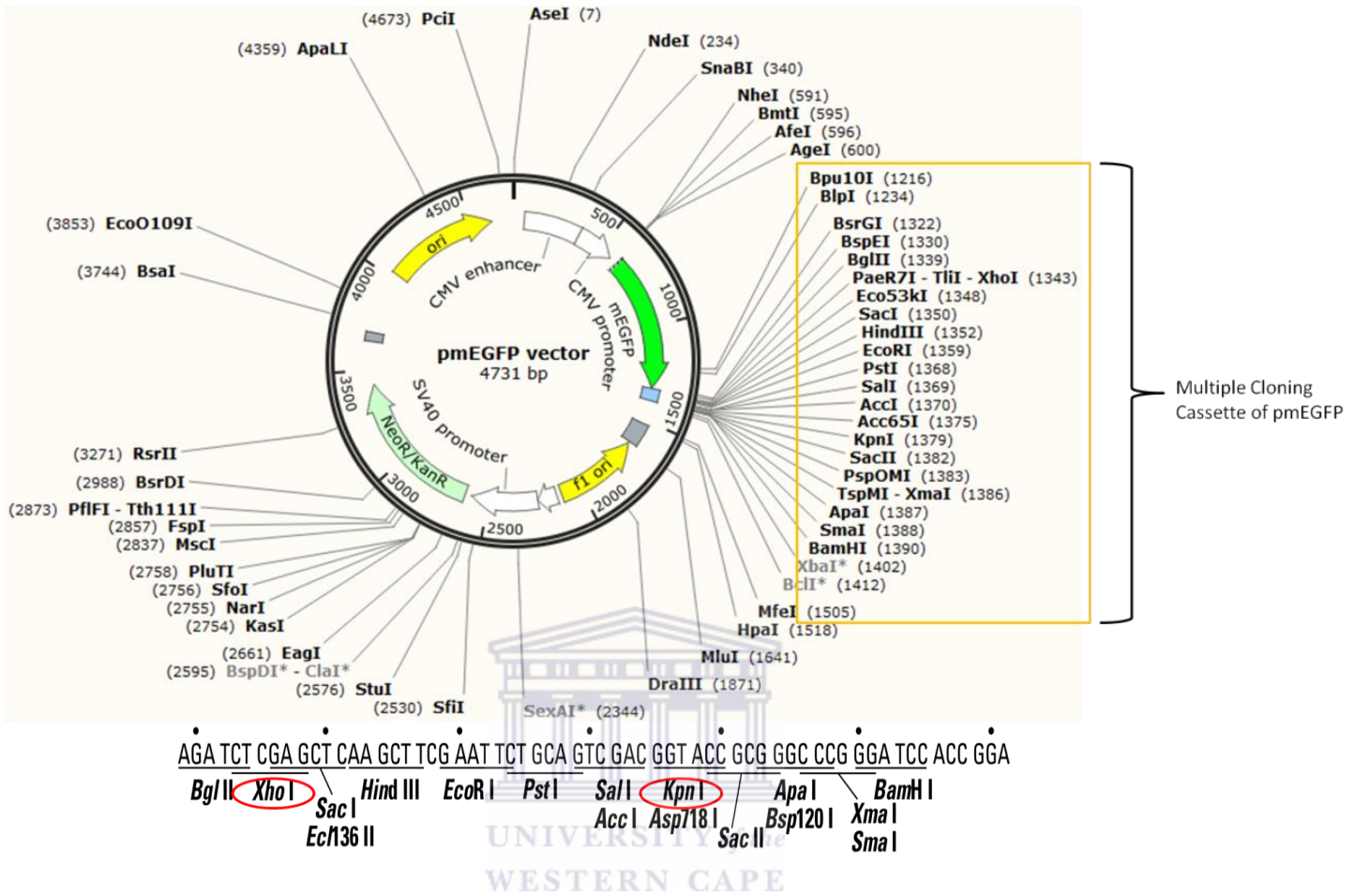


Figure 3.1. Plasmid map of pmEGFP-C1 with the restriction enzymes used for cloning circled in red. Target proteins are fused to the C-terminus of mEGFP. XhoI is not in frame with the promoter, with the result that additional bases must be inserted between the XhoI site and the beginning of the target sequence in order to re-establish the frame.

(a) Primers used to subclone DWNN13 from pEGFP-C1 into pmEGFP-C1, reversing the orientation

Forward primer: 5' - GAGGCG CT CGA GCT TCC TGT GTG CAT TAT AAA TTT T -3'
 Reverse primer: 5' - GAGGCG GGTACC TCA TTA TAA AGG TAA AAG CAA TGT G -3'

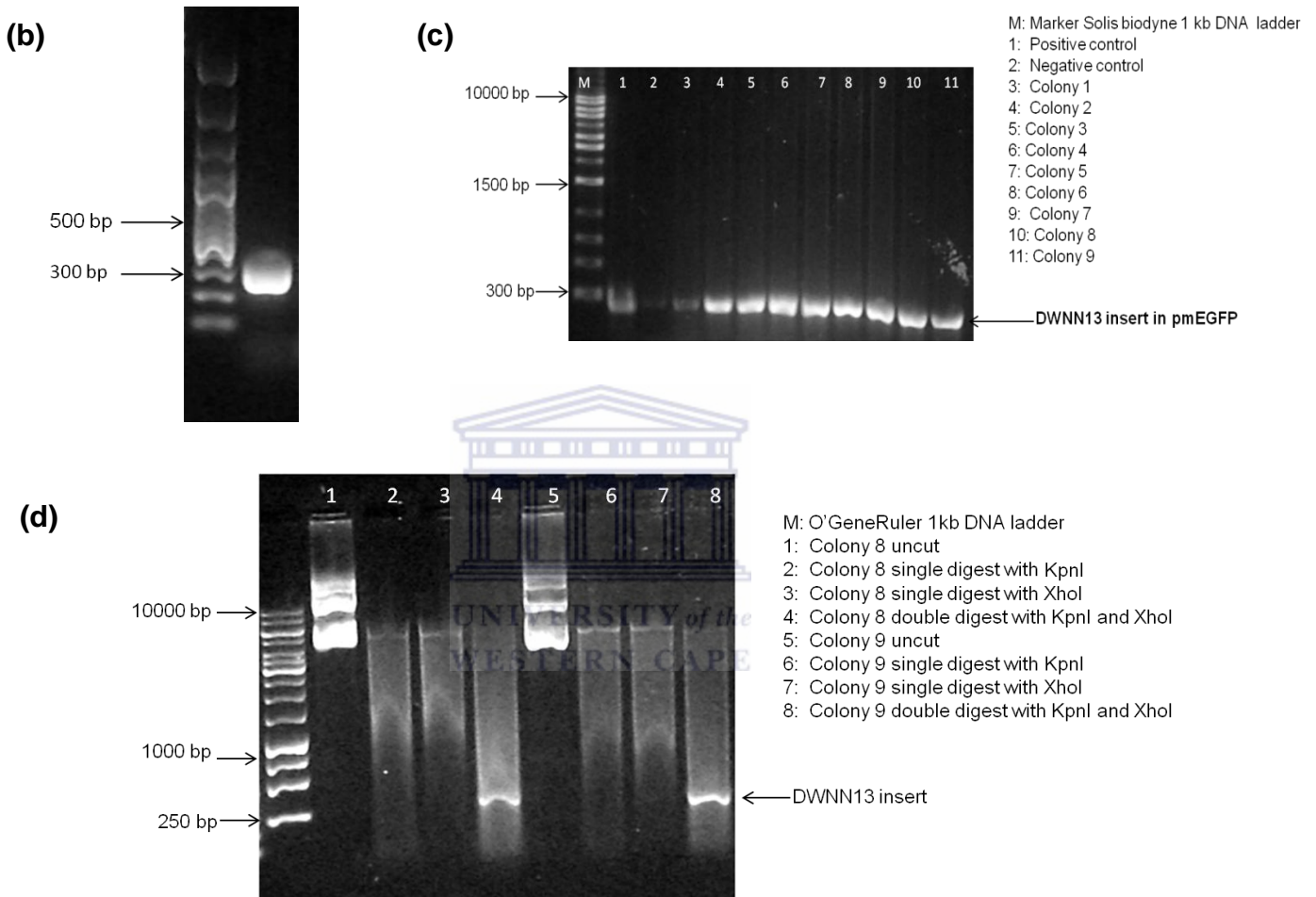


Figure 3.2 Cloning of DWNN13 into pmEGFP-C1 (a) Primer sequences used for amplification of DWNN13 into pmEGFP-C1. The XhoI and KpnI restriction sites are indicated by the blue and orange boxes respectively. The dinucleotide CT, indicated in yellow, was introduced to restore the frame of DWNN13 after the XhoI site. Two stop codons are indicated by red boxes. (b) Successful amplification of a 290 bp fragment corresponding to DWNN13 (right lane). (c) Colony-PCR screening of selected colonies using the specific primers shows that all of them contain an insert of the expected size. The positive control used was the original DWNN13 in pEGFP construct (d) Double digestion of two selected colonies with XhoI and KpnI releases a fragment of the expected size of 290 bp (as indicated).

3.3. Generation of an expression construct for the E2 UbchH1

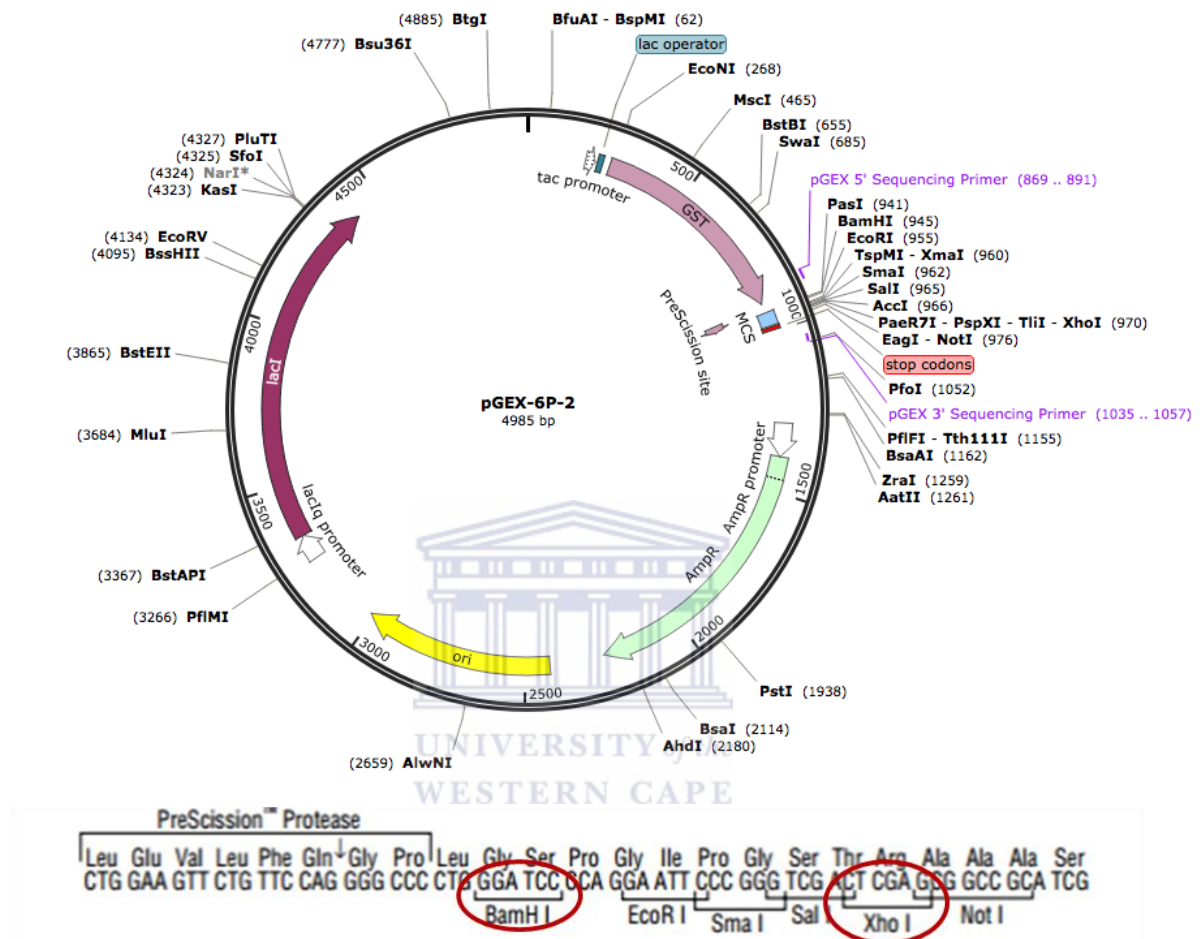


Figure 3.3 Plasmid map of pGEX-6P-2 expression vector with restriction enzymes used for cloning circled in red.

UbchH1, also known as HIP2 or UBE2K, has been reported to act as a ubiquitin conjugating enzyme (E2) for p53, in conjugation with MDM2. A construct coding for UbchH1, cloned into the pACT2 vector, was a kind gift from Prof Rachel Klevit of the University of Washington, Seattle (Addgene plasmid No: 31436). Forward and reverse primers incorporating BamHI and XhoI sites respectively were designed as shown in Figure 3.4(a) and used to amplify UbchH1 for ligation into

the same sites of the bacterial expression vector pGEX-6P-2. A map of pGEX-6P2 can be seen in Figure 3.3. In this case the BamHI site is “in frame” with the promoter, negating the need for additional bases between the BamHI site and the start of UbchI. Two stop codons (TAA TAA) were inserted immediately before the XhoI site.

PCR amplification using the pACT2-UbchI1 template yielded a band of approximately 400-500 bp, which corresponds to the expected size of full-length UbchI1, as can be seen in lane 1 of Figure 3.4(b). No amplification is seen in lane 2, to which no template DNA was added. The PCR product was purified and digested with BamHI and XhoI restriction enzymes and ligated into pGEX-6P-2, following digestion with the same restriction enzymes. Six putative positive colonies were screened using colony-PCR using the same primers in order to confirm the presence of the expected insert (Fig 3.4(c)); all six amplified a band of the same size as the original PCR product (lane 1), confirming that they were positive transformants. The positive control was a PCR reaction using the original template. No negative control was included in this screen. The sequence was verified by direct sequencing (Inqaba Biotechnical Industries, Hatfield, South Africa) and found to be in 100% agreement with the expected sequence.

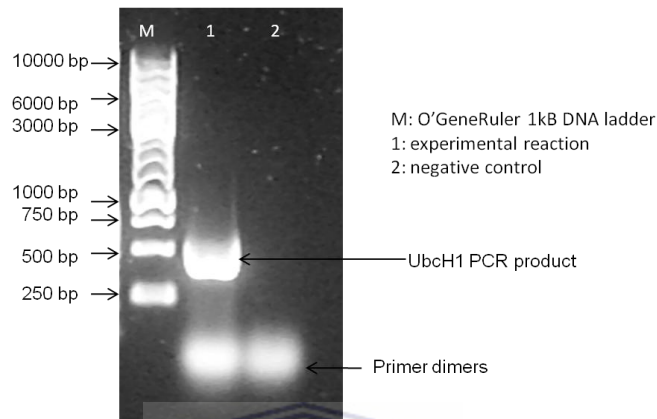
Primer set to subclone pACT2-UbcH1 into pGEX-6P-2

(a)

Forward primer: 5'- GAG GCG GGA TCC ATG GCC AAC ATC GCG GTG C -3'

Reverse primer: 5'- GAG GCG CTC GAG TTA TTA GTT ACT CAG AAG CAA TTC TGT T -3'

(b)



(c)

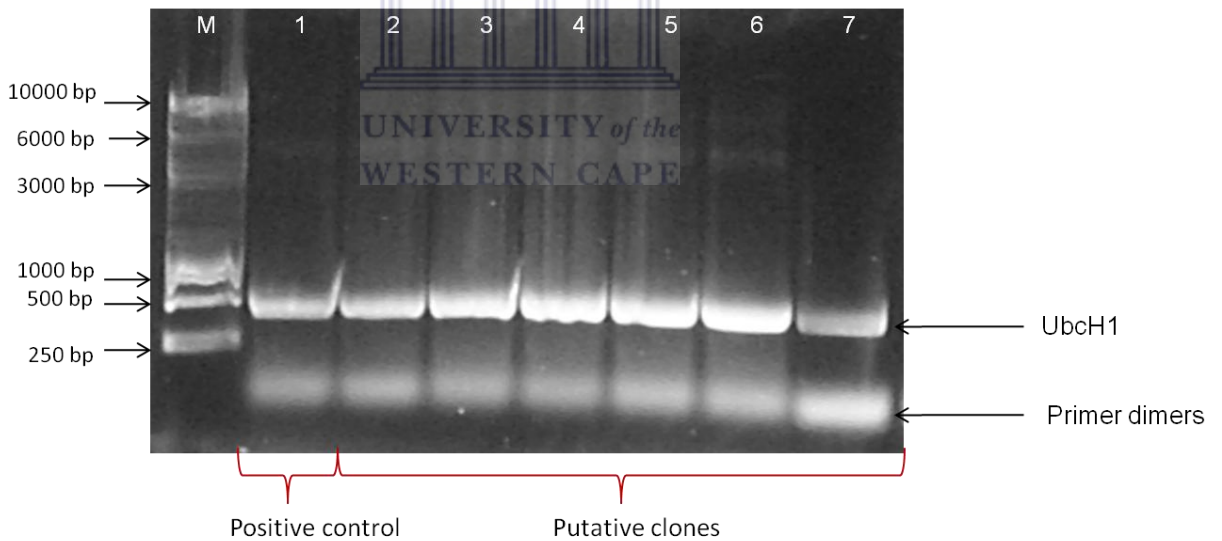


Figure 3.4 Amplification and PCR-colony screening of UbcH1. (a) Primers used to amplify UbcH1 from pACT2-UbcH1. The BamHI and XhoI restriction sites are indicated in the pink box and green boxes respectively. The start of UbcH1 is indicated in the blue box. Two TTA stop codons are indicated by the red box. (b) PCR amplification of UbcH1. A PCR product of about 500 bp, which corresponds to the expected size of the UbcH1 coding sequence, can be seen in lane 1. Lane 2 is the negative control which contains no template DNA. Lane M contains the O'GeneRuler 1kb DNA ladder mix (Thermo Scientific, Massachusetts, USA). (c) PCR-colony screening of putative transformants for the presence of the UbcH1 insert. Lanes 2-7 are all positive for the UbcH1 insert. Lane 1 is the positive control which included the original construct pACT2-UbcH1 as template.

3.4. Generation of expression construct for stabilised p53 quadruple mutant

A DNA sequence coding for the M133L/V203A/N239Y/N268D mutant of p53, codon-optimised for expression in bacteria and flanked by NdeI and BamHI restriction sites, was synthesized by Genscript Inc. (Piscataway, NJ, USA.) and supplied in a pUC57 vector. The plasmid was transformed into *E. coli* and digested with NdeI and BamHI, which released an insert of the expected size, as shown in lane 4 of Figure 3.5(b) (denoted p53-QM, for “p53 quadruple mutant”). The insert was then cloned into pET28a; as can be seen from panel (a), the NdeI restriction sites was chosen so that the protein would be expressed with an N-terminal His₆ tag. A 5'-TGA stop codon was included immediately before the BamHI site to ensure that the C-terminal His₆ tag in the vector would not form part of the expressed protein.

Fifteen putative positive colonies were picked and screened by double digestion with NdeI and BamHI for the presence of the p53-QM insert, as shown in panel (c). An insert of the expected size (1192 bp) was visible in 8 of the 15 colonies, of which 2 were subjected to direct sequencing and found to be in 100% agreement with the expected sequence (see Appendix).

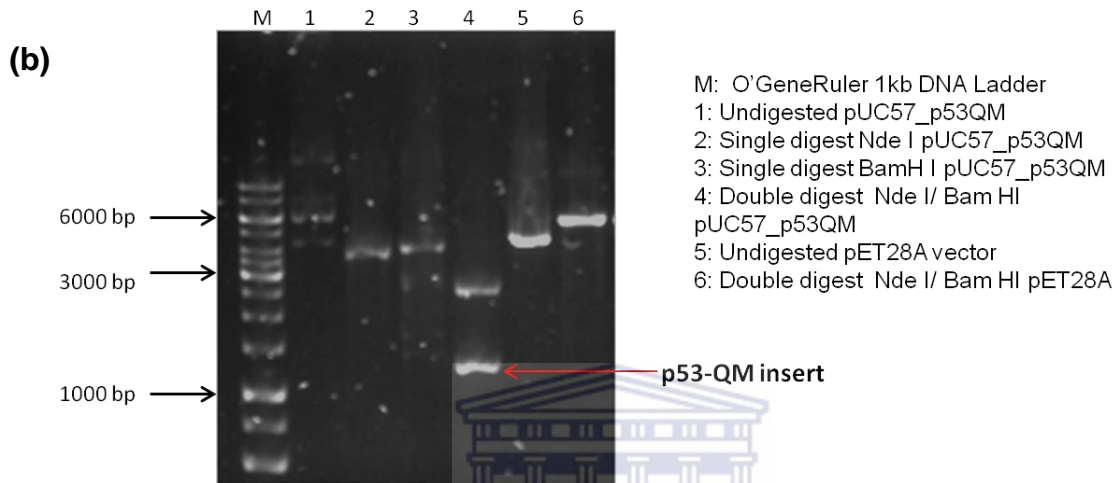
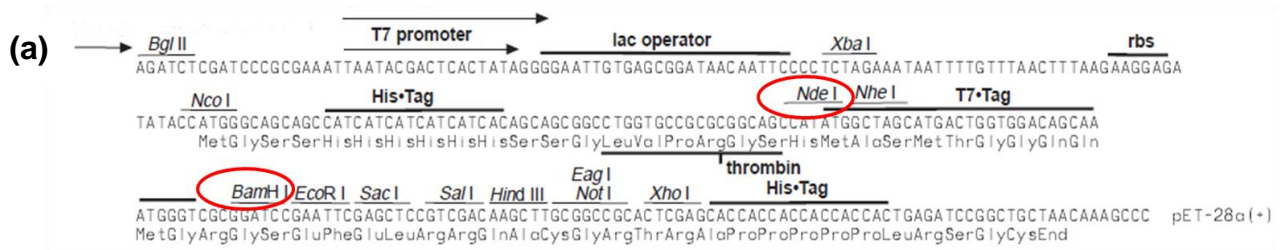


Figure 3.5 Subcloning of the quadruple mutant p53 (p53-QM) from a pUC57 vector into the expression vector pET28a. (a) The pET28a vector sequence and multiple cloning cassette. Indicated in red are the NdeI and BamHI restriction sites respectively. (b) Agarose gel showing preparation of the vector and insert. The undigested pUC57-p53-QM vector can be seen in lane 1. Single digestion of the pUC57-p53-QM vector with NdeI and with BamHI can be seen in lanes 2 and 3 respectively; double digestion with both NdeI and BamHI released the expected p53-QM insert (lane 4). Lanes 5 and 6 contain the pET28A vector, undigested and digested with both NdeI and BamHI respectively. (c) Screening DNA preparations from colonies 1-15 using double digestion with NdeI and BamHI (even lanes) and undigested (odd lanes). The released p53-QM insert is clearly visible in lanes 2, 4, 6, 12, 16, 22, 24 and 26. Colonies 8 (lanes 15 and 16) and 13 (lanes 25 and 26) were selected for sequencing.

3.5. Expression and purification of three different p53 constructs: GST-p53 (wild type), His₆-p53 (wild type) and His₆-p53-QM (quadruple mutant)

Human p53 was used as the substrate in all *in vitro* ubiquitination assays. Three different expression constructs were tested in an effort to maximise expression and minimise degradation.

GST-p53 (wild type)

A pGEX-6P-2 expression vector containing wild type human p53 was a gift from Dr Andrew Faro in our research group. The protein was expressed as a fusion with glutathione-S-transferase (GST) and purified using a glutathione-conjugated agarose column as described in Section 2.9. The protein was expressed at low levels (Figure 3.6), so Western blotting using a rabbit polyclonal anti-p53 antibody (sc-6243 Santa Cruz Biotechnology, Inc., Santa Cruz, CA, USA) was used to confirm the presence of the GST-fusion protein. The GST was successfully removed using GST-3C protease (lane 2) and the sample returned to the glutathione column following dialysis to remove free glutathione. Cleaved p53 was collected in the flow-through (lanes 3-5) and appears at the expected size of slightly more than 50 kDa. GST was retained by the column and eluted in lanes 6-8, although it is not visible in the p53-detected Western blot. The amount of residual GST along with p53 in lanes 3-5 is also not apparent from the blot since only p53 is detected.

Appreciable levels of low molecular weight degradation products were detected in all lanes; note that while full length p53 was not retained by the column, as expected, the degradation products leach continuously from the column, as would be expected for unfolded protein fragments. Full length p53 forms a single tight band at its expected molecular weight, which suggests that it is folded and intact; unfortunately it was found to degrade rapidly following removal of the GST tag, making it difficult to use in the subsequent *in vitro* assays.

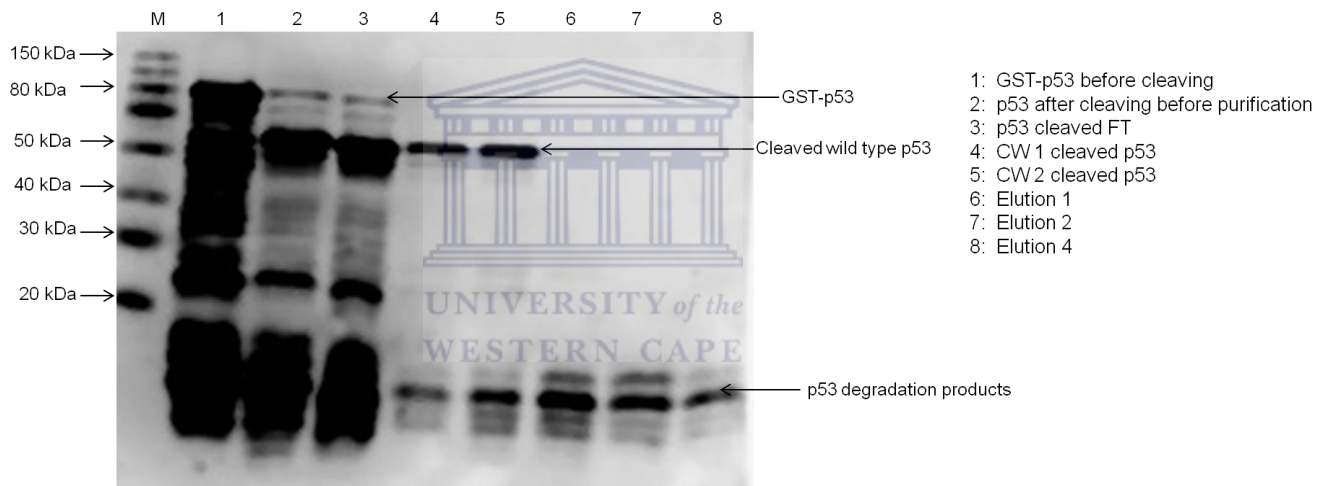


Figure 3.6 Western blot showing cleavage and purification of GST-p53. Western blotting was used due to low levels of expression. The primary antibody used was polyclonal anti-p53 antibody raised against full length p53 (dilution 1:1000). Lane 1 contains GST-p53 following affinity purification out of bacterial lysate using glutathione agarose, prior to cleavage with 3C protease. Lane 2 is the same sample following cleavage using 3C protease—the band corresponding to the fusion protein is almost completely depleted, leaving a band at around 50 kDa corresponding to p53 and a number of smaller fragments which are detected due to the fact that the antibody was raised against full length p53. All of the full length p53 is found in the flow through (lane 3 or the washes—lanes 4 and 5, but not in the elution (lanes 6-7)). However, since this is a p53-detected Western blot it does not reveal how much GST remains in lanes 2-5 along with the full length p53.

His₆-p53 (wild type)

A pET15b plasmid coding for wild type p53 with an N-terminal His₆ tag was a gift from Prof Cheryl Arrowsmith, University of Toronto, Canada (Addgene plasmid number: 24859). The protein was expressed and purified using immobilised nickel ion affinity chromatography, as described in Sections 2.10. Expression levels of His₆-p53 were still not high as shown using SDS-PAGE (lane 7, Figure 3.7), but were generally better than those of GST-p53 (a Western blot was not necessary to show the expressed levels as it was visible directly on an SDS-PAGE gel). Nevertheless, they were deemed sufficient for ubiquitination assays as the end-point analysis by Western blotting can detect as little as femtograms of protein. His₆-p53 wild type appears to be running slightly low on the SDS-PAGE in Figure 3.7, possibly due to the marker on the gel running slightly askew. However, the Western blot of this sample shown in Figure 4.2 confirms that it does migrate at the expected size.

His₆-p53-QM

Construction of a pET28a plasmid coding for the p53 quadruple mutant (p53-QM) is described in Section 3.4. p53-QM was expressed and purified using immobilised nickel ion affinity chromatography, as shown in Figure 3.8. In our hands this protein was found to express in low levels, as is apparent in lanes 7-9, and to be highly susceptible to degradation, even immediately after purification. Nevertheless this construct has subsequently been used extensively by a co-worker in the laboratory to reproduce many of the results presented in this thesis (Dr Andrew Faro, manuscript in preparation),

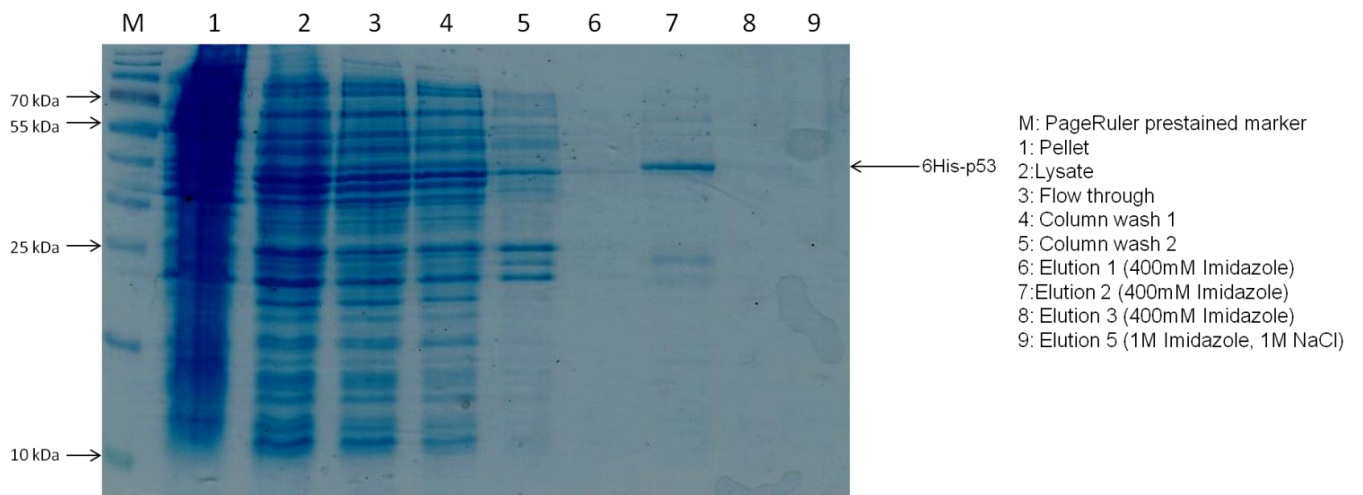


Figure 3.7 SDS-PAGE gel showing expression and purification of wild-type His₆-p53 using nickel ion affinity chromatography. Lane 1 contains the insoluble fraction and lane 2 the soluble fraction prior to purification. Lane 3 contains the flow through and lanes 4 and 5 the column washes with 20 mM imidazole to suppress non-specific binding to the column. Lanes 6-8 contain elutions with 400 mM imidazole. Lane 9 is the cleaning step with 1M imidazole and 1M NaCl. The band eluting at approximately 50 kDa in lane 7 corresponds to p53. This band appears to migrate a little faster than expected, but the Western blot in Figure 4.2 confirms that it is indeed p53.

and generation of the construct has therefore contributed significantly to understanding of the process of ubiquitination of p53 by RBBP6.

In summary, all three methods of expressing p53 were found to be susceptible to extensive degradation, both pre- and post-lysis. Overall, the most stable form was found to be His₆-p53

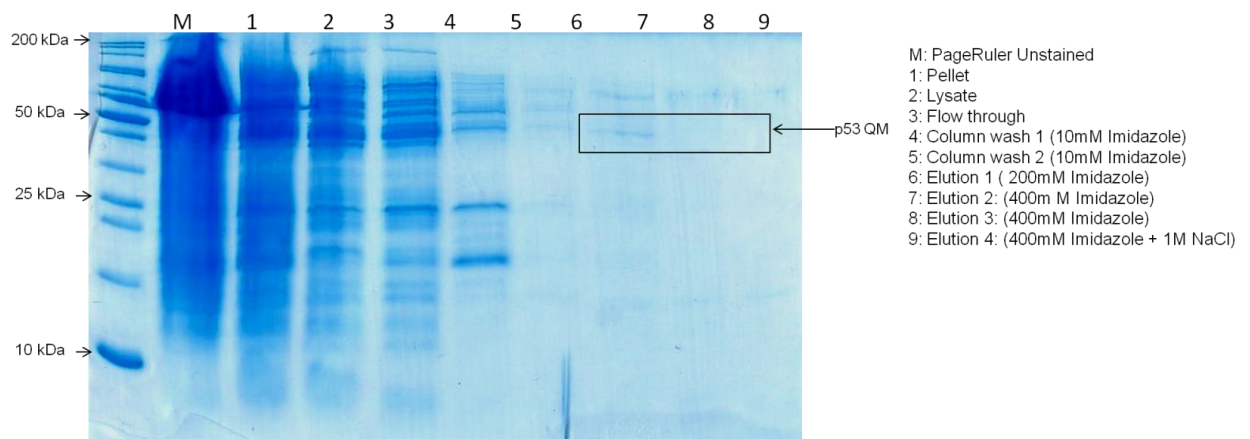


Figure 3.8 SDS-PAGE gel showing small-scale expression and purification of the quadruple mutant p53-QM. Low levels of p53-QM can be seen in the elution fraction in lane 7. Lane 1 contains the insoluble fraction and lane 2 the soluble fraction. Washes with 10 mM imidazole to remove any non-specific adhering of proteins are shown in lanes 4 and 5 respectively. Elution with 200mM imidazole is shown lane 6 and with 400mM imidazole is shown in lanes 7-9. Elution 4 also has additional 1M NaCl to clean any residual proteins off the column.

3.6. Expression and purification of ubiquitin-ligating enzymes MDM2 and R3

A pGEX-4T3 expression vector coding for GST-MDM2 was a gift from Mien-Chie Hung, University of Texas, Houston, USA (Addgene plasmid number 16237). A pGEX-6P-2 vector coding for the R3 fragment of RBBP6 (residues 1 – 335) was previously cloned by a co-worker in our laboratory. This fragment contains the RING finger domain known to be essential for enhancing the ubiquitination activity of RBBP6 against p53 (Li *et al*, 2007), and was shown to be suitable for soluble expression in bacteria (Dr Andrew Faro, PhD thesis, University of the Western Cape 2011).

GST-fusion proteins were expressed and purified using glutathione agarose affinity chromatography as described in Section 2.9. Elution of GST-MDM2 can be seen in Figure 3.9, lanes 6-8, migrating at the expected size of

approximately 90 kDa. MDM2 is known to migrate at a higher effective size than would be expected from its true molecular weight of 54 kDa (Cheng & Cohen, 2007). Elution of GST-R3 can be seen in Figure 3.10, lanes 6-7, migrating higher than the expected size of approximately 65 kDa (full length protein 38 kDa + GST 27 kDa). Significant evidence of lower molecular weight degradation products can be seen in both cases, but especially for GST-MDM2. Depending on the required application, GST was either left in place or removed using thrombin protease, in the case of GST-MDM2, or 3C protease in the case of GST-R3. Levels of expression of both of these proteins were sufficient for use in *in vitro* assays; however both were susceptible to on-going degradation post-purification. Lower bands below each protein are simply due to degradation products and are not contaminating proteins. Further purification was not shown as the degradation became increasingly worse when upon further handling of these proteins and degradation products were not an issue for the application of the proteins.

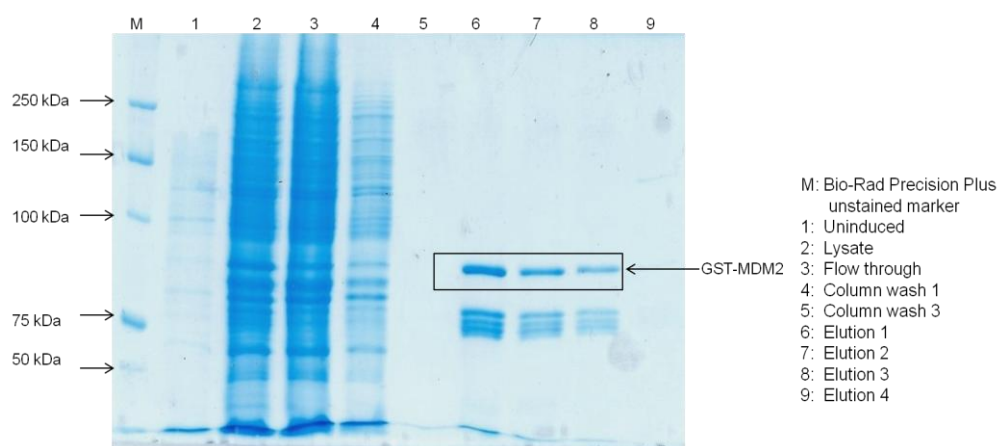


Figure 3.9 SDS-PAGE gel showing expression and purification of GST-MDM2. The box indicates elution of GST-MDM2 from the glutathione agarose matrix following addition of free glutathione. Lane 1 contains bacterial lysate prior to induction with IPTG and lane 2 the lysate following induction. Lane 3 is the flow through and lanes 4 and 5 are the column washes. Lanes 6-8 are the GST-MDM2 elutions with 20 mM reduced glutathione. Lane 9 is the final wash elution with 20 mM reduced glutathione and 1M NaCl.

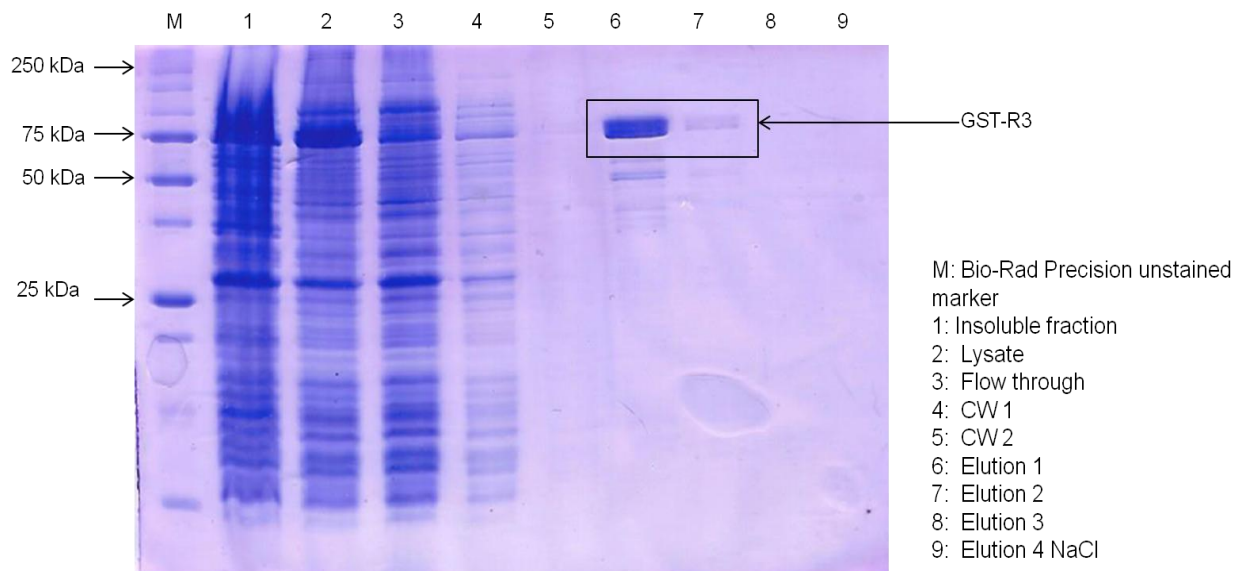


Figure 3.10 SDS-PAGE gel showing expression and purification of GST-R3. Lane 6-8 shows the elution of GST-R3 by 20 mM reduced glutathione. Lane 1 is the insoluble fraction and lane 2 the soluble fraction. Lane 3 is the flow through. Lanes 4 and 5 are the column washes. Lane 9 is the final wash elution by 20 mM reduced glutathione and 1M NaCl.

3.7. Expression and purification of various ubiquitin conjugating enzymes (E2s) and ubiquitin



Purification of UbchH1

Generation of an expression construct for the E2 enzyme GST-UbchH1 was described above. The fusion protein was expressed in *E.coli*, retained on a glutathione agarose column and subsequently eluted with free glutathione as shown in Figure 3.11(a), lanes 6-8. Cleavage with 3C protease produced two bands on SDS-PAGE of very similar molecular weight, corresponding to GST (25 kDa) and UbchH1 (23 kDa) respectively. After being returned to the glutathione agarose column the lower band was found in the flow through, confirming that it was UbchH1 (Fig 3.11(b), lanes 3 & 4), whereas the upper band was retained on the column and eluted with free glutathione, confirming that it was GST (lanes 7 & 8). A small amount of residual GST remaining in the

UbcH1 sample was removed using three 5 ml GSTrap columns (GE Healthcare Life Sciences) connected in series, operated using an ÄKTA Protein Purification System (GE Healthcare Life Sciences). In order to retain the UbcH1 in a soluble form, a high salt buffer was required. A buffer of 400 mM NaCl and 50 mM Tris was made up and the protein was dialysed into the high salt buffer overnight at 4 °C. The triple GSTrap column was pre-equilibrated with the buffer of 400 mM NaCl and 50 mM Tris prior to purification. The protein was loaded onto the column and 5 CV washes of 1 ml each were collected which were expected to contain the highly purified protein of interest (Fig 3.12(a) fractions 5-13; (b) lanes 3-7). The elution buffer was made up of 20 mM reduced glutathione in 400 mM NaCl and 50 mM Tris buffer. 3 ml elutions were collected which were expected to contain residual GST (lane 9) and GST-fusion protein only. Selected fractions were analysed by SDS-PAGE. Note that while GST is not apparent in lane 1 of Fig 3.12(b) because it was too dilute, it does appear in lane 9 as a result of the concentrating effect of affinity chromatography. The dilute band visible below UbcH1 in lane 3-7 represents a degradation product of UbcH1. The intensity of this band typically increased with time following purification, while that of the upper band decreased, which is consistent with proteolytic removal of a portion of UbcH1. Since UbcH1 contains a C-terminal ubiquitin-like domain in addition to the typical E2-like domain, it is possible that this corresponds to proteolytic removal of the ubiquitin-like domain.

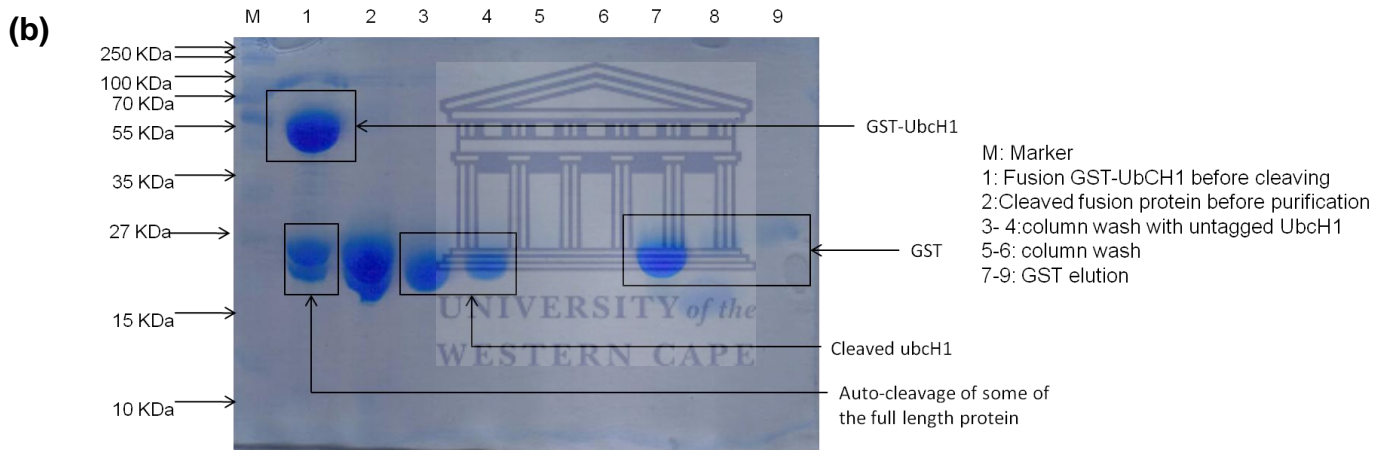
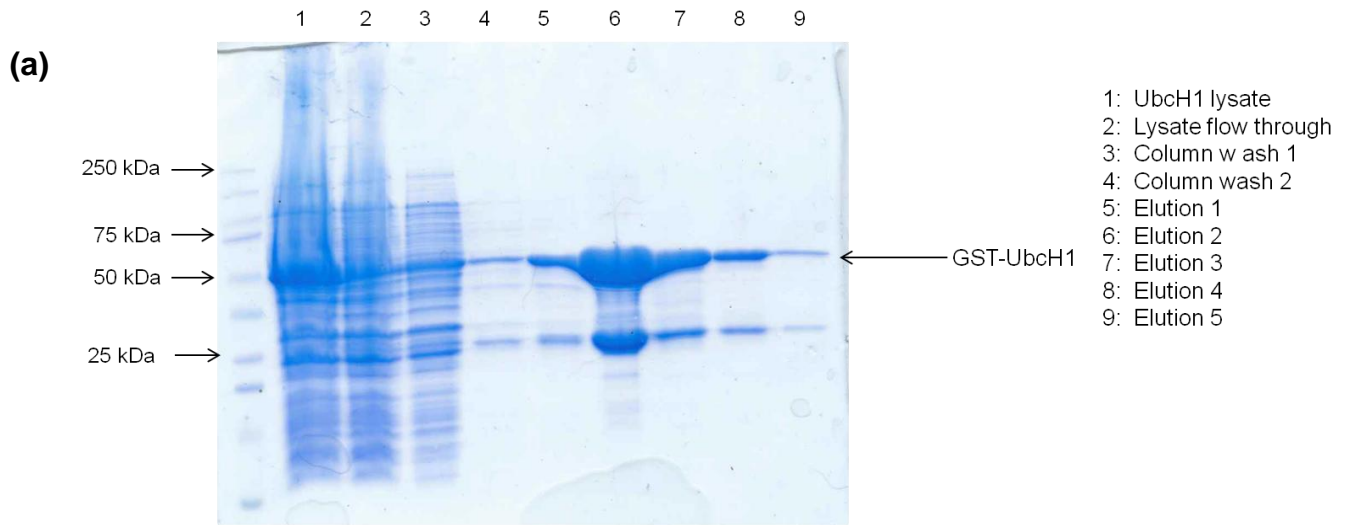


Figure 3.11 SDS-PAGE gels showing expression, purification and cleavage of GST-UbcH1. (a) Glutathione affinity purification of GST-UbcH1, which can be seen eluting in lanes 5-8 following immobilisation on the glutathione agarose column. Free GST is also observed, from which we conclude that there was a degree of cleavage of the linker between GST and UbcH1 either before or after lysis. Lane 1 is the soluble fraction before purification and lane 2 is the flow through. Lanes 3 and 4 are column washes. The elutions 1 to 5 with 20mM reduced glutathione are shown in lanes 5-9 respectively. (b) Cleavage of GST-UbcH1 with GST-3C protease can be seen in lane 2, which should be compared with the uncleaved sample in lane 1. Cleavage produces two very similarly sized bands corresponding to UbcH1 and GST. The cleaved UbcH1 was not retained on the column due to its GST tag being cleaved off and elutes in lanes 3 and 4 with the column washes. The GST protein elutes in lanes 7-9 with 20 mM reduced glutathione. The marker used was BioRad Precision Plus unstained marker.

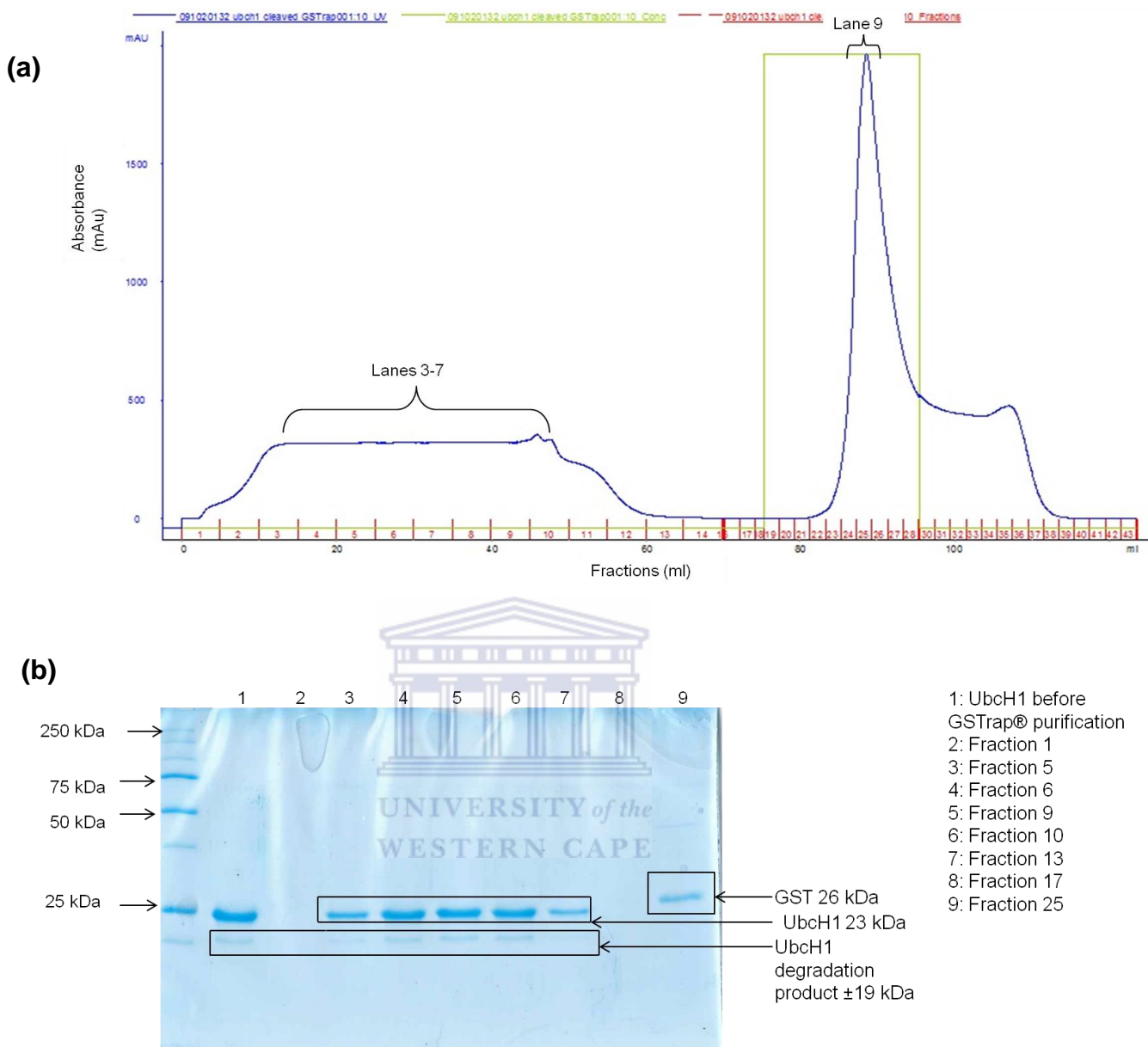


Figure 3.12 Removal of residual GST from Ubch1 using three 5 ml GSTrap™ columns connected in series. (a) Chromatogram from an ÄKTA purification system showing the flow through (labelled “lanes 3-7”) and the elution fraction (labelled “lane 9”) (b) SDS-PAGE confirming that GST, which is eluted from the column (lane 9) corresponds to the higher of the two bands, whereas Ubch1, which is found in the flow through (lanes 3-7) corresponds to the lower band. All residual GST has been removed from the flow through. The even lower band in lanes 3-7 corresponds to a degradation product of Ubch1. The marker used was BioRad Precision Plus unstained marker.

Purification of UbchH13

An expression plasmid coding for the E2 enzyme UbchH13 in a pET24 vector was a gift from Prof Rachel Klevit, University of Washington, Seattle, USA. UbchH13 was expressed with a C-terminal His₆ tag, and was purified using gravity-flow immobilised nickel affinity chromatography. Elution of large quantities of UbchH13 from the column is shown in lane 8 of Figure 3.13. The higher molecular weight contaminants seen in lane 8 were subsequently partially removed using a HisTrap™ purification column on the ÄKTA Protein Purification System (data not shown). Unfortunately the majority of the protein was lost due to precipitation during this second step purification process; however the quantity that remained was deemed more than sufficient for *in vitro* ubiquitination assays.

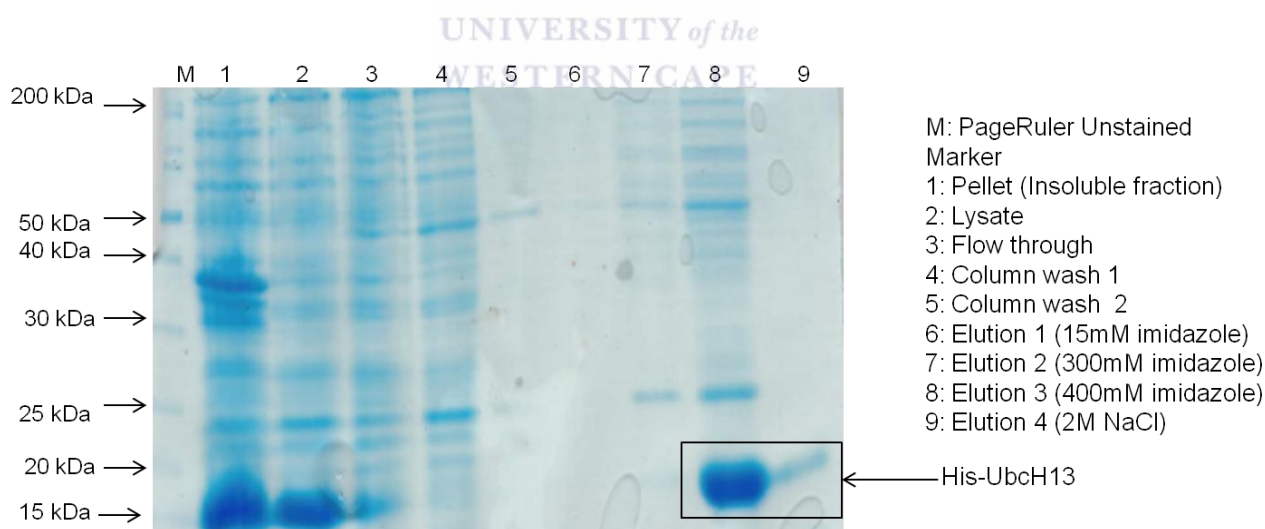
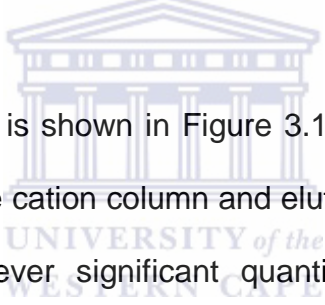


Figure 3.13 Expression and purification of the E2 His₆-UbchH13 using nickel ion affinity chromatography. Partially purified His₆-UbchH13 is seen in lanes 8 and 9 as indicated in the black box. Lane 1 shows the insoluble fraction (pellet) and lane 2 is the soluble fraction (lysate) prior to purification. Lane 3 contains the flow through and lanes 4 and 5 the column washes with 20 mM imidazole to suppress non-specific binding to the column. Lane 6 contains the first elution with 15 mM imidazole and Lane 7 contains the second elution with 300 mM imidazole. Lane 8 is the third elution with 400 mM imidazole and lane 9 the final elution with 2 M NaCl to remove any protein still bound to the column.

Purification of wild type and K(0) mutant ubiquitin

Expression plasmids for wild type ubiquitin and the K(0) mutant (all lysine residues replaced with arginines) were kind gifts from Prof Rachel Klevit (affiliation as above). Both were expressed without an affinity tag and purified according to the protocol supplied in Section 2.9.4, which takes advantage of the stability of ubiquitin at pH 4.5 to denature and precipitate host proteins. The proteins were purified further by cation exchange chromatography at pH 4.5; since the pI of both wild type and K(0) ubiquitin as determined by the ExPasy ProtParam server are in the vicinity of 6.5, at pH 4.5 they are expected to be highly positively charged and therefore retained by the cation column.



Purification of ubiquitin-K(0) is shown in Figure 3.14. As expected, most of the ubiquitin was retained by the cation column and eluted with a step-wise gradient of NaCl (lanes 4-7); however significant quantities of contaminating host proteins were still co-purified. To purify the target protein further, the fractions in lanes 4-7 were pooled, dialysed against 1mM PBS to reduce the concentration of NaCl and subjected to a further round of purification. The final eluate in 600 mM NaCl (panel (b), lane 6) is highly purified. This sample was dialysed into 20 mM sodium acetate for use in *in vitro* assays.

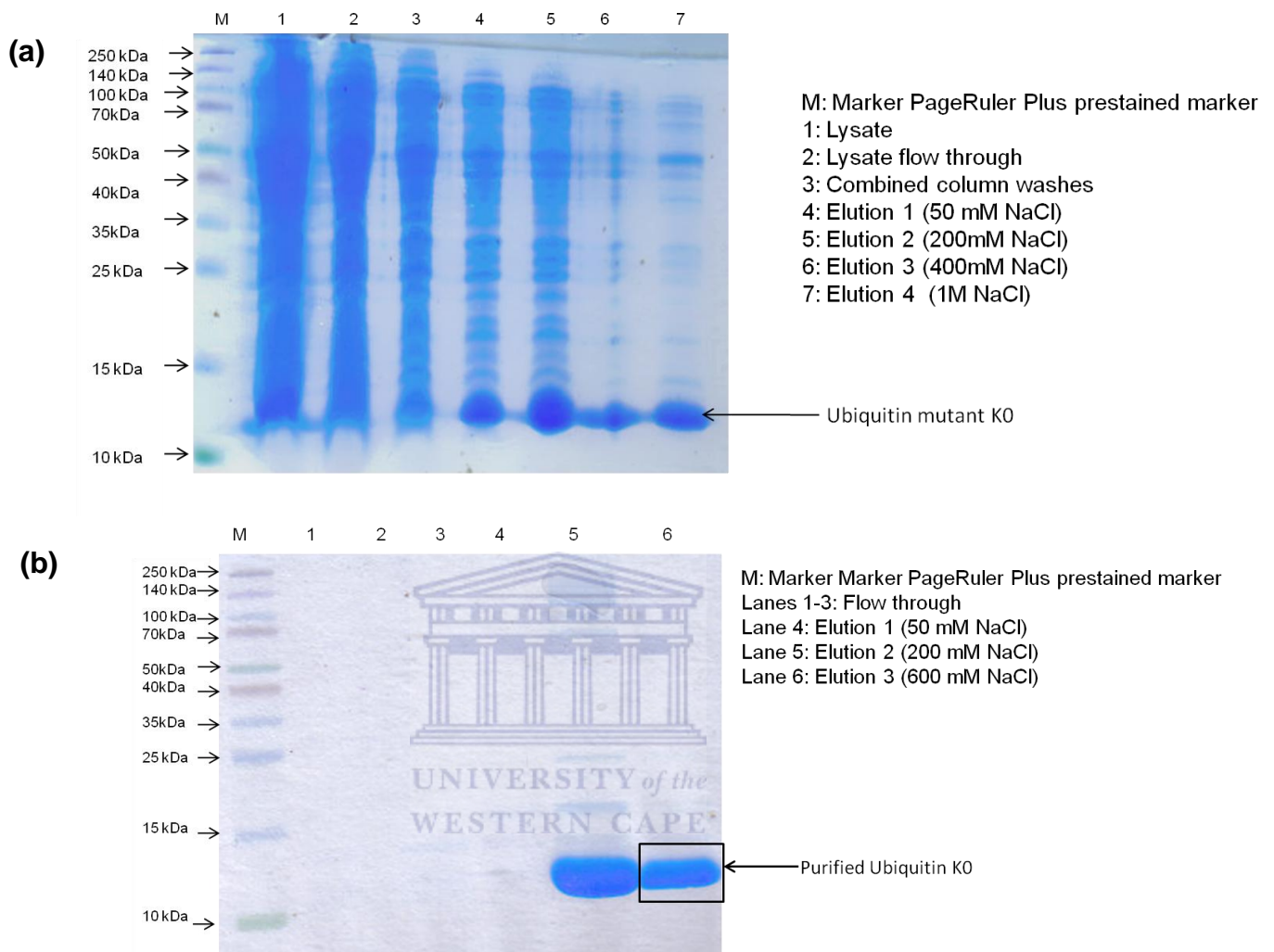


Figure 3.14 SDS-PAGE gel showing the purification of the ubiquitin-K(0) mutant. (a) Partial purification of the ubiquitin mutant-K0 mutant is indicated by the arrow in lanes 4-7. This initial purification of the ubiquitin mutant was performed after dialysis with 20 mM sodium acetate. The soluble fraction is shown in lane 1 and the flow through in lane 2. The column washes were combined and produced a sample that was taken to produce the result in lane 3. Elutions 1-4 were performed with a stepwise gradient of NaCl (50 mM, 200 mM, 400 mM and 1 M NaCl respectively). **(b)** Re-purification of ubiquitin mutant-K0. Due to their being a lot of contaminating bacterial proteins still present in the partially purified Ubch13 preparation in (a), the elutions from lanes 4-7 were pooled and subjected to a second round of purification. Large quantities of highly pure ubiquitin-K(0) can be seen in lane 6. Lanes 1-3 contain the flow through and lanes 4-6 contain the three elutions with 50 mM, 200 mM and 600 mM NaCl respectively.

3.8. Purification of intact proteasomes from human cell lysates

Intact 26S proteasomes were precipitated from human HeLa cell lysates using an antibody raised against the α_2 subunit, using lysate prepared from MCP21 hybridoma cells (Sigma-Aldrich, Missouri, USA) by a co-worker, Ms Ania Szmyd-Potapczuk. The antibody was coupled to Affigel beads (Bio-Rad, Hercules, California) as described in Section 2.12-2.13.

A Western blot showing successful detection of the purified 26S proteasome is shown in Figure 3.15. A number of background bands are visible in lanes 1-3, which are likely to correspond either to cross-reactivity with lysate proteins or to heavy and light chains of the anti- α_2 antibody, which is expected since the same antibody was used for both immunoprecipitation and detection. However the presence of additional bands in lane 7 which are not present in lane 2 is evidence that α_2 subunit has been precipitated. The new bands are in the range of 20-40 kDa which is consistent with the mass of the α_2 subunit (26 kDa). The bands are unlikely to correspond to β -subunits, since they are not likely to be detected by the antibody against the α_2 subunit. Nevertheless, the fact that at least the α_2 subunit is present in the immunoprecipitate makes it likely that the entire intact proteasome has been precipitated as well.

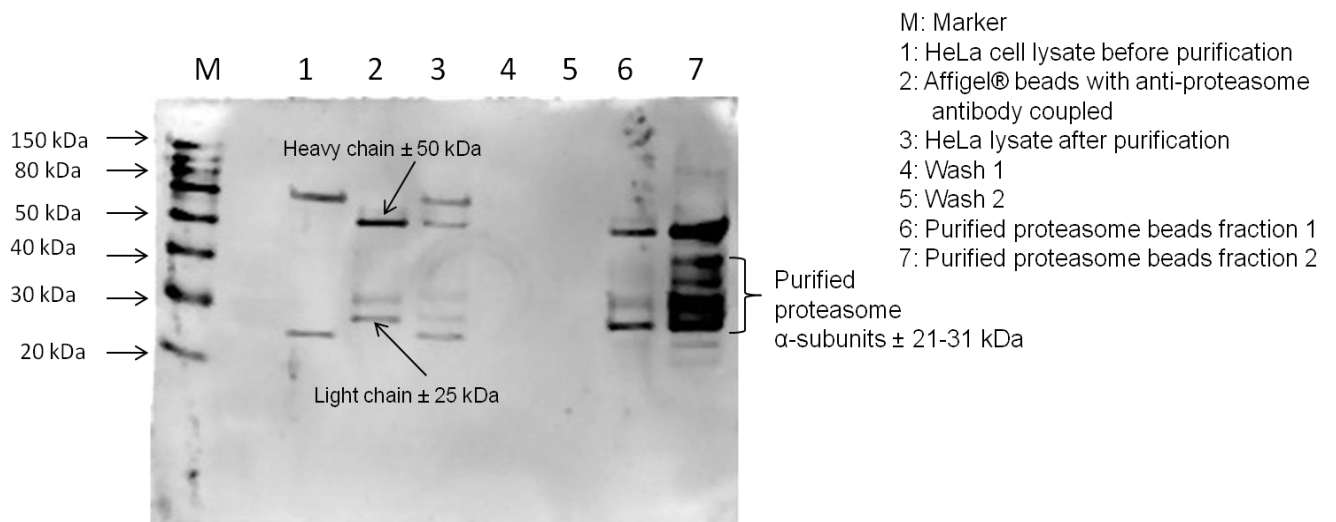


Figure 3.15 Immuno-blot showing purification of the 20S α_2 -subunit of the 26S proteasome from HeLa cell lysate. Proteasome purified using anti-proteasome antibody raised against the α -subunit of the 20S core subunit which was coupled to Affigel® matrix beads. Lane 1 is the HeLa human cell lysate. Lane 2 is the Affigel matrix beads coupled to the antibody. Lane 3 is the lysate after proteasome purification. Lanes 4 and 5 are the supernatants from wash buffers 1 and 2 respectively. Lane 6 and 7 are the purified proteasome beads. Western blot antibody dilution 1:500 primary, 1:1000 goat-anti mouse secondary (Santa Cruz).

CHAPTER 4

***In vitro* investigation of the ubiquitination of p53 by RBBP6 and MDM2**

4.1. Introduction

Studies in knock-out mice suggested that RBBP6 plays a role in facilitating poly-ubiquitination and degradation of p53 by MDM2. In the same study Li and co-workers showed that RBBP6 (referred to as PACT in their report) interacts directly with MDM2 in U2OS and MCF7 cell lysates. Since RBBP6 had previously been shown to interact with p53 via its C-terminus (Simons *et al.*, 1995), Li and co-workers hypothesised that RBBP6 may function as a molecular scaffold, bringing p53 and MDM2 together to catalyse ubiquitination of p53 by MDM2 (Li *et al.*, 2007). Using immunoprecipitation they showed that a stronger interaction exists between p53 and MDM2 in the presence of RBBP6. They also showed that over-expression of Myc-PACT alone in HEK293 cells did not lead to a decrease in exogenous Flag-p53, but did lead to a decrease when MDM2 was co-expressed together with Myc-PACT. Hence they concluded that RBBP6 does not participate directly in the ubiquitination reaction, but only indirectly by facilitating the ubiquitination activity of MDM2 (Li *et al.* 2007).

At the same time RBBP6 contains its own RING finger domain and has been shown to have its own E3 ligase activity against the cancer-associated protein

YB-1 and DNA damage-associated protein zBTB38, in both cases leading to degradation in the proteasome (Chibi *et al.*, 2008; Miotto *et al.*, 2011). The possibility that RBBP6 has its own ubiquitin ligase activity against p53 is therefore worthy of more detailed investigation.

We therefore set out to investigate using *in vitro* assays whether RBBP6 is able to mono- or poly-ubiquitinate p53 with or without the assistance of MDM2. Due to the (expected) poor solubility of the full length RBBP6 protein, a truncated form of RBBP6 consisting of the first 335 amino acid residues was used. This fragment was named “R3” because it contains the first three domains of RBBP6, namely the DWNN domain, the zinc knuckle and the RING finger. Since R3 does not contain the C-terminal region previously characterised as the p53-binding domain (Simons *et al.*, 1997), utilising R3 should therefore rule out the scaffold mechanism proposed by Li and co-workers. Nevertheless, a protein orthologous to human R3 is expressed in all invertebrate eukaryotic genomes (see Figure 1.4), which suggests that this fragment may contain most, if not all, of the ubiquitination-related activity of the protein.

4.2. R3 is able to ubiquitinate p53 in a partially in vitro system

As a first step, a partially *in vitro* ubiquitination assay was set up in which human HepG2 cell lysate was used to supply the E1 and E2 enzymes, to which bacterially-expressed R3 and/or MDM2 were added. Since endogenous p53 was not detectable in the lysate (HepG2 are expected to express wild type p53 (Volmer *et al.*, 1999) which might be quite low for this application as p53 is kept

at low levels), bacterially-produced p53 was added and detected by Western blot using anti-p53 antibodies.

Due to the expected presence of other endogenous E3 enzymes in the lysate, any effect observed using this assay could not be attributed exclusively to R3. Nevertheless, the expectation in setting up this assay was that it may provide a rapid means of determining whether R3 promotes ubiquitination of p53, either directly or indirectly, and whether addition of R3 together with MDM2 leads to increased ubiquitination suggestive of cooperative behaviour. It should also allow for investigation of whether the resulting ubiquitination was mono- or poly-ubiquitination and whether it resulted in proteasomal degradation.

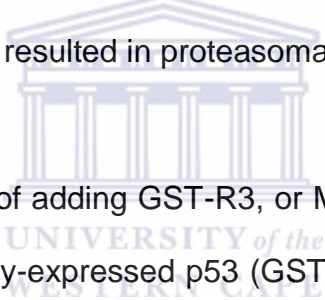


Figure 4.1 shows the result of adding GST-R3, or MDM2 (GST tag removed) to HepG2 cell lysate. Bacterially-expressed p53 (GST tag removed) was added to all lanes except lane 1 and was detected by Western blotting with rabbit polyclonal anti-p53 antibody (sc-6243 Santa Cruz Biotechnology, Inc., Santa Cruz, CA, USA). p53 was detected as a doublet at approximately 50 kDa. The absence of similar bands in lane 1, which contains only lysate, confirms that endogenous p53 was not expressed at detectable levels in these cells. Bacterially-expressed ubiquitin, E1 and a panel of E2s (UbcH1, UbcH5b, UbcH5c, UbcH6, UbcH7, UbcH8 and UbcH13) were added to all lanes except lane 1.

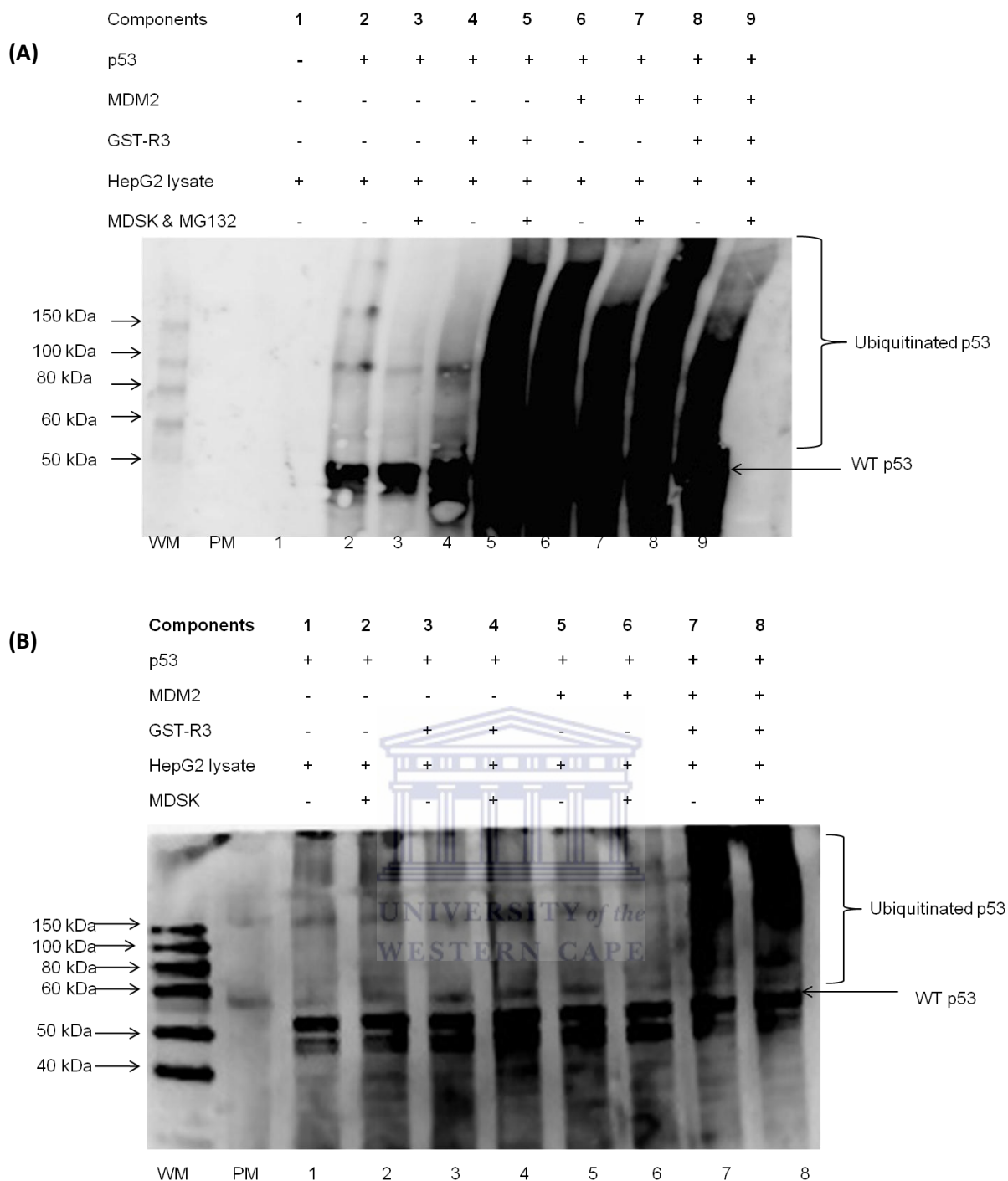


Figure 4.1 R3 and MDM2 promote the poly-ubiquitination of p53 in the presence of human HepG2 lysate (A) GST-R3 (lane 5) and MDM2 (lane 7) catalyses massive ubiquitination of p53 in the presence of HepG2 lysate, which is not present when exogenous E3 is not added (lane 3). Unmodified p53, migrating as a doublet at an apparent molecular weight of around 50 kDa, can be seen in lanes 2 and 3, to which no exogenous E3 enzymes were added. The absence of endogenous p53 in the HepG2 lysate (lane 1) is expected and shows that the p53 in lanes 2-9 corresponds exclusively to exogenous, bacterially-expressed p53. Omission of proteasome inhibitors MG132 and MultiDsk appears to result in a decrease of the poly-ubiquitination (lane 4), possibly due to degradation of the poly-ubiquitinated p53 in proteasome. However, an expected similar effect is not seen in lanes 6 and 8, rendering the results inconclusive. **(B)** Same assay as in (A), but with only MultiDsk added in odd lanes rather than a combination with MG132. The same massive poly-ubiquitination is observed when GST-R3 and MDM2 are used together, although the evidence for poly-ubiquitinated p53 in lane 8, which contains MultiDsk, as compared to lane 7 which contains no MultiDsk, is not convincing. The lack of degradation in lane 7 suggests that MultiDsk was either not present or not functional.

Lane 5 of Figure 4.1(A) suggests that R3 promotes poly-ubiquitination of p53 in HepG2 lysate. A thick smear stretches right up to the top of the Western blot, most likely corresponding to poly-ubiquitination of p53, which is not present when R3 is not added (lanes 2 and 3). Higher molecular weight bands up to 150 kDa are typically identified with mono-ubiquitination of p53 on multiple sites (Wang *et al.*, 2011); however bands such as these, stretching much higher than the top marker band at 150 kDa, are more likely to correspond to poly-ubiquitination of p53.

Note that this result does not allow the conclusion that R3 is capable of poly-ubiquitinating p53 on its own. It is possible that R3 cooperates with other endogenous E3s present in the lysate, including MDM2. However it does confirm the conclusion of Li and co-workers that R3 promotes poly-ubiquitination of p53.

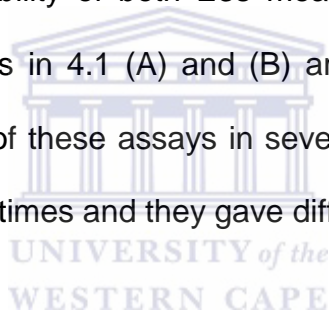
As expected, MDM2 produces similar high molecular weight smears when added to the lysate (lane 7). Here too, the potential presence of other E3s in the lysate, such as MDMX, means that this result does not contradict the view that MDM2 can only mono-ubiquitinate p53. In addition to other ubiquitination enzymes, cell lysate is also likely to contain de-ubiquitination enzymes (DUBs), which may reduce the amount of ubiquitination, and 26S proteasomes, which may degrade poly-ubiquitinated p53 and lead to a decrease of the high molecular weight smears. In an attempt to control for these two effects, MultiDsk, a synthetic protein reported to oppose the effects of DUBs and

proteasomal degradation, and MG132, which is well known to block the 26S proteasome, were added together to odd-numbered lanes. This is expected to lead to increased ubiquitination in odd-numbered lanes. While there does appear to be evidence for this in the case of GST-R3 (compare lanes 4 and 5), the effect appears to be the wrong way around in the case of MDM2 (lanes 6 and 7). When GST-R3 and MDM2 are added together the poly-ubiquitination is still present but there is no considerable increase suggestive of cooperation between them (lane 9). Nevertheless Fig 4.1(A) provides strong evidence that R3 promotes poly-ubiquitination of p53 in cell lysates.

Figure 4.1(B) shows a repeat of the result in (A), but this time using only MultiDsk in odd-numbered lanes to determine whether MultiDSK was capable of performing its concentrating effect of poly-ubiquitinated proteins and preventing degradation without the aid of MG132. It could only concentrate if a pull down was performed – was anything like that done? Again there is evidence of heavy poly-ubiquitination when R3 and MDM2 are present together (lanes 7 and 8), but much less evidence when they are used separately (lanes 3-6). There may be evidence of more poly-ubiquitination when MultiDsk is present (lane 8), suggesting that degradation has taken pace in lane 7, but it is not convincing. The lack of any effect from MultiDsk suggests that MultiDsk was either not present in the expected concentration or was not functional.

The R3 used in these assays was a fusion with GST. MDM2 was expressed as a fusion with GST, but the GST was subsequently removed using the thrombin protease site present in the expression vector. A number of authors have

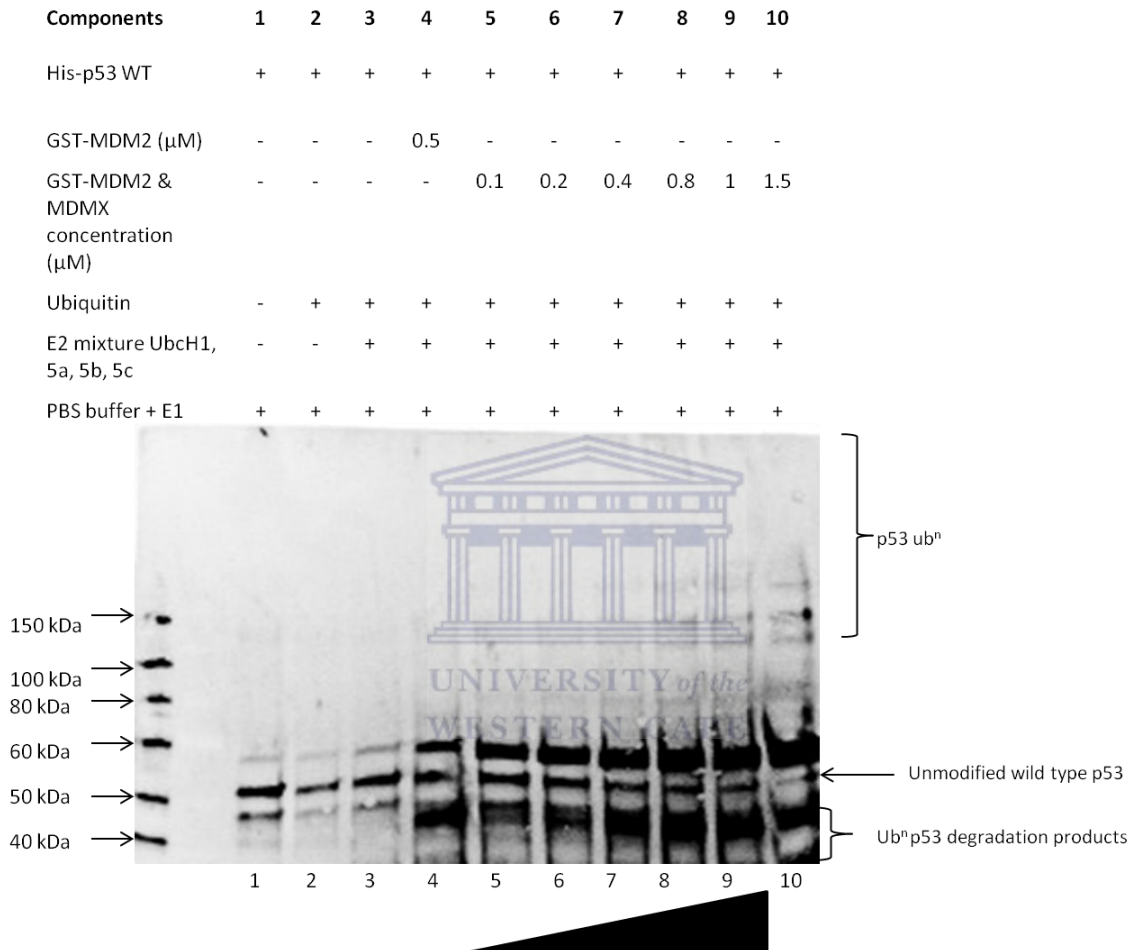
warned that the presence of GST may artificially enhance the poly-ubiquitination activity of GST-MDM2 by stabilising the homo-dimeric state (Hadelman *et al.*, 1997; Wang *et al.*, 2011). Since R3 forms a homodimer in solution (P. M Maumela and D.J.R. Pugh, manuscript in preparation), it is possible that GST artificially enhances the ubiquitination activity of GST-R3 in the same manner. However size exclusion data suggests that the strength of the homodimer is already sufficiently strong that GST is unlikely to have much effect on the stability of the R3 homodimer (P. M Maumela and D.J.R. Pugh, unpublished data). Un-tagged R3 and MDM2 were therefore used wherever possible, although the inherent instability of both E3s meant that this was not always possible. These two Figures in 4.1 (A) and (B) are the representative results presented in the repetition of these assays in seven attempts – what does this mean – that you did them 7 times and they gave different results in the other 5?



4.3. Optimisation of fully *in vitro* ubiquitination assays

The previous assays were conducted using a mammalian cell lysate to provide essential associated enzymes such as E1 and E2s. As a first step in setting up full *in vitro* ubiquitination assays, protocols were bench-marked against the MDM2/MDMX system, which is known to produce poly-ubiquitination when both MDM2 and MDMX are present, but only mono-ubiquitination when MDM2 is used on its own (Wang *et al.*, 2011). The E2s selected for this screening were UbcH1, UbcH5a, UbcH5b and UbcH5c to provide a variety as the preferred E2 would be selected from this pool. His₆-p53 was used and detected using a rabbit polyclonal antibody, as previously described. As can be seen from Figure

4.2, addition of increasing amounts of GST-MDM2 and a fixed amount of MDMX led to a dose-dependent increase of high molecular weight bands above 100 kDa. We concluded that bacterially expressed MDM2 and MDMX are



successfully producing poly-ubiquitination of p53 in a fully *in vitro* system and that a MDM2 concentration of 1 μM was sufficient for detectable ubiquitination.

Figure 4.2 MDM2 and MDMX titration to find the optimal conditions for p53 ubiquitination. A mix of GST-MDM2 and MDMX was titrated with concentrations are indicated above. Lane 1 contains only the substrate p53 and the PBS buffer with E1. Lane 2 contains p53 and the PBS buffer with E1 and ubiquitin. Lane 3 contains the same as lane 2 with an E2 mix of UbcH1, 5a, 5b and 5c. Lane 4 contains the same as lane 3 with 0.5 μM of the E3 GST-MDM2. Lanes 5-10 contain the same as lane 3 with increasing concentrations of the combination of GST-MDM2 and MDMX.

A similar titration assay was carried out using GST-MDM2 and GST-R3, and Figure 4.3 shows some evidence of dose-dependent ubiquitination of p53 by GST-MDM2/GST-R3 extending to above 150 kDa. Disappointingly this was far less than previous assays. Despite being repeated several times, the quantity of ubiquitination remained low. It is possible that one of the many components in our assays was not functional, not present in sufficient quantities or degraded. However it does suggest that the amounts of ubiquitination seen in many of our assays are nevertheless significant, since they are comparable with the effect seen for the standard system of MDM2/MDMX.

4.4. UbcH5a is the preferred E2 for in vitro poly-ubiquitination of p53 by GST-MDM2 and GST-R3

The in-lysate assays shown in Figure 4.1(A) and (B) indicate that R3 is able to promote poly-ubiquitination of p53. However these assays do not indicate whether R3 is sufficient, or whether any other proteins are required for this ubiquitination.

In order to identify one or more E2s which work in combination with R3 to ubiquitinate p53 *in vitro*, an E2 screen was conducted using a number of bacterially-expressed E2s. The screen was performed using bacterially His₆-tagged p53, which was tested in an attempt to circumvent the serious degradation found with GST-tagged p53.

Components	1	2	3	4	5	6	7	8	9
His-p53 WT	+	+	+	+	+	+	+	+	+
GST-R3 (μM)	-	-	-	-	0.6	-	-	-	-
GST-MDM2 (μM)	-	-	-	0.5	-	-	-	-	-
GST-MDM2 & GST-R3 concentration (μM)	-	-	-	-	-	0.1	0.4	0.8	1
Ubiquitin	-	+	+	+	+	+	+	+	+
E2 UbcH5a	-	-	+	+	+	+	+	+	+
PBS buffer + E1	+	+	+	+	+	+	+	+	+

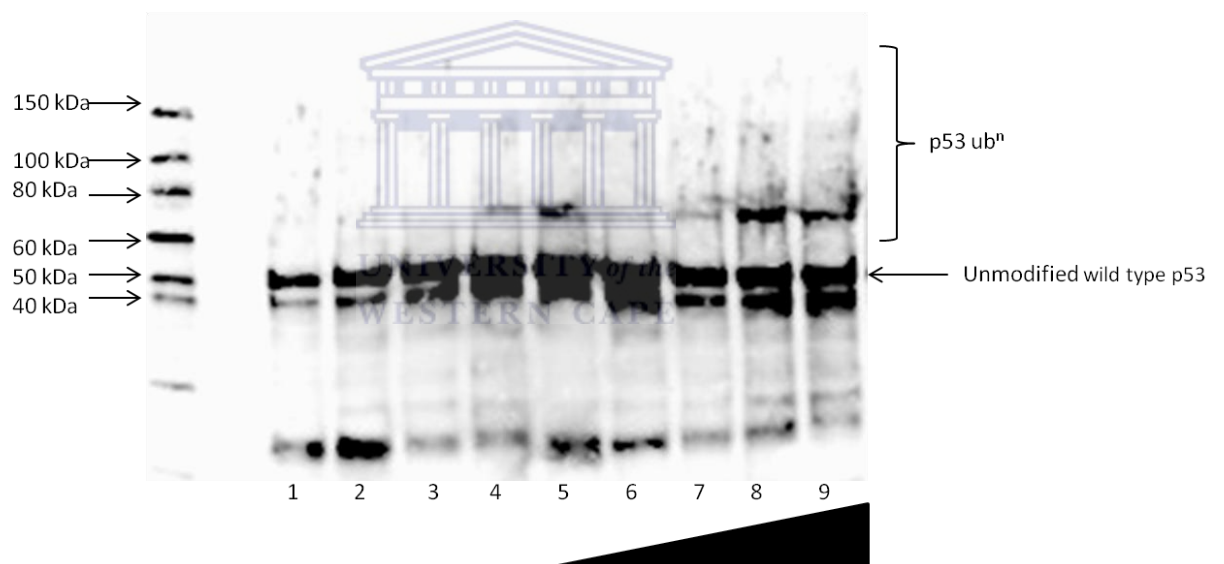


Figure 4.3 GST-MDM2 and GST-R3 titration to find the optimal conditions for p53 ubiquitination. Lane 1 contains only the substrate p53 and the PBS buffer with E1. Lane 2 contains p53 and the PBS buffer with E1 and ubiquitin. Lane 3 contains the same as lane 2 with the E2 UbcH5a. Lane 4 contains the same as lane 3 with 0.5 μM of the E3 GST-MDM2. Lane 5 contains the same as lane 3 with 0.6 μM GST-R3. Lanes 6-10 contains the same as lane 3 with increasing concentrations of the combination of GST-MDM2 and GST-R3.

1 μM of GST-MDM2 and 1 μM of GST-R3 was added to each lane in Figure 4.4, along with 0.35 μM of E1, 2 μM of each E2 and 1 mM HA-ubiquitin and 1 μM His₆-p53.

Although the samples appear to have run anomalously on the gel, there is nevertheless clear evidence that Ubch5a (lane 5) and Ubch5c (lane 7) are the most effective E2s for ubiquitinating p53, both producing high molecular weight smears right to the top of the gel. Consistent with this conclusion, the band corresponding to unmodified p53 appears lighter in the lane containing Ubch5a (lane 5) than in all the others, as would be expected if a significant fraction of p53 were migrating at higher molecular weight. Ubch5c appears to be not as effective as Ubch5a in ubiquitinating p53, since the band corresponding to unmodified p53 band is not as light in lane 7 as it is in lane 5. However the majority of the p53 remained unmodified at 53 kDa. The other E2s did not show ubiquitination activity with this MDM2/R3 combination.

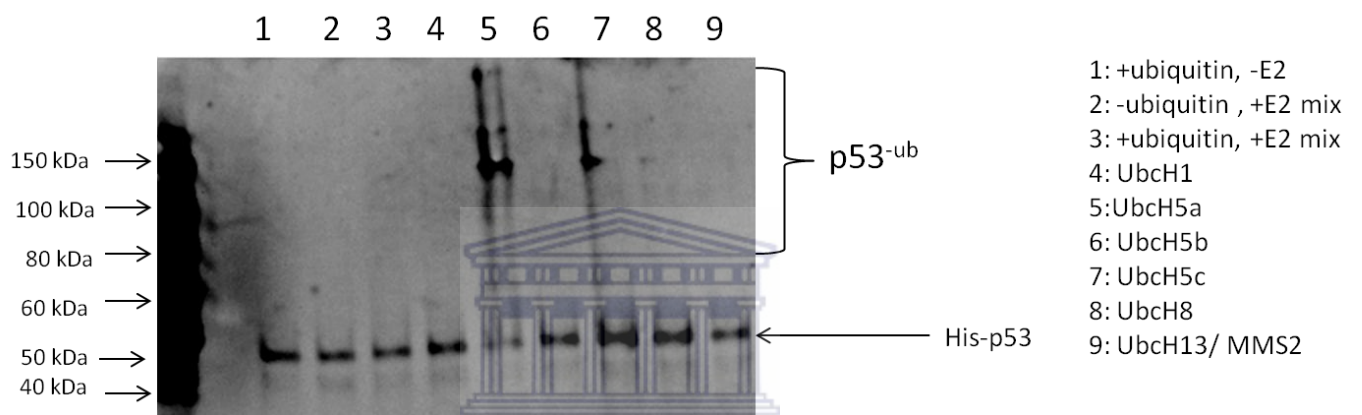


Figure 4.4 *In vitro* E2 screen using His₆-p53 confirms that UbcH5a acts as E2 with E3s GST-MDM2 and GST-R3 to poly-ubiquitinate p53. Lanes 1-9 contain 10 μM each of GST-R3 and GST-MDM2. Lane 1 contains ubiquitin with no E2s. Lane 2 contains a mixture of all the E2s used without ubiquitin. Lane 3 contains an E2 mix with ubiquitin. Lanes 4-10 all contain ubiquitin. Lanes 2-9 contain 2 μM each of the E2s shown in the key. High molecular weight smears in lanes 5 and 7 show that UbcH5a and UbcH5c are able to catalyse poly-ubiquitination of p53 by GST-MDM2 and GST-R3.

Up to this point, in the *in vitro* assays R3 has been shown to produce ubiquitination of p53 in combination with MDM2. In order to test whether it has its own E3 activity against p53 a fully *in vitro* assay was set up using 2 μ M UbcH5a as the E2. Lanes 3 of Figure 4.5 suggests that R3 is able to mono-ubiquitinate p53, with higher molecular weight species apparent at least up to 150 kDa. It is possible that the bands extends further, but the poor resolution of this 16% self-cast SDS-PAGE gel makes it difficult to discriminate between high molecular weight bands. The effect is similar to that produced by GST-MDM2 alone (lane 4). Similar high molecular weight bands are seen in lane 2, which contains no E3, but they are much fainter than when R3 is present. When GST-MDM2 is added jointly with R3 the density of the ubiquitination increases; whether this is due to cooperation between MDM2 and R3 or simply the combined effect of the two E3s working individually is not clear from this assay. Densitometry could be used to quantify signals produced through Western blotting, however this method of quantification was not investigated in this thesis.

Components	1	2	3	4	5
p53	+	+	+	+	+
Buffer +E1 +E2	-	+	+	+	+
ubiquitin	-	+	+	+	+
R3 (no GST)	-	-	+	-	+
GST-Mdm2	-	-	-	+	+

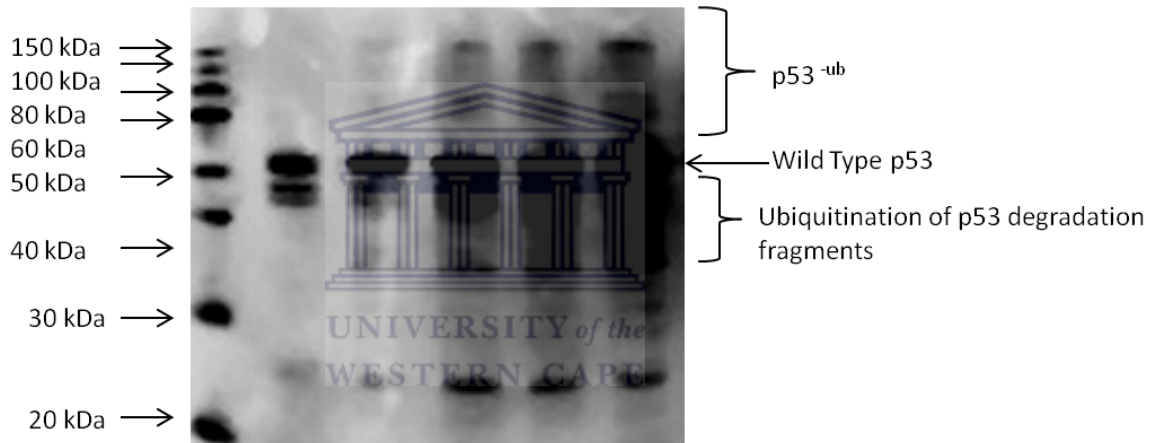
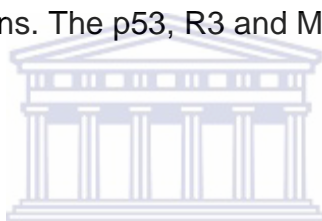


Figure 4.5 R3 is able to ubiquitinate p53 independently of MDM2 using UbcH5a in an *in vitro* assay. Lane 1 is non-modified p53. Lane 2 is p53 with the reagents for ubiquitination without the E3s. Lane 3 has R3 (cleaved of its GST tag) added in addition to the reagents in lane 2. Lane 4 GST-MDM2 with the reagents in lane 2. Lane 5 contains both R3 and GST-MDM2.

4.5. Ubiquitination by a combination of R3 and MDM2 leads to enhanced ubiquitination of p53 and proteasomal degradation *in vitro*

The results of the previous section suggest that R3 may be able to catalyse poly-ubiquitination of p53 in conjunction with UbcH5a as E2. If so, then it may also be expected to catalyse proteasomal degradation of p53, provided the poly-ubiquitination involved lysine-48 internal linkages. UbcH5a is known to catalyse lysine-48 linked poly-ubiquitination with a number of different E3s (Kim *et al.*, 2015). To test this hypothesis, intact proteasomes were immunoprecipitated from A549 human cell lysates and added to all tubes in the *in vitro* ubiquitination reactions. The p53, R3 and MDM2 used in this assay were all tagged with GST.



The results are shown in Figure 4.6(A). Lanes 2 and 3 show evidence of poly-ubiquitination produced by GST-R3 and GST-MDM2 respectively, with bands stretching up at least to 150 kDa and possibly higher, which are not present in the absence of E3 (lane 1). When GST-R3 and GST-MDM2 are added together both the un-modified p53 and the higher molecular weight bands almost completely disappear (lane 4), suggesting that poly-ubiquitinated p53 has been degraded in the proteasome. Crucially, in the presence of the proteasome inhibitor MG132 (lane 5) both the unmodified and higher molecular weight species of GST-p53 are restored completely, which is clear evidence that the reduction in lane 4 is due to degradation by the proteasome. Due to no MG132 controls being included for lanes 2 and 3, it cannot be concluded that there was no degradation in these lanes; nevertheless it is noticeably less than that seen

in lanes 4 and 5. p53 degradation products are clearly seen in all the lanes due to the instability of GST-p53.

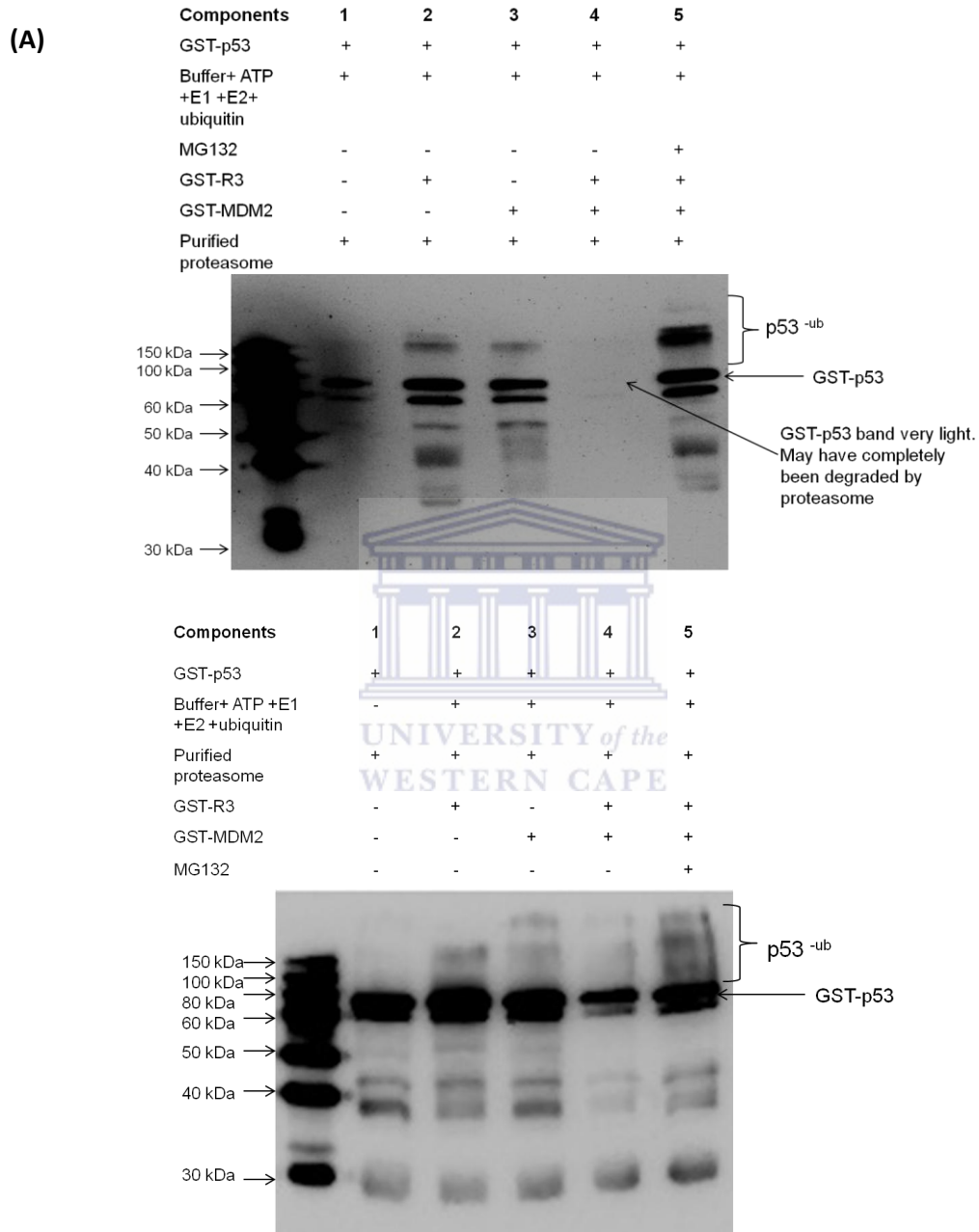
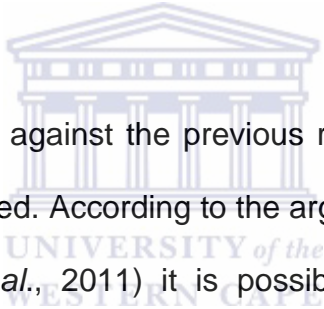


Figure 4.6 Enhanced degradation using both GST-R3 and GST-MDM2 *in vitro* (A) *In vitro* assay showing degradation when both GST-R3 and GST-MDM2 are used. All lanes contain purified proteasome from A549 human cell lysate, GST-p53, E1, and a cocktail of E2 including UbcH1, UbcH5a, UbcH5b, UbcH5c, UbcH6 and UbcH8. Lane 1 is GST-p53 only. In addition, lane 2 contains additional GST-R3, lane 3 contains GST-MDM2, lane 4 contains both GST-R3 and GST-MDM2 and lane 5 contains GST-MDM2 and GST-R3 together with MG132 to inhibit the purified proteasome. **(B)** An independent repeat of the assay in panel (A), including the same components.

This conclusion is confirmed by the repeat assay shown in Figure 4.6(B). As before, both un-modified p53 and higher-molecular weight bands are reduced when GST-R3 and GST-MDM2 are used together (lane 4), and re-appear when MG132 is added (lane 5). Furthermore, p53 is not reduced when GST-R3 or GST-MDM2 are used individually. These results suggest strongly that GST-R3 and GST-MDM2 are individually incapable of catalysing degradation of GST-p53, but that when used together they produce poly-ubiquitin capable of causing degradation of p53. This appears to confirm previous *in vivo* reports that RBBP6 cooperates with MDM2 in catalysing poly-ubiquitination and degradation of p53.



An objection may be raised against the previous result that the substrate and the E3s all have GST attached. According to the argument put forward by Wang and co-workers (Wang *et al.*, 2011) it is possible that GST enhances the ubiquitination activity of R3 and MDM2 by promoting their dimerisation. Alternatively, the GST attached to the substrate may promote recruitment of either or both of the E3s. In reply to this objection, it can be pointed out that GST-MDM2 was not able to cause degradation of GST-p53 (lane 3 of panel A), despite the presence of GST on both proteins.

Despite the above argument, in order to eliminate all uncertainty resulting from the presence of GST was attempted to reproduce the results in Figure 4.6 following removal of the GST from the substrate and E3s. However, this proved very difficult due to the instability of all three proteins following removal of the

GST tag. Instead of GST- or His₆-tagged wild type p53, we therefore generated an expression construct for the quadruple mutant form of p53 reported by Joergher and co-workers (Joergher *et al.*, 2004), and expressed it with an N-terminal His₆ tag (His₆-p53-QM). Following removal of the GST tag the amounts of MDM2 recovered dropped significantly, and no consistent ubiquitination could be generated using MDM2, leading us to the conclusion that the amount of active MDM2 had been reduced to ineffective levels. However Western blots detecting MDM2 to show this directly were not undertaken.

Figure 4.7 shows the result of an *in vitro* assay using His₆-p53-QM as substrate and either GST-MDM2 or R3 (no GST tag) as E3. Ubch5c was used as E2 in all lanes. His₆-p53-QM appears as a doublet at around 50 kDa, as seen in previous results. The band consistently seen at around 100 kDa in all lanes is considered to be an artefact and subsequent work has shown that this band is not present when a different anti-p53 antibody is used (A. Faro, unpublished data). In the absence of ubiquitin there is very little evidence of ubiquitination, as would be expected (lanes 1-4). However addition of either R3 (lane 7) or GST-MDM2 (lane 5) yielded clear evidence of poly-ubiquitination corresponding to molecular weights substantially greater than 150 kDa.

Significantly more ubiquitination was produced when R3 and GST-MDM2 were used together (lane 10), a conclusion supported by the disappearance of unmodified p53. In fact the level of ubiquitination appears to be significantly greater than the sum of the amounts produced by R3 and GST-MDM2 alone, suggesting that the effect is cooperative rather than simply additive. Lane 9

contains the same reagents as lane 10, with the addition of proteasome purified from A549 cell lysates.

Components	1	2	3	4	5	6	7	8	9	10
p53QM	+	+	+	+	+	+	+	+	+	+
GST-MDM2	-	-	+	+	+	+	-	-	+	+
R3	-	-	+	+	-	-	+	+	+	+
Ubiquitin	-	-	-	-	+	+	+	+	+	+
Proteasome	+	-	+	-	+	-	+	-	+	-
PBS +E1+UbcH5c	+	+	+	+	+	+	+	+	+	+

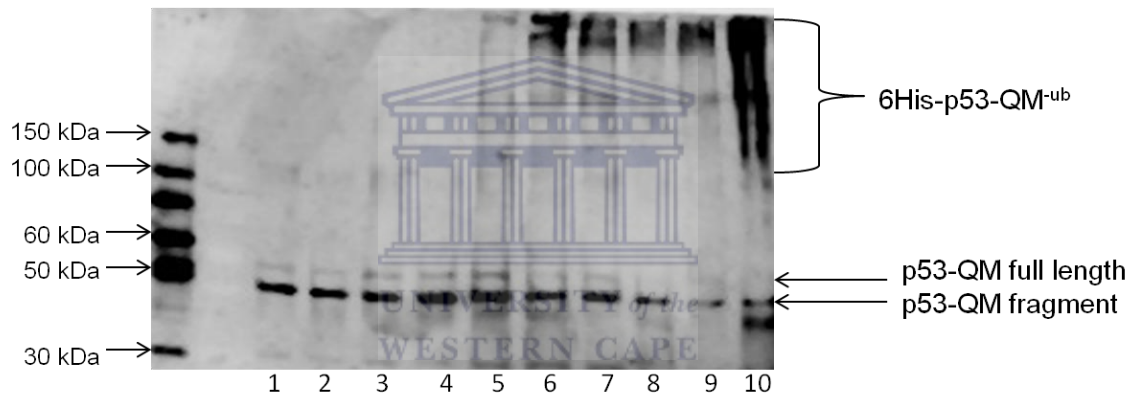


Figure 4.7 Ubiquitination of p53-QM using a combination of R3 (no GST tag) and GST-MDM2 leads to enhanced ubiquitination and results in proteasomal degradation of p53-QM. Showing fully *in vitro* ubiquitination and degradation assay of the p53 quadruple mutant. All lanes contain p53-QM and ubiquitination buffer. Lanes 1, 3, 5, 7 and 9 all contain purified proteasome and the others do not. Lanes 1-4 do not contain ubiquitin and 4-12 contain ubiquitin. Lanes 3 and 4 also contain both R3 and GST-MDM2. Lanes 5 and 6 contain GST-MDM2 with and without proteasome respectively. Lanes 7 and 8 contain GST-R3 with and without proteasome respectively. Lanes 9 and 10 contain both R3 and GST-MDM2 with and without proteasome respectively.

While not as dramatic as the result in Figure 4.6, the significant reduction of high molecular weight bands in lane 9 compared to lane 10, strongly suggests that p53 is being degraded by the proteasome. Comparison of lanes 5 and 6 suggests that poly-ubiquitination catalysed by GST-MDM2 may be susceptible

to degradation, although there is no evidence that the same is true for R3 (lanes 7 and 8). Figures 4.6 and 4.7 provide clear evidence that MDM2 and R3 acting together are able to catalyse proteasome-mediated degradation of p53, whereas the E3s acting alone are not. In addition it provides clear evidence that the proteasome immunopurified from mammalian cell lysates as part of this work is indeed active.

Given the degree of variability of the ubiquitination seen in these assays, an objection (albeit an unlikely one) that could be raised is that the ubiquitination reaction failed to work exactly in those lanes to which MG132 was added. To counter this objection it would indeed have been better to have performed the ubiquitination reaction and then split it into 2, adding proteasome to one half but not to the other. That would have ensured that the same amount of ubiquitination was present in the reaction to which proteasome was added and to which it was not added. This procedure has since been adopted in our laboratory for all similar assays involving purified proteasome.

4.6. The DWNN domain is not required for ubiquitination of p53

The ubiquitin-like structure of the DWNN domain has previously led us to propose that it plays some role in the ubiquitination activity of RBBP6 (Pugh *et al.*, 2006). Such a role would not necessarily promote ubiquitination; it could also be inhibitory, such as that recently reported for the N-terminal ubiquitin-like domain of Parkin (Chaugule *et al.*, 2011). To investigate whether the DWNN domain is required for ubiquitination of p53, a truncated form of R3 containing

only the zinc knuckle and the RING finger (and hence the named “R2”) was amplified from R3 and cloned into a pGEX-6P-2 expression vector by a co-worker, Ms A'tieyah Salie. The final construct was codon optimised for expression in bacteria (inherited from the R3 construct) and contained a C-terminal His₆ tag in addition to the N-terminal GST-tag.

Bioinformatic analysis of the sequence of RBBP6 suggests that the region between the DWNN domain and the zinc knuckle is unstructured and plays the role of a flexible linker (unpublished observation). As reported above, R3 was found to be highly susceptible to degradation *in vitro*, leading to the hypothesis that it may be subject to proteolytic cleavage in this region. If that were the case then excluding the flexible region may yield a construct that was more stable and therefore more suitable for future structural studies. R2 was therefore designed to begin immediately after the linker region of R3, yielding a fragment corresponding to residues 143-335 of RBBP6. Including the N-terminal GPLGS stemming from the vector and the C-terminal His₆ tag, the resulting protein had a molecular weight of 22.7 kDa.

GST-R2-His₆ was expressed in bacteria by a co-worker, Ms A'tieyah Salie and the GST affinity tag removed prior to use in *in vitro* ubiquitination assays. The quadruple mutant form of p53, p53-QM, served as substrate and was detected using the same rabbit polyclonal anti-p53 antibody used in earlier assays (sc-6243 Santa Cruz Biotechnology, Inc., Santa Cruz, CA, USA). As mentioned

earlier, this antibody produces an artifactual band at 100 kDa and can therefore be ignored.

The results are shown in Figure 4.8. Despite high background and evidence of uneven transfer of proteins from the gel to the membrane (two whitish sloping lines over lanes 1-4), there is nevertheless evidence of poly-ubiquitination of p53-QM by GST-R3 and GST-MDM2, acting either separately or together (lanes 3-5). This is in line with previous data shown in Figure 4.7. Lane 6 shows that R2 (note, no GST) on its own is able to produce poly-ubiquitination of p53-QM that is at least as significant as that produced by GST-R3 (lane 4). The pattern of ubiquitination produced by MDM2 acting with R2 (lane 7) is similar to that produced by MDM2 acting with MDMX (lane 8), and is more significant than that produced by GST-MDM2 alone (lane 3). It is possible that the strength of the signal at the top of lane 6 has been reduced due to poor blotting efficiency; if so the effect produced by R2 alone may in fact be more significant than that produced by GST-R3. It should be noted that the lanes 6 and 7 include E2s UbchH1 and UbchH5b in addition to the UbchH5a used in lanes 3-5.

Since the ubiquitination activity of R2 appears to be at least as high as that of R3, we conclude that the DWNN domain does not enhance the poly-ubiquitination activity of RBBP6 for p53. On the other hand, despite repeated attempts we did not find strong evidence that the ubiquitination activity of R2 is significantly greater than that of R3, from which we conclude that the DWNN domain does not appear to inhibit the activity of RBBP6 for p53. However the

greater susceptibility of R3 to proteolysis makes it possible that the “R3” samples used earlier in this work were in fact R2. This question will be the focus of careful investigation in future work. It can nevertheless be concluded that the R2 fragment is more stable than R3 and therefore represents a more promising choice for studies of the ubiquitination activity of RBBP6 against p53.

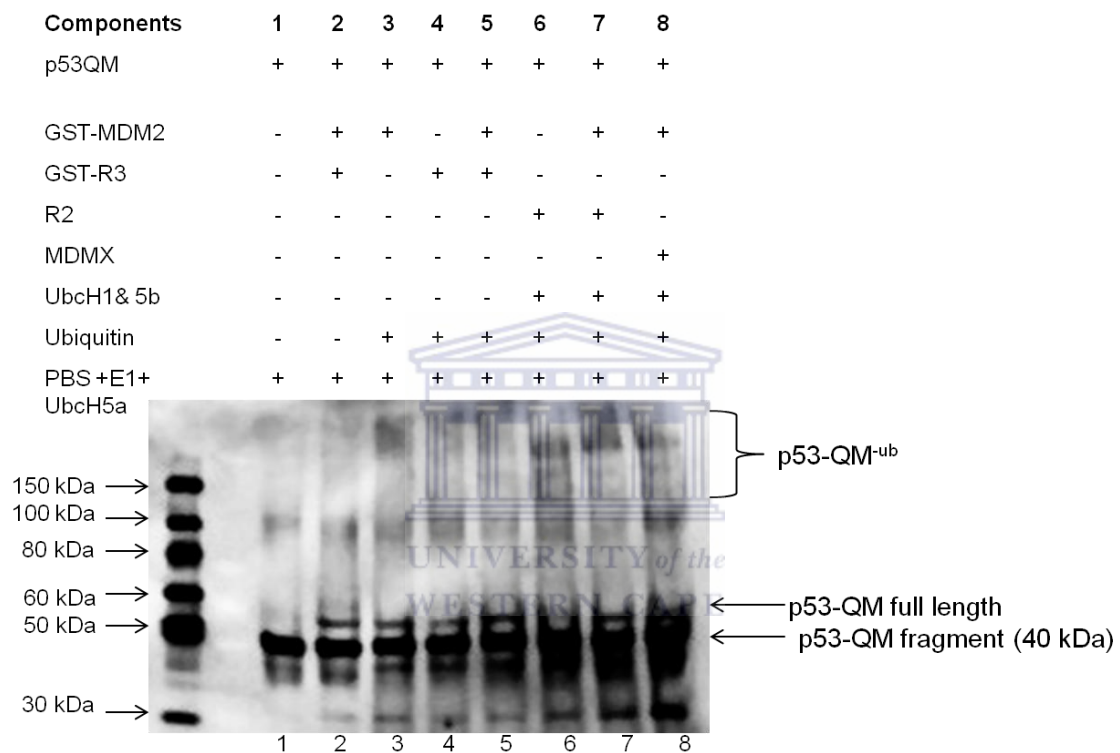
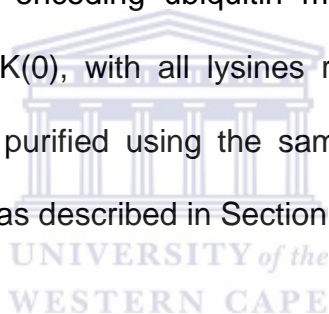


Figure 4.8 The DWNN domain is not required for the ubiquitination of p53. The ubiquitination of the p53 quadruple mutant (p53-QM) using GST-MDM2, GST-R3, and R2. All lanes contain p53-QM and the ubiquitination buffer. Lanes 1 and 2 are no ubiquitin controls, with lane 2 containing both E3s as well. Lanes 3-8 all contain ubiquitin. Lane 3 contains GST-MDM2 and Lane 4 contains GST-R3 with lane 5 containing both GST-MDM2 and GST-R3. Lane 6 contains R2 with additional E2s UbcH1 and UbcH5b. Lane 7 is the same as lane 6 with additional GST-MDM2. Lane 8 is a control lane containing GST-MDM2 and MDMX with additional E2s UbcH1 and UbcH5b. Note that the band at 100 kDa is an artefact of the anti-p53 antibody which can therefore be ignored.

4.7. Poly-ubiquitination of p53 catalysed by RBBP6 is Lys-48 linked

If all of the intra-chain isopeptide bonds making up a poly-ubiquitin chain involve lysine 48 of ubiquitin, then the chain is described as being “lysine48-linked”.

Lysine48-linked chains are strongly associated with recognition and degradation by the proteasome, although other linkages have recently also been linked with proteasomal degradation (Saeki *et al.*, 2009). Hence our earlier conclusion that a combination of MDM2 and R3 is sufficient to produce degradation of p53 in the presence of the proteasome makes it likely, but not certain, that the resulting poly-ubiquitin chains are lysine48-linked. Hence a more reliable method is required to establish whether the chains are lysine48-linked. Ubiquitin mutants lacking lysine48 cannot form such chains and have therefore been used to determine whether particular poly-ubiquitin chains are lysine48-linked or not. Expression constructs encoding ubiquitin mutants K48R, with lysine48 replaced by arginine, and K(0), with all lysines replaced by arginines, were expressed in bacteria and purified using the same cation exchange method used for wild type ubiquitin, as described in Section 3.7.



Using His₆-p53 as the substrate and Ubch5a as E2, fully *in vitro* assays were conducted to establish whether GST-R3, GST-MDM2 and MDMX could produce ubiquitination using the different forms of ubiquitin. The results are as shown in Figure 4.9. As expected GST-MDM2/MDMX produced clear evidence of poly-ubiquitination with wild type ubiquitin (lane 6) but not with ubiquitin-K0 (lane 7) or ubiquitin-K48R (lane 8), nor when ubiquitin was omitted altogether (lane 5), indicating that the poly-ubiquitin chains are lysine48-linked. Similarly, GST-MDM2/GST-R3 was able to produce poly-ubiquitination using wild-type ubiquitin (lane 2) but not with ubiquitin-K0 (lane 3) or ubiquitin-K48R (lane 4),

nor when ubiquitin was omitted altogether (lane 1), confirming that the poly-ubiquitin chains produced by GST-MDM2/GST-R3 are lysine48-linked.

Other faint bands can be seen between 50 and 100 kDa and above 150 kDa which are present in most lanes, including the no-ubiquitin lanes 1 and 5. Rather than being evidence of mono-ubiquitination these are more likely to be background similar to the artifactual band at 100 kDa seen in earlier assays.

An important draw-back of the results shown in Figure 4.9 are that there are no positive controls for the ubiquitin mutants, to show that they were present in similar quantities to wild type ubiquitin and competent to produce ubiquitination under the right circumstances. Ideally the Western blot should have been stripped and re-probed with anti-ubiquitin antibodies in order to show that similar quantities of all three were present in the assays. Alternatively, using anti-ubiquitin to detect ubiquitinated p53 would also have allowed the amount of ubiquitin present to be gauged. More sophisticated controls would include the use of substrates known to be poly-ubiquitinated with chain-linkages other than lysine48, in order to verify that ubiquitin-K48R is competent to produce such chains. However, the preliminary nature of the result in Figure 4.9 did not justify the use of such complex controls.

In addition, in light of the earlier discussion of the possible effects of GST on the ubiquitination activity of MDM2, Figure 4.9 does not rule out the possibility that the poly-ubiquitination in lanes 2 and 6 is due to GST-MDM2 alone, in which

case no conclusions could be drawn about the linkages of chains catalysed only by the combination of MDM2 and R3. For this reason it would have been useful to have included E3s without GST attached. Unfortunately time constraints did not allow this, but it is the focus of ongoing research in the laboratory.

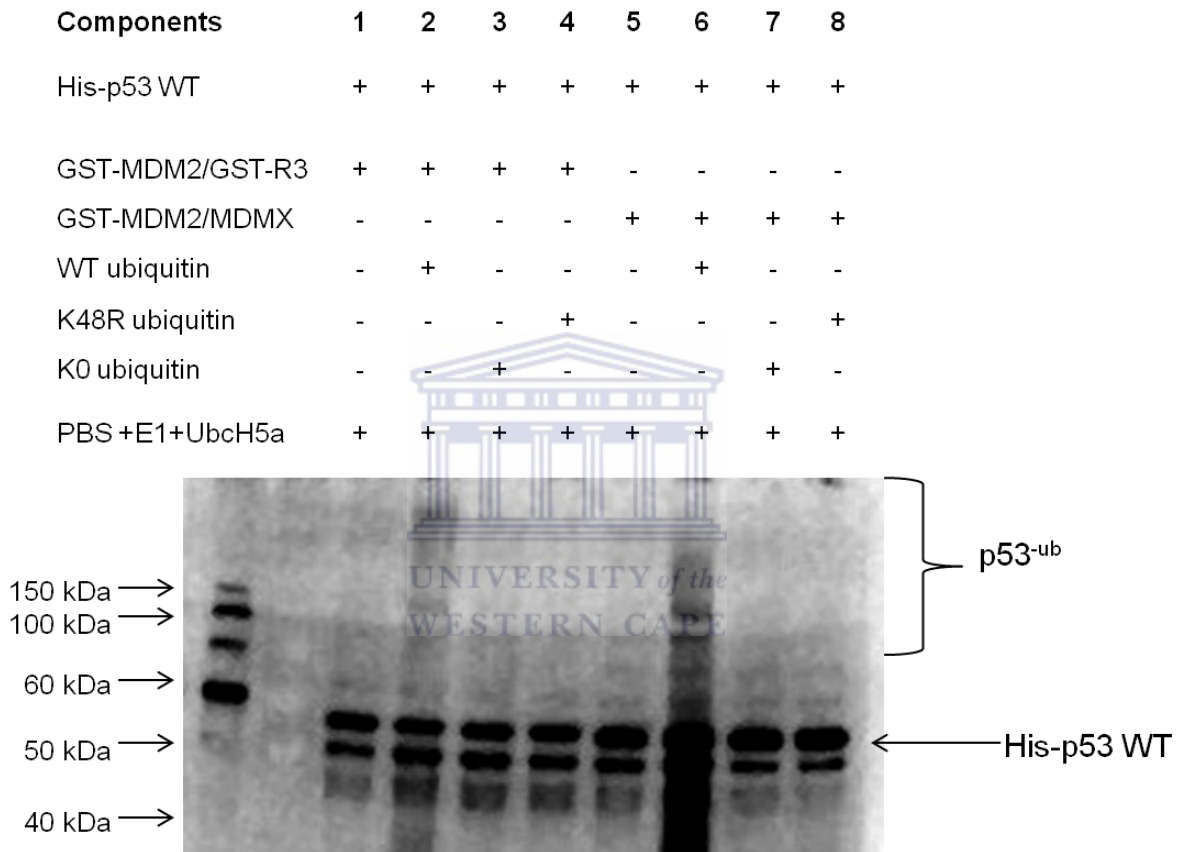


Figure 4.9. Poly-ubiquitination of p53 by GST-MDM2/GST-R3 is lysine48-linked. Poly-ubiquitination by GST-MDM2/GST-R3 is apparent when wild type ubiquitin is used (lane 2) but not when the K48R (lane 3) or K0 (lane 4) mutants are used, nor when ubiquitin is omitted entirely (lane 1). Similar results are observed for GST-MDM2/MDMX, which is as expected and therefore lends credibility to the results for GST-MDM2/GST-R3.

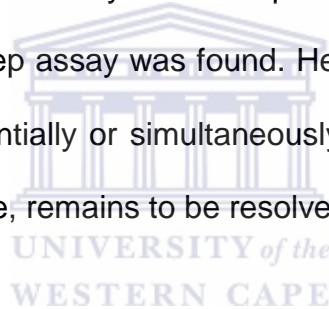
4.8. RBBP6 could potentially serve as an E4 poly-ubiquitin chain extension factor for p53

An E4 chain extension factor is an enzyme that catalyses the extension of an existing poly-ubiquitin chain, but not the addition of the first ubiquitin to the substrate. Due to the fact that RBBP6 has been reported to facilitate poly-ubiquitination of p53 by MDM2, but not to be able to catalyse ubiquitination itself, the question should be asked whether RBBP6 plays the role of an E4 for p53. Wu and co-workers showed that Ube4b is an E4 for p53 using a 2-step assay in which MDM2 was first used to mono-ubiquitinate p53, whereafter p53 was immunoprecipitated and then added to a fresh ubiquitination reaction including Ube4b but not MDM2 (Wu *et al.*, 2011). The results of an initial investigation using the above protocol are shown in Figure 4.10(A). The assay was conducted using p53, MDM2 and R3, with all GST tags removed.

High molecular weight bands are seen when MDM2 was added in Step 1 (before immunoprecipitation) and R3 in Step 2 (after immunoprecipitation) (lane 5) but not when R3 was omitted from Step 2 (lane 4), which suggests that R3 is required for poly-ubiquitination of p53. But similar bands are not seen when MDM2 was omitted from Step 1 (lane 3), which suggests that R3 cannot poly-ubiquitinate without prior mono-ubiquitination by MDM2. As expected, poly-ubiquitination was also not seen when R3 was added to Step 1 and MDM2 to Step 2 (lane 6), nor when both E3s were omitted from both steps (lanes 1 and 2). The heavy signal between 25 and 50 kDa is largely due to detection by the secondary antibody of the heavy and light chains of the anti-p53 primary

antibody, which was present on the membrane because of its presence in the SDS-PAGE due to its use in the immunoprecipitation step.

The result shown in panel (A) suggests that R3 is only able to poly-ubiquitinate p53 following prior mono-ubiquitination by MDM2. It also implies that MDM2 and R3 do not have to be present simultaneously at the substrate in order to poly-ubiquitinate it, which contrasts with a model in which MDM2 and R3 have to associate directly during ubiquitination, such as in the scaffold model proposed by Li and co-workers (Li *et al.*, 2007). However, despite numerous attempts to repeat this result, such as the assay shown in panel (B), no further evidence of poly-ubiquitination in a 2-step assay was found. Hence the question of whether R3 and MDM2 work sequentially or simultaneously or, in other words whether R3 functions as an E4 ligase, remains to be resolved.



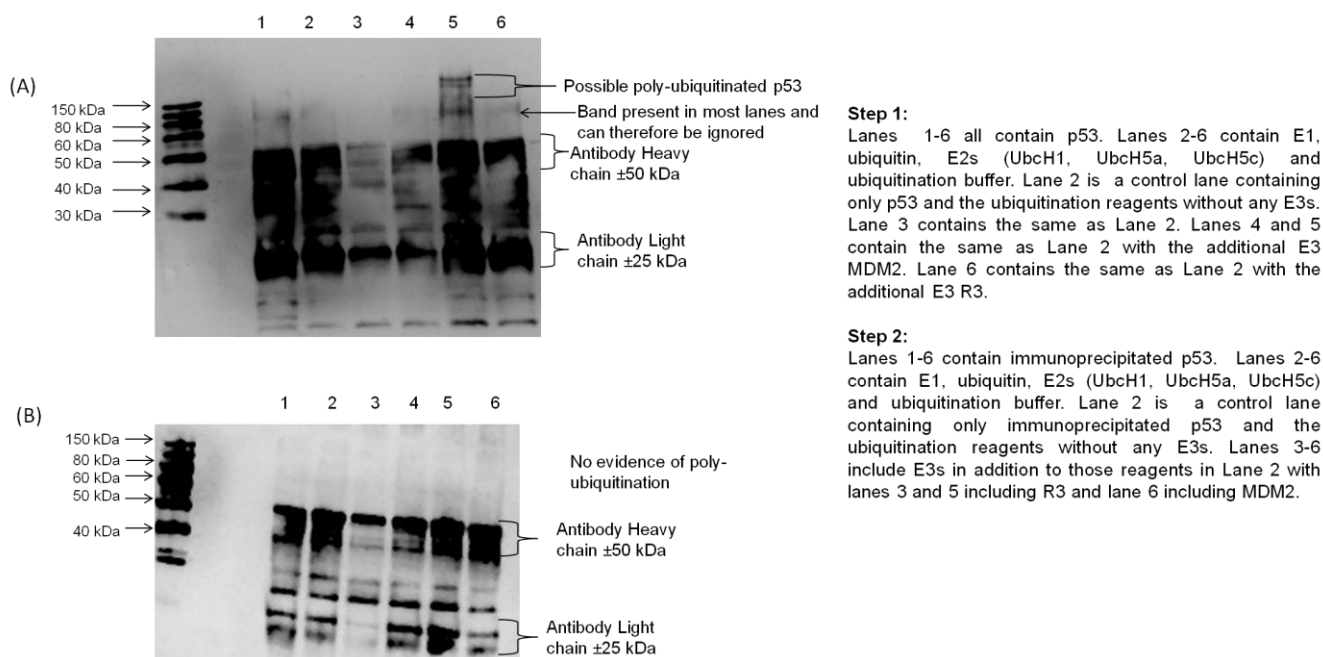


Figure 4.10 “Two-step” assay to determine if R3 functions as an E4. (A) and (B) Step I is MDM2 mono-ubiquitination. p53 is then immunoprecipitated using anti-p53 and step II is the R3 poly-ubiquitinating step using the mono-ubiquitinated p53 from step I. p53, MDM2 and R3 have been cleaved and purified of their GST tags. Lane 1 and 2 are the controls containing no E3s. Lane 3 has nothing added in step I, but R3 is added in step II. Lane 4 has MDM2 only added in step I and nothing in step II. Lane 5 has MDM2 added in step I and R3 added in step II. Lane 6 has R3 added in step I and MDM2 added in step II. The immunoprecipitation was done with anti-p53 rabbit polyclonal antibody and Western blotted using 1:1000 anti-p53 rabbit polyclonal antibody; secondary 1:2000 donkey anti-rabbit antibody.

4.9. p53 and R3 interact directly in vitro

Simons and co-workers have previously reported that RBBP6 interacts directly with p53, and identified a “p53 binding region” near the C-terminus of RBBP6 (Simons *et al.*, 1997). Our results suggest that the R2 and R3 fragments of RBBP6, which do not contain the domain identified by Simons and co-workers is nevertheless able to ubiquitinate p53 raising the question of whether the R3 fragment can bind directly to p53. A Far Western blot, or “blot overlay”, was performed to test this possibility. In a Far Western blot, a PVDF membrane onto

which one of the putative interactors (call it Protein 1) has been blotted, is incubated with the other interactor (call it Protein 2) and then washed to remove non-interacting Protein 2. The membrane is then immunodetected using antibodies recognising Protein 2. If the two proteins interact then Protein 2 will be detected at molecular weights characteristic of Protein 1. An advantage of the method is that the interactions of a single Protein 2 can be investigated simultaneously with a number of different Protein 1s (R. Hall, 2004).

The results can be seen in Figure 4.11(A). In this case, Protein 2 was p53 and the set of Protein 1s contained GST-R3 (lane 6; approximately 60 kDa), as well as proteins expected to interact with p53 including GST-MDM2 (lane 1; full length at 100 kDa and major degradation product at 60 kDa) and the E2 Ubch5c (lane 2; 17 kDa), as well as GST (lane 3; 27 kDa), which is not expected to interact with p53. The above proteins were separated by SDS PAGE, transferred to a PVDF membrane and incubated with p53, after which the membrane was washed thoroughly to remove unbound p53. The membrane was then immunodetected with rabbit poly-clonal anti-p53 antibody (sc-6243 Santa Cruz Biotechnology, Inc., Santa Cruz, CA, USA). Figure 4.11(B) is an independent repeat of (A) with proteins loaded as indicated.

The detection of p53 in lane 2 at the molecular weight of Ubch5c and the lack of p53 at the molecular weight of GST in lane 3 generate confidence that the assay is working as expected. In addition, the ladder of bands in lane 1 in both (A) and (B) suggests that p53 interacts with MDM2 and its degradation

products, again as expected. The ladder of bands in lane 4 in (A) and lane 3 in (B), at molecular weights consistent with GST-R3 and its degradation products suggests that there is a direct interaction between R3 and p53.

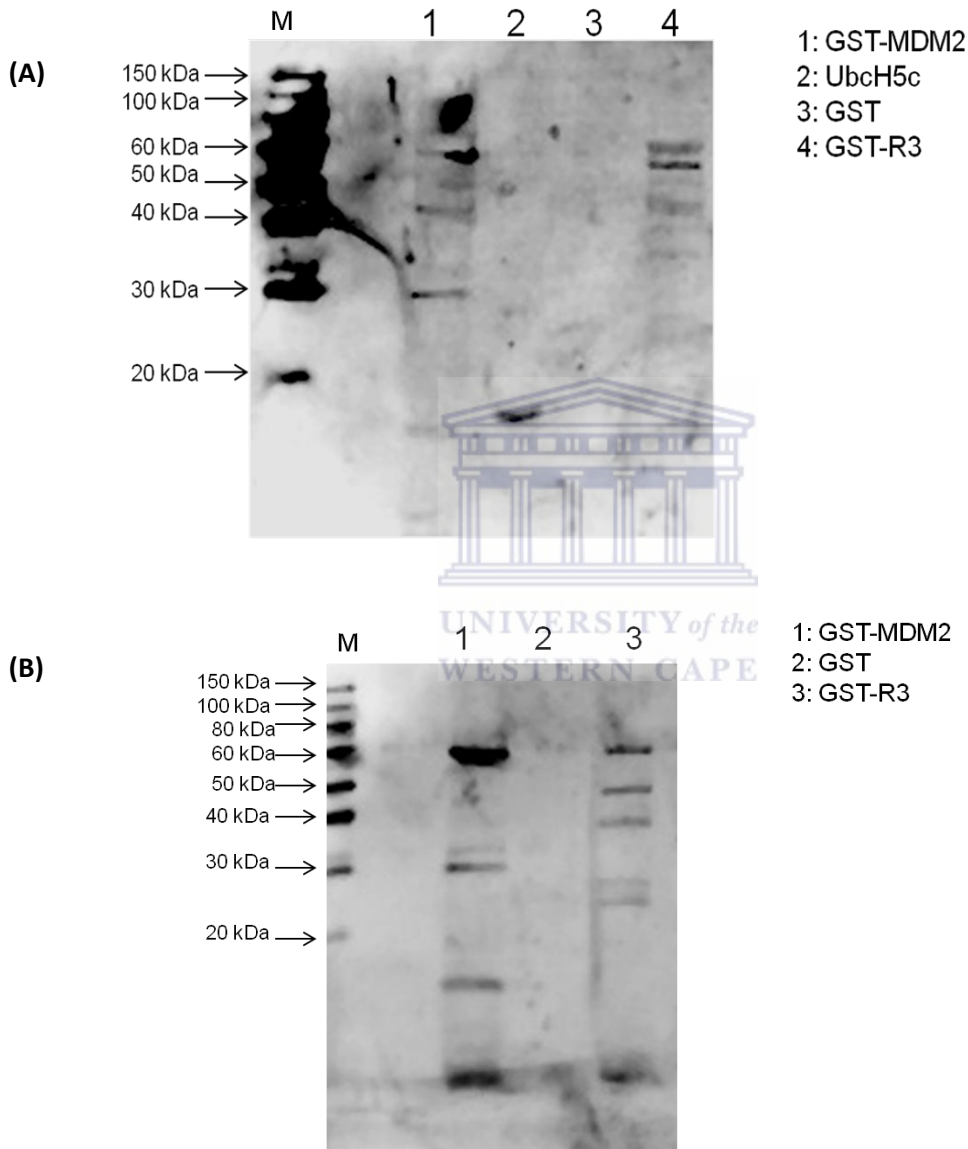


Figure 4.11 Far Western blot overlay showing interaction between p53 and GST-R3. GST-R3 interact directly with p53 ((A) lane 4 and (B) lane 3) M is the marker lane. (A) Lanes 1 and 2 contain the positive controls GST-MDM2 and Ubch5c respectively. Lane 3 the negative control GST. Lane 4 contains GST-R3. (B) Lane 1 is the positive control GST-MDM2. Lane 2 is the negative control GST and lane 3 is GST-R3. Equal amounts of each protein were loaded onto the gel and separated. Transfer onto PVDF membrane, blocking and subsequent probing using 100 ng of His-p53 protein. A 1:750 dilution of anti-p53 rabbit polyclonal antibody and 1:1000 dilution of donkey anti-rabbit secondary antibody used.

CHAPTER 5

Discussion and Conclusion

It has been previously established by Li and co-workers that Retinoblastoma Binding Protein 6 (RBBP6) plays a major role in suppressing levels of p53 levels during development by promoting its poly-ubiquitination and degradation in the proteasome (Li *et al.*, 2007). The main objective of this project was therefore to investigate the role of RBBP6 in ubiquitination of p53 in more detail using *in vitro* assays. Since RBBP6 is a large, multi-domain protein that is unsuited to expression in bacteria, a shortened fragment dubbed R3 and containing the first three domains of RBBP6 (DWNN, zinc knuckle and RING finger domains), was used *in vitro* assays. The fact that this fragment corresponds to the major isoform of RBBP6 found in lower eukaryotes lends support to the hypothesis that R3 contains most, if not all, of the ubiquitination activity of full length RBBP6. However, since it excludes the reported p53 binding domain near the C-terminus of RBBP6, if it were able to catalyse ubiquitination of p53 it would potentially rule out the model proposed by Li and co-workers whereby RBBP6 functions as a scaffold bringing p53 and MDM2 together.

In vitro ubiquitination reactions required the bacterial expression and purification of a number of different proteins, including the substrate p53 (wild type, both His₆- and GST-tagged and the stabilised quadruple mutant which was His₆-tagged), ubiquitin-ligating enzymes R3 and MDM2, E1, a number of different

ubiquitin conjugating enzymes (E2s), ubiquitin activating enzyme (E1) and ubiquitin (wild-type and mutants K0 and K48R). The 26S proteasome was immunopurified from human cell lysates supplied by a co-worker.

As a first step, “partially *in vitro*” assays were conducted using human cell lysate to supply E1 and E2 enzymes, as well as the proteasome. The proteasome inhibitor MG132 and the poly-ubiquitin-binding protein MultiDsk were added to block the action of the proteasome and de-ubiquitination enzymes respectively. Addition of both R3 and MDM2 to HepG2 lysate led to massive increase of higher molecular weight species of p53 consistent with poly-ubiquitination (Figure 4.1, panel A). However there was no consistent decrease indicative of proteasome-induced degradation when MG132 was omitted. This could be due to the proteasome not being active or to the poly-ubiquitination not targeting p53 to the proteasome. When the assay was repeated the same heavy poly-ubiquitination was observed, but only when both R3 and MDM2 were present (panel B). Addition of MultiDsk again had no significant effect; whether this was due to lack of active proteasome or de-ubiquitination enzymes, or to insufficient or non-functional MultiDsk is difficult to determine from this preliminary summary.

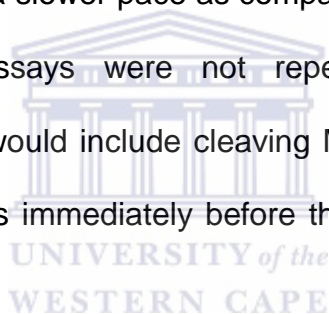
Although this assay provides no evidence about the mechanism behind the effect, it nevertheless shows conclusively that R3 stimulates poly-ubiquitination of p53. Since roughly equal amounts of R3 and MDM2 were used in the assay

(data not shown), it suggests that the activity of R3 is of the same order as that of MDM2, which is known to be the most important regulator of p53.

The first fully *in vitro* assays were conducted using the MDM2/MDMX system as a bench-mark as it is well known to produce poly-ubiquitination of p53. A simple titration assay was conducted using a small selection of E2s (UbcH1, UbcH5a, UbcH5b and UbcH5c) in which concentrations of GST-MDM2/MDMX were progressively increased in order to determine which concentration gave the best ubiquitination of p53. This was repeated for GST-MDM2/GST-R3 and although the results were not as impressive as that of the MDM2/MDMX combination, it established that we were able to produce ubiquitination of p53 in a fully *in vitro* assay using approximately 1 μ M of GST-MDM2 and GST-R3. However it should be admitted that the lack of a no-MDM2 control means that the possibility that the effect is entirely due to MDM2 is not ruled out.

Ubiquitin conjugating enzymes (E2s) UbcH5a and UbcH5c were found to work best with GST-MDM2 and GST-R3 in ubiquitinating p53. As previously, the lack of a no-MDM2 control means that this assay does not rule out the possibility that the effect is entirely due to GST-MDM2 which has been reported to be able to catalyse poly-ubiquitination. Nevertheless, this result prompted us to use UbcH5a and UbcH5c as first choice E2s in subsequent investigations. In order to address the problems raised in the previous two assays, R3 and MDM2 were added separately and in combination in the next *in vitro* reaction. GST was also removed from GST-R3 in order to avoid potential artefacts resulting from GST-

driven dimerisation. Figure 4.5 shows that un-tagged R3 was able to at least mono-ubiquitinate p53 *in vitro* (lane 3), producing an effect similar to that of GST-MDM2. When R3 and GST-MDM2 were combined the effect was stronger, although whether this qualifies as cooperative behaviour or is simply additive is not clear from this assay. Although from this assay we could establish that GST-R3 independently plays a role in the ubiquitination of p53, the GST attached to MDM2 may cast a negative shadow on these promising results. MDM2 was found to be able to degrade quickly once expressed and purified, even with the GST tag attached (Figure 4.11 B), although the GST did provide a mechanism for this process to occur at a slower pace as compared without the GST. Due to time limitations, these assays were not repeated with their non-GST counterparts. Future work would include cleaving MDM2 and R3 from its GST tag and utilising it in assays immediately before the degradation becomes too severe.



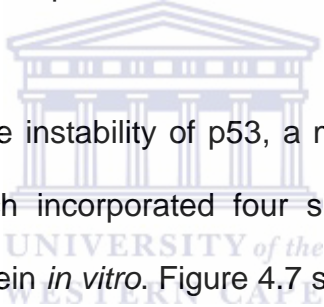
The previous assay suggested that R3 was at least able to multiply mono-ubiquitinate p53, and that R3 and MDM2 may show cooperative behaviour. This posed the question of whether R3, acting either alone or in combination with MDM2, was able to catalyse poly-ubiquitination leading to proteasomal degradation. In order to investigate this, intact proteasomes were immunopurified from human cell lysates and added to *in vitro* ubiquitin reactions. Figure 4.6(A) shows that although both GST-R3 and GST-MDM2 were able to catalyse what appears to be poly-ubiquitination, producing a number of bands greater than 150 kDa, it did not appear to result in degradation

in the proteasome. In contrast, when GST-R3 and GST-MDM2 were used together the p53 appeared to be completely degraded. Supporting this conclusion, addition of MG132 completely rescued p53 and poly-ubiquitinated bands. This result suggests strongly that R3 and MDM2, acting together, are able to catalyse poly-ubiquitination that is recognised by the proteasome, whereas acting independently they are not.

The above result therefore supports the conclusions of Li and co-workers (Li *et al.*, 2007) that RBBP6 cooperates with MDM2 to poly-ubiquitinate p53, leading to degradation in the proteasome. However, whereas their result was achieved *in vivo*, where un-identified factors may be present, this result was achieved in the defined environment of an *in vitro* assay. In addition, this result was obtained using the smaller R3 fragment of RBBP6 (residues 1–335), which does not contain the putative p53-binding domain identified previously (Simons *et al.*, 1997). It would therefore appear to rule out the scaffold model proposed by Li and co-workers in which RBBP6 brings MDM2 and p53 together.

An objection that can be raised against the result shown in Figure 4.6 is that p53, MDM2 and R3 are all tagged with GST. It may be suggested that homo-dimerisation of GST may influence the results, as shown for GST-MDM2 by Wang and co-workers (Wang *et al.*, 2011). However the fact that GST-MDM2 and GST-R3 were unable to catalyse degradation of p53 under exactly the same conditions suggests strongly that GST is not responsible for the effect. Nevertheless attempts were therefore made to remove GST from the substrate

and both E3s; however this proved extremely difficult as the protein became unstable and prone to precipitation, reducing concentrations and introducing degradation products which complicated analysis of ubiquitination ladders. This was particularly problematic for MDM2, and the concentrations of MDM2 in many of our assays were possibly lower than expected due to degradation and precipitation. For this reason, it would have been a good idea to strip Western blots following detection of p53, re-probing with anti-MDM2 and anti-R3 to establish how much of each E3 was present in each assay. However this proved technically very challenging and time-consuming and was therefore deemed to be outside of the scope of this thesis.



In an attempt to address the instability of p53, a mutant form was cloned and expressed in bacteria which incorporated four single amino acid mutations reported to stabilise the protein *in vitro*. Figure 4.7 shows that this form, denoted p53-QM for “quadruple mutant”, can also be poly-ubiquitinated by R3 (no GST tag). As before, R3 appears to be more effective in poly-ubiquitinating p53 when acting in conjunction with GST-MDM2, and this poly-ubiquitinating is able to catalyse degradation in the proteasome (compare lanes 9 and 10).

The ubiquitin-like structure of DWNN domain raised the question as to whether it plays a role in the ubiquitination activity of R3. To address this question a shortened form of R3, excluding the DWNN domain and denoted R2, was cloned and expressed by a co-worker and incorporated into *in vitro* ubiquitination assays.

The ubiquitination activity of R2 (no GST tag) was not significantly different from that of GST-R3 (Figure 4.8). This would appear to rule out the hypothesis that the DWNN domain functions as an inhibitory domain similar to that of Parkin (Chaugule *et al.*, 2011), but rather suggests that it is not required for the ubiquitination of p53. However R2 was found to be more stable than R3 and therefore more suitable for future functional and structural studies. Attempts to express sufficient quantities of R2 for NMR-based structural analysis are ongoing in the laboratory.

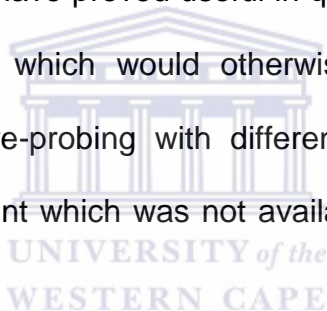
In this thesis we have shown unequivocally that R3 and MDM2, acting together, are able to catalyse addition of poly-ubiquitin chains to p53. The disappearance of both p53 and its ubiquitinated isoforms in the presence of immunoprecipitated proteasome, and their re-appearance in the presence of MG132, suggest that these chains are lysine48-linked. In order to further investigate the mode of linkage, ubiquitin mutants K(0) (all seven lysines replaced with arginines) and K48R (lysine48 replaced with arginine) were expressed and purified and incorporated in our *in vitro* ubiquitination assays. As shown in figure 4.9, poly-ubiquitination was seen when wild type ubiquitin was used, but neither when K(0) nor when K48R was used. This result reinforces the conclusion that the poly-ubiquitin chains produced by R3 and MDM2 are lysine48-linked. The three forms of ubiquitin behaved similarly during expression and purification, yielded similar amounts of protein and the same amounts were added to each assay; it would nevertheless have improved the assay if the blot shown in Figure 4.9 had been stripped and re-probed with anti-

ubiquitin to demonstrate that sufficient quantities of the mutants were present. This was not attempted for the reason outlined earlier.

A major drawback encountered in this thesis was the large variability of *in vitro* ubiquitination assays. A number of factors contribute to this. The first is the complex nature of the ubiquitination reaction, which consists of not one, but three consecutive enzymatic reactions. As with all enzymatic reactions, each is highly sensitive to the purity and quantity of reactants, including the presence of degradation products and contaminants, among other factors. The result is that the overall reaction depends sensitively on a number of unknown factors, leading to large variation in the results.

A second factor contributing to variability is the method of detection. Western blots rely on transfer of proteins from a poly-acrylamide gel to a membrane, a process which is not always equally efficient for all proteins and often shows different efficiency within different parts of the same gel. Western blotting relies furthermore on the binding of antibodies to target proteins; antibodies are themselves highly unreliable and their efficacy may differ significantly from one batch to another. Chemiluminescence, because it is also an enzymatic process, is again a highly variable process. It also has poor linearity, which means that the strength of the signal is not always well correlated with the quantity of protein being detected. In particular they saturate easily, which makes them particularly poor at distinguishing between strong signals.

Despite all of these drawbacks, Western blotting remains the standard method for studying ubiquitination. Nevertheless, there are a number of improvements could be made in future to reduce the variability of our results. One is the replacement of chemiluminescent detection with fluorescent detection. Instead of using secondaries conjugated to horseradish peroxidase, secondaries conjugated to fluorophores are used, with detection using a fluorescence-enabled camera. This has been shown to be significantly more linear than chemiluminescence. An additional advantage is that it is compatible with multiplexing, which means that more than one protein can be detected simultaneously. This would have proved useful in quantitating enzymes such as the various E2s and E3s which would otherwise have required repeated stripping of the blot and re-probing with different antibodies. However this requires specialised equipment which was not available in our laboratory during the course of this project.



Another possible improvement would involve replacing Western blot detection with a plate-based solution assay. An example is the AlphaLisa technology from Perkin Elmer, in which the substrate is coupled to a fluorophore and another fluorophore is coupled to a protein with high affinity for poly-ubiquitin chains. Poly-ubiquitination of the substrate causes the two fluorophores to come into close proximity with one another, leading to modulation of their fluorescence spectra which is detected by a plate reader. Use of this technology was attempted at the very beginning of this project, but it was not found to be easy to use and was abandoned in favour of Western blot-based detection.

Perhaps the easiest way of improving the assays used here would be to replace the p53-specific antibodies, which were repeatedly found to be of poor quality and variable from batch to batch, with a reliable antibody targeting an immuno-tag. Since p53 was heterologously produced in bacteria, it would have been very simple to engineer the expression plasmid to include an immuno-tag such as HA, cMyc or FLAG.

Another way in which ubiquitination assays could be simplified and therefore rendered less variable would be through use of E2 enzymes pre-charged with ubiquitin, thereby eliminating both the E1 activation step and the transfer of the ubiquitin from the E1 to the E2. UbcH5a, which was found to be active with respect to p53, RBBP6 and MDM2, is commercially available as an ubiquitin conjugate (for example Cat E2-802, R&D Systems, Inc., Minneapolis MN, USA). Such a system may be useful in situations where the role of UbcH5a had already been established; however in other investigations it may also be too restrictive and eliminate a number of alternative ubiquitination mechanisms.

RBBP6 was previously found to interact with p53 in a region near to the C-terminus of RBBP6 (Sakai *et al.*, 1995). The ability of the R3 fragment of RBBP6, which does not include the putative p53-binding domain, to catalyse ubiquitination of p53, with or without the assistance of MDM2, suggests that RBBP6 contains another p53 binding site, located within R3. Far Western blots were conducted in order to test this hypothesis, which involved incubating a membrane containing R3 and other potential interactors with recombinant p53,

followed by immunoblotting with anti-p53 antibody both (Figure 4.11). As shown in Figure 4.11, this method confirmed the presence of an interaction between GST-MDM2 and GST-R3, both of which are known to interact with p53, but no interaction was detected with GST, as expected.

In conclusion, this thesis provided strong support for the hypothesis that Retinoblastoma Binding Protein 6 (RBBP6) has ubiquitin ligase activity against p53 *in vitro*, using members of the UbcH5 family of ubiquitin conjugating enzymes (E2s). Although the results do not distinguish clearly between poly-ubiquitination and multiple mono-ubiquitination, there is at least some evidence that R3 may be able to catalyse poly-ubiquitination of p53. There is also strong evidence that when R3 and MDM2 are used together p53 is poly-ubiquitinated, leading to degradation in the proteasome. As expected these poly-ubiquitin chains are lysine48-linked, as was shown using the K48R mutants of ubiquitin. Assays were carried out using the stabilised quadruple mutant of p53 which demonstrated that the mutant is susceptible to ubiquitination and therefore a suitable substrate for *in vitro* investigations of the ubiquitin-mediated regulation of p53 (Joergher *et al.*, 2004).

Since R3 does not contain the reported p53-binding site of RBBP6, and the DWNN domain is not required for ubiquitination activity, the minimal active region of RBBP6 appears to be contained within the smaller R2 fragment. It is therefore unlikely that RBBP6 plays the role of a scaffold suggested by Li and co-workers (Li *et al.*, 2007), bringing p53 and MDM2 together. What then could

be the mechanism whereby R3 influences MDM2 in ubiquitination of p53? A possible scenario is that RBBP6 and MDM2 form a hetero-dimer through their respective RING finger domains, similar to the hetero-dimer formed between MDMX and MDM2. Future structural investigations will concentrate on this fascinating possibility.

Bibliography

Bai, L. & Zhu, W. 2006. p53 : Structure , Function and Therapeutic Applications. *Journal of Cancer Molecules*, 2(4): 141–153.

Braithwaite, A.W., Del Sal, G. & Lu, X. 2006. Some p53-binding proteins that can function as arbiters of life and death. *Cell death and differentiation*, 13(6): 984–93. Brooks, C.L. & Gu, W. 2011. P53 Regulation By Ubiquitin. *FEBS letters*, 585(18): 2803–9.

Brooks, C.L. & Gu, W. 2011. P53 Regulation By Ubiquitin. *FEBS letters*, 585(18): 2803–9.

Brooks, C.L., Li, M. & Gu, W. 2004. Monoubiquitination: The Signal for p53 Nuclear Export? *Cell Cycle*, 3(4): 436–438. Brown, C.J., Lain, S., Verma, C.S., Fersht, A.R. & Lane, D.P. 2009. Awakening guardian angels: drugging the p53 pathway. *Nature reviews. Cancer*, 9(12): 862–73.

Brown, C.J., Lain, S., Verma, C.S., Fersht, A.R. & Lane, D.P. 2009. Awakening guardian angels: drugging the p53 pathway. *Nature reviews. Cancer*, 9(12): 862–73.

Bullock, A. & Fersht, A. 2001. Rescuing the function of mutant p53. *Nature Reviews Cancer*, 1(October): 1–11.

Cayrol, C., Knibiehler, M. & Ducommun, B. 1998. p21 binding to PCNA causes G1 and G2 cell cycle arrest in p53-deficient cells. *Oncogene*, 16(3): 311–20.

Chaugule, V.K., Burchell, L., Barber, K.R., Sidhu, A., Leslie, S.J., Shaw, G.S. & Walden, H. 2011. Autoregulation of Parkin activity through its ubiquitin-like domain. *The EMBO journal*, 30(14): 2853–67.

Chen, C., Gherzi, R., Andersen, J.S., Gaietta, G., Ju, K., Royer, H., Mann, M. & Karin, M. 2000. Nucleolin and YB-1 are required for JNK-mediated interleukin-2 mRNA stabilization during T-cell activation. *Genes & development*, 14: 1236–1248.

Chen, J., Tang, H., Wu, Z., Zhou, C., Jiang, T., Xue, Y., Huang, G., Yan, D. & Peng, Z. 2013. Overexpression of RBBP6, alone or combined with mutant TP53, is predictive of poor prognosis in colon cancer. *PloS one*, 8(6): e66524.

Cheng, T.-H. & Cohen, S.N. 2007. Human MDM2 isoforms translated differentially on constitutive versus p53-regulated transcripts have distinct functions in the p53/MDM2 and TSG101/MDM2 feedback control loops. *Molecular and cellular biology*, 27(1): 111–9.

Chibi, M., Meyer, M., Skepu, A., G Rees, D.J., Moolman-Smook, J.C. & Pugh, D.J.R. 2008. RBBP6 interacts with multifunctional protein YB-1 through its RING finger domain, leading to ubiquitination and proteosomal degradation of YB-1. *Journal of molecular biology*, 384(4): 908–16.

Ciechanover, A. & Stanhill, A. 2014. The complexity of recognition of ubiquitinated substrates by the 26S proteasome. *Biochimica et biophysica acta*, 1843(1): 86–96.

Dantuma, N.P. & Lindsten, K. 2010. Stressing the ubiquitin-proteasome system. *Cardiovascular research*, 85(2): 263–71.

David, Y., Ternette, N., Edelmann, M.J., Ziv, T., Gayer, B., Sertchook, R., Dadon, Y., Kessler, B.M. & Navon, A. 2011. E3 ligases determine ubiquitination site and conjugate type by enforcing specificity on E2 enzymes. *The Journal of Biological Chemistry*, 286(51): 44104–15.

Efeyan, A. & Serrano, M. 2007. The Guardian of the Genome and Policeman of the Oncogenes. *Cell Cycle*, 6(9): 1006–1010.

Di Giammartino, D., Li, W., Ogami, K., Yashinski, J., Hoque, M., Tian, B. & Manley, J. 2014. RBBP6 isoforms regulate the human polyadenylation machinery and modulate expression of mRNAs with AU-rich 3'UTRs. *Genes & Development*, 28: 2248–2260.

Haldeman, M.T., Xia, G., Kasperek, E.M. & Pickart, C.M. 1997. Structure and Function of Ubiquitin Conjugating Enzyme E2-25K: The Tail Is a Core-Dependent Activity Element †. *Biochemistry*, (36): 10526–10537.

Hall, R. 2004. Studying protein-protein interactions via blot overlay or Far Western blot. *Methods in Molecular Biology*, 261: 167–174.

Hayter, J.R., Doherty, M.K., Whitehead, C., McCormack, H., Gaskell, S.J. & Beynon, R.J. 2005. The subunit structure and dynamics of the 20S proteasome in chicken skeletal muscle. *Molecular & cellular proteomics : MCP*, 4(9): 1370–81.

Hjerpe, R., Aillet, F., Lopitz-Otsoa, F., Lang, V., England, P. & Rodriguez, M.S. 2009. Efficient protection and isolation of ubiquitylated proteins using tandem ubiquitin-binding entities. *EMBO reports*, 10(11): 1250–8.

Hock, A.K. & Vousden, K.H. 2014. The role of ubiquitin modification in the regulation of p53. *Biochimica et biophysica acta*, 1843(1): 137–49.

Hoe, K.K., Verma, C.S. & Lane, D.P. 2014. Drugging the p53 pathway: understanding the route to clinical efficacy. *Nature reviews. Drug discovery*, 13(3): 217–36.

Homer, C., Knight, D. a, Hananeia, L., Sheard, P., Risk, J., Lasham, A., Royds, J. a & Braithwaite, A.W. 2005. Y-box factor YB1 controls p53 apoptotic function. *Oncogene*, 24(56): 8314–25.

Honda, R., Tanaka, H. & Yasuda, H. 1997. Oncoprotein MDM2 is a ubiquitin ligase E3 for tumor suppressor p53. *FEBS letters*, 420(1): 25–7.

Huang, P., Ma, X., Zhao, Y. & Miao, L. 2013. The C. elegans Homolog of RBBP6 (RBPL-1) regulates fertility through controlling cell proliferation in the germline and nutrient synthesis in the intestine. *PloS one*, 8(3): e58736.

Jensen, J.P., Bates, P.W., Yang, M., Vierstra, R.D. & Weissman, A.M. 1995. Identification of a Family of Closely Related Human Ubiquitin Conjugating Enzymes *. *The Journal of biological chemistry*, 270(51): 30408–30414.

Joerger, A.C., Allen, M.D. & Fersht, A.R. 2004. Crystal structure of a superstable mutant of human p53 core domain. Insights into the mechanism of rescuing oncogenic mutations. *The Journal of biological chemistry*, 279(2): 1291–6.

Kao, A., Randall, A., Yang, Y., Patel, V.R., Kandur, W., Guan, S., Rychnovsky, S.D., Baldi, P. & Huang, L. 2012. Mapping the structural topology of the yeast 19S proteasomal regulatory particle using chemical cross-linking and probabilistic modeling. *Molecular & cellular proteomics : MCP*, 11(12): 1566–77.

Kappo, M., AB, E., Hassem, F., Atkinson, R.A., Faro, A., Muleya, V., Mulaudzi, T., Poole, J.O., McKenzie, J.M., Chibi, M., Moolman-Smook, J.C., Rees, D.J.G. & Pugh, D.J.R. 2011. Solution Structure of RING Finger-like Domain of

Retinoblastoma-binding Protein-6 (RBBP6) Suggests It Functions as a U-box. *The Journal of biological chemistry*, 287(10): 7146–58.

Khan, F., Allam, M., Tincho, M. & Pretorius, A. 2014. Implications of RBBP6 in various types of Cancer. In *Proceedings IWBBIO*. 727–737.

Koegl, M., Hoppe, T., Schlenker, S., Ulrich, H.D., Mayer, T.U. & Jentsch, S. 1999a. A Novel Ubiquitination Factor , E4 , Is Involved in Multiubiquitin Chain Assembly. *Cell*, 96: 635–644.

Koegl, M., Hoppe, T., Schlenker, S., Ulrich, H.D., Mayer, T.U. & Jentsch, S. 1999b. A Novel Ubiquitination Factor , E4 , Is Involved in Multiubiquitin Chain Assembly. *Cell*, 96: 635–644.

Lai, Z., Ferry, K. V, Diamond, M. a, Wee, K.E., Kim, Y.B., Ma, J., Yang, T., Benfield, P. a, Copeland, R. a & Auger, K.R. 2001. Human mdm2 mediates multiple mono-ubiquitination of p53 by a mechanism requiring enzyme isomerization. *The Journal of biological chemistry*, 276(33):

Lee, J.T. & Gu, W. 2010. The multiple levels of regulation by p53 ubiquitination. *Cell death and differentiation*, 17(1): 86–92.

Lee, S.D. & Moore, C.L. 2014. Efficient mRNA polyadenylation requires a ubiquitin-like domain, a zinc knuckle, and a RING finger domain, all contained in the Mpe1 protein. *Molecular and cellular biology*, 34(21): 3955–67.

Lee, S.W., Seong, M.W., Jeon, Y.J. & Chung, C.H. 2012. Ubiquitin E3 ligases controlling p53 stability. *Animal Cells and Systems*, 16(3): 173–182.

Levine, A.J. 1997. p53 , the Cellular Gatekeeper for Growth and Division. , 88: 323–331.

Li, L., Deng, B., Xing, G., Teng, Y., Tian, C., Cheng, X., Yin, X., Yang, J., Gao, X., Zhu, Y., Sun, Q., Zhang, L., Yang, X. & He, F. 2007. PACT is a negative regulator of p53 and essential for cell growth and embryonic development. *Proceedings of the National Academy of Sciences of the United States of America*, 104(19): 7951–6.

Liu, D.P., Song, H. & Xu, Y. 2010. A common gain of function of p53 cancer mutants in inducing genetic instability. *Oncogene*, 29(7): 949–56.

Mather, A., Rakgotho, M. & Ntwasa, M. 2005. SNAMA, a novel protein with a DWNN domain and a RING finger-like motif: a possible role in apoptosis. *Biochimica et biophysica acta*, 1727(3): 169–76.

Metzger, M.B., Pruneda, J.N., Klevit, R.E. & Weissman, A.M. 2014. RING-type E3 ligases: master manipulators of E2 ubiquitin-conjugating enzymes and ubiquitination. *Biochimica et biophysica acta*, 1843(1): 47–60.

Miotto, B., Chibi, M., Xie, P., Koundrioukoff, S., Moolman-Smook, H., Pugh, D., Debatisse, M., He, F., Zhang, L. & Defossez, P.-A. 2014. The RBBP6/ZBTB38/MCM10 axis regulates DNA replication and common fragile site stability. *Cell reports*, 7(2): 575–87.

Morisaki, T., Yashiro, M., Kakehashi, A., Inagaki, A., Kinoshita, H., Fukuoka, T., Kasashima, H., Masuda, G., Sakurai, K., Kubo, N., Muguruma, K., Ohira, M., Wanibuchi, H. & Hirakawa, K. 2014. Comparative proteomics analysis of gastric cancer stem cells. *PloS one*, 9(11): e110736.

Motadi, L.R., Bhoola, K.D. & Dlamini, Z. 2011. Expression and function of retinoblastoma binding protein 6 (RBBP6) in human lung cancer. *Immunobiology*, 216(10): 1065–73.

Newton, K., Matsumoto, M.L., Wertz, I.E., Kirkpatrick, D.S., Lill, J.R., Tan, J., Dugger, D., Gordon, N., Sidhu, S.S., Fellouse, F. a, Komuves, L., French, D.M., Ferrando, R.E., Lam, C., Compaan, D., Yu, C., Bosanac, I., Hymowitz, S.G., Kelley, R.F. & Dixit, V.M. 2008. Ubiquitin chain editing revealed by polyubiquitin linkage-specific antibodies. *Cell*, 134(4): 668–78.

Niklova, P., Henckel, J., Lane, D. & Fersht, A. 1998. Semirational design of active tumor suppressor p53 DNA binding. *Proceedings of the National Academy of Sciences*, 95: 14675–14680.

Pant, V. & Lozano, G. 2014. Limiting the power of p53 through the ubiquitin proteasome pathway. *Genes & development*, 28: 1739–1751.

Pretorius, A., Kaur, M., Wamalwa, M., Essack, M., Bajic, V. & Rees, D. 2011. Functional analysis and characterization of the human RBBP6 promoters based on a combination of molecular biology and in silico approaches provide additional evidence for RBBP6 role in apoptosis. *GSTF Journal of BioSciences* doi: 10.5176/ 2251-3159_1.1.2.

Pugh, D.J.R., Ab, E., Faro, A., Lutya, P.T., Hoffmann, E. & Rees, D.J.G. 2006. DWNN, a novel ubiquitin-like domain, implicates RBBP6 in mRNA processing and ubiquitin-like pathways. *BMC structural biology*, 6: 1.

Rodriguez, M.S., Desterro, J.M.P., Lain, S. & Lane, D.P. 2000. Multiple C-Terminal Lysine Residues Target p53 for Ubiquitin-Proteasome-Mediated Degradation. *Molecular and Cellular Biology*, 20(22): 8458–8467.

Saeki, Y., Kudo, T., Sone, T., Kikuchi, Y., Yokosawa, H., Toh-e, A. & Tanaka, K. 2009. Lysine 63-linked polyubiquitin chain may serve as a targeting signal for the 26S proteasome. *The EMBO journal*, 28(4): 359–71.

Sakai, Y., Saijo, M., Coelho, K. & Kishino, T. 1995. cDNA sequence and chromosomal localization of a novel human protein, RBQ-1 (RBBP6), that binds to the retinoblastoma gene product. *Genomics*, 30: 98–101.

Saville, M.K., Sparks, A., Xirodimas, D.P., Wardrop, J., Stevenson, L.F., Bourdon, J.-C., Woods, Y.L. & Lane, D.P. 2004. Regulation of p53 by the ubiquitin-conjugating enzymes UbcH5B/C in vivo. *The Journal of biological chemistry*, 279(40): 42169–81.

Shi, D., Pop, M.S., Kulikov, R., Love, I.M., Kung, A.L. & Grossman, S.R. 2009. CBP and p300 are cytoplasmic E4 polyubiquitin ligases for p53. *Proceedings of the National Academy of Sciences*, 106(38): 16275–16280.

Shloush, J., Vlassov, J.E., Engson, I., Duan, S., Saridakis, V., Dhe-Paganon, S., Raught, B., Sheng, Y. & Arrowsmith, C.H. 2011. Structural and functional comparison of the RING domains of two p53 E3 ligases, Mdm2 and Pirh2. *The Journal of biological chemistry*, 286(6): 4796–808.

Simons, A., Melamed-Bessudo, C., Wolkowicz, R., Sperling, J., Sperling, R., Eisenbach, L. & Rotter, V. 1997. PACT: cloning and characterization of a cellular p53 binding protein that interacts with Rb. *Oncogene*, 14(2): 145–55.

Sorokin, A. V., Kim, E.R. & Ovchinnikov, L.P. 2009. Proteasome system of protein degradation and processing. *Biochemistry (Moscow)*, 74(13): 1411–1442.

Vo, L., Minet, M., Schmitter, J., Lacroute, F. & Wyers, F. 2001. Mpe1, a Zinc Knuckle Protein, Is an Essential Component of Yeast Cleavage and Polyadenylation Factor Required for the Cleavage and Polyadenylation of mRNA. *Molecular and Cellular Biology*, 21(24): 8346–8356.

Vousden, K. H. 2000. p53 : Death Star Minireview. , 103: 691–694.

Walerych, D., Napoli, M., Collavin, L. & Del Sal, G. 2012. The rebel angel: mutant p53 as the driving oncogene in breast cancer. *Carcinogenesis*, 33(11): 2007–17.

Wang, X., Wang, J. & Jiang, X. 2011. MdmX protein is essential for Mdm2 protein-mediated p53 polyubiquitination. *The Journal of biological chemistry*, 286(27): 23725–34.

Weinberg, R. 2007. *The Biology of Cancer*. 7th Edition. New York: Garland Sciences.

Van Wijk, S.J.L. & Timmers, H.T.M. 2010. The family of ubiquitin-conjugating enzymes (E2s): deciding between life and death of proteins. *FASEB journal: official publication of the Federation of American Societies for Experimental Biology*, 24(4): 981–93.

Wilson, M.D., Saponaro, M., Leidl, M. a & Svejstrup, J.Q. 2012. MultiDsk: a ubiquitin-specific affinity resin. *PloS one*, 7(10): e46398.

Windheim, M., Peggie, M. & Cohen, P. 2008. Two different classes of E2 ubiquitin-conjugating enzymes are required for the mono-ubiquitination of proteins and elongation by polyubiquitin chains with a specific topology. *The Biochemical journal*, 409(3): 723–729.

Witte, M. & Scott, R. 1997. The proliferation potential protein-related (P2P-R) gene with domains encoding heterogeneous nuclear ribonucleoprotein association and Rb1 binding shows repressed. *Cell biology*, 94: 1212–1217.

Woelk, T., Sigismund, S., Penengo, L. & Polo, S. 2007. The ubiquitination code: a signalling problem. *Cell division*, 2: 11.

Wu, H., Pomeroy, S.L., Ferreira, M., Teider, N., Mariani, J., Nakayama, K.I., Hatakeyama, S., Tron, V. a, Saltibus, L.F., Spyrapoulos, L. & Leng, R.P. 2011. UBE4B promotes Hdm2-mediated degradation of the tumor suppressor p53. *Nature medicine*, 17(3): 347–55.

Xie, Y. 2010. Structure, assembly and homeostatic regulation of the 26S proteasome. *Journal of molecular cell biology*, 2(6): 308–17.

Xu, G., Paige, J. & Jaffrey, S. 2010. Global analysis of lysine ubiquitination by ubiquitin remnant immunoaffinity profiling. *Natural Biotechnology*, 28(8): 868–873.


Xu, P. & Peng, J. 2007. Dissecting the ubiquitin pathway by mass spectrometry. *Biochimica et Biophysica Acta*, 1764(12): 1940–1947.

Ye, Y. & Rape, M. 2009. Building ubiquitin chains: E2 enzymes at work. *Nature reviews. Molecular cell biology*, 10(11): 755–64.

Yoshitake, Y., Nakatsura, T., Monji, M., Senju, S., Matsuyoshi, H., Tsukamoto, H., Hosaka, S., Komori, H., Fukuma, D., Ikuta, Y., Katagiri, T., Furukawa, Y., Ito, H., Shinohara, M., Nakamura, Y. & Nishimura, Y. 2004. Proliferation Potential-Related Protein , an Ideal Esophageal Cancer Antigen for Immunotherapy , Identified Using Complementary DNA Microarray Analysis. *Clinical Cancer Research*, 10: 6437–6448.

Appendix

(A) Materials and suppliers



40% 37.5:1 acrylamide: bis-acrylamide	Merck
Agarose	Separations
Ammonium persulphate	Merck
Ampicillin	Sigma
Antibodies	Santa Cruz Biotechnology
Calcium chloride	Merck
Casein	Sigma
Coomassie Blue R-250	Sigma
Ethanol	Merck
Ethylene diamine tetra acetic acid (EDTA)	Merck
Glacial acetic acid	Merck
Glycerol	Merck
Glycine	Merck
Hydrochloric acid	Merck

Imidazole	Sigma
Isopropanol (Propan-2-ol)	Merck
Kanamycin mono-phosphate	Sigma
Magnesium chloride	Merck
Methanol	Merck
<i>N, N, N', N'</i> -Tetra methylethylene-diamine (TEMED)	Sigma
Nutrient agar	Merck
Potassium acetate	Merck
Potassium chloride	Merck
Protease inhibitor cocktail	Roche
Restriction enzymes	Thermo Scientific
Sodium chloride	Merck
Sodium dodecyl sulphate	Merck
T4 ligase	Thermo Scientific
Tris [hydroxymethyl] aminomethane	Merck
Triton X-100	Merck
Tryptone	Merck
Yeast extract	Merck
Glutathione agarose	Sigma
Nickel sepharose	Sigma



(B) General Stock solutions and buffer preparation

Ammonium Persulphate: A 10% stock solution was prepared in deionised water. The solution was stored at 4 °C.

Ampicillin: A 100 mg/ml stock solution was prepared in deionised water. The solution was filter-sterilized using a 0.22 micron filter and stored at -20 °C.

Binding buffer (Proteasome purification): 1 x PBS, 10% Glycerol, 1 mM DTT

Coomassie Staining Solution: 0.25 g Coomassie Blue R-250, 40% ethanol and 10% acetic acid in 250 ml deionised water.

Destaining Solution: 40% ethanol (v/v) and 10% acetic acid (v/v) in 250 ml deionised water.

DTT: 1M stock prepared and stored at -20 °C.

GTE: 50 mM glucose, 50 mM Tris-HCl and 10 mM EDTA, pH 8.0.

Immunoprecipitation buffer (IP buffer): 1 x PBS, 10% glycerol and 0.5 mM ZnSO₄

IPTG: A 1 M stock solution was prepared in deionised water. The solution was filter-sterilized, aliquoted and stored at -20 °C.

Kanamycin: A 50 mg/ml stock solution was prepared in deionised water and stored at -20 °C.

Luria Agar: 10 g/l tryptone powder, 5 g/l yeast extract, 5 g/l NaCl and 14 g/l bacteriological agar.

Luria Broth: 10 g/l tryptone powder, 5 g/l yeast extract, 5 g/l NaCl and 2 g/l glucose.

Protein Elution Buffer: 20 mM reduced glutathione, 1x PBS (for GST tagged proteins) and 300-400 mM imidazole, 1 x PBS (for His₆- tagged proteins).

Protein Extraction Buffer: 1x PBS, 100 µg/ml lysozyme, 10 mM β-mercaptoethanol, 0.5% Triton X-100, 20 µg/ml ZnSO₄, Complete™ EDTA-free protease inhibitor cocktail.

Protein Wash Buffer: 1x PBS, 1 mM β-mercaptoethanol.

2x SDS PAGE Sample Buffer: 4% SDS, 0.125 M Tris-HCl pH 6.8, 15% glycerol and 1 mg/ml Bromophenol Blue. The buffer was stored at room temperature and 100 mM freshly prepared DTT was added immediately prior to use.

10x SDS PAGE Electrophoresis Buffer: 30.2 g Tris, 144.1 g glycine and 10 g SDS dissolved in 1 L distilled water. The buffer was stored at room temperature and diluted 10-fold when needed.

Separating Buffer: 1.5 M Tris-HCl, adjusted to pH 8.8 with HCl. The buffer was stored at 4 °C.

Stacking Buffer: 0.5 M Tris-HCl, adjusted to pH 6.8 with HCl. The buffer was stored at 4 °C.

1x TAE: 40 mM Tris, 20 mM acetic acid and 1 mM EDTA.

TYM Broth: 20 g/l tryptone powder, 5 g/l yeast extract, 3.5 g/l NaCl and 2 g/l MgCl₂.

(C) Strategy behind cloning DWNN13 into pmEGFP (originally cloned in the incorrect orientation in pEGFP)

Clone into **XhoI** and **KpnI** sites of pEGFP-C1; note that the XhoI site is in frame 2 in pEGFP, so needs an insertion of 2 bases (**in yellow**) to complete the frame. Neither of these enzymes occurs in the target sequence.

GFP-DWNN13-f: 5' - GAGGCG **CT CGA GCT** TCC TGT GTG CAT TAT AAA
TTT T -3'

$$T_m = 7 \times 4 + 17 \times 2 = 28 + 34 = 62$$

GFP-DWNN13-r: 5' - GAGGCG **GGTACC** **TCA TTA** TAA AGG TAA AAG CAA
TGT G -3'

$$T_m = 7 \times 4 + 18 \times 2 = 28 + 36 = 64$$

Sequence of amplicon used to clone DWNN13 into pmEGFP

GGTACCGCGGGCCCGGGATCCACCGGATCTAGATAACTGATCATAATCAGCCATACCAC
ATTTGTAGAGGTTTTACTTGTCTTTAAAAAACCTCCACACCTCCCCCTGAACCTGAAAC
ATAAAATGAATGCAATTGTTGTTGTTAACTTGTATTATTGCAGCTTATAATGGTTACAAA
TAAAGCAATAGCATCACAAATTTACAAATAAAGCATTTTTTTTTCACTGCATTCTAGTTG
TGGTTTGTCCAAACTCATCAATGTATCTTAACGCGTAAATTGTAAGCGTTAATATTTTG
TTAAAATTCGCGTTAAATTTTTGTAAATCAGCTCATTTTTTTAACCAATAGGCCGAAAT
CGGCAAAATCCCTTATAAATCAAAGAATAGACCGAGATAGGGTTGAGTGTTGTTCCAG
TTTGGACAAGAGTCCACTATTAAAGAACGTGGACTCCAACGTCAAAGGGCGAAAAACC
GTCTATCAGGGCGATGGCCCACTACGTGAACCATCACCTAATCAAGTTTTTTGGGGTC
GAGGTGCCGTAAAGCACTAAATCGGAACCTAAAGGGAGCCCCGATTTAGAGCTTGAC
GGGAAAGCCGCGCAACGTGGCGAGAAAGGAAGGAAGAAAGCGAAAGGAGCGGGCGCT
AGGGCGCTGGCAAGTGTAGCGGTCACGCTGCGCGTAACCACCACACCCGCCGCGCTTAA
TGCGCCGCTACAGGGCGCGTCAGGTGGCACTTTTCGGGGAAATGTGCGCGGAACCCCTA
TTTGTATTATTTTTCTAAATACATTCAAATATGTATCCGCTCATGAGACAATAACCCTGA
TAAATGCTTCAATAATATTGAAAAGGAAGAGTCCTGAGCGGAAAGAACCAGCTGTGG
AATGTGTGTCAGTTAGGGTGTGGAAAGTCCCCAGGCTCCCCAGCAGGCAGAAGTATGCA
AAGCATGCATCTCAATTAGTCAGCAACCAGGTGTGGAAAGTCCCCAGGCTCCCCAGCAG
GCAGAAGTATGCAAAGCATGCATCTCAATTAGTCAGCAACCATAGTCCCGCCCCCTAACT
CCGCCCATCCCGCCCCCTAACTCCGCCAGTTCGCCCATTTCTCCGCCCATGGCTGACT
AATTTTTTTTTATTTATGCAGAGGCCGAGGCCGCTCGGCCTCTGAGCTATTCAGAAGT
AGTGAGGAGGCTTTTTTGGAGGCCTAGGCTTTTGCAAAGATCGATCAAGAGACAGGATG
AGGATCGTTTTCGCATGATTGAACAAGATGGATTGCACGCAGGTTCTCCGGCCGCTTGGG
TGGAGAGGCTATTCGGCTATGACTGGGCACAACAGACAATCGGCTGCTCTGATGCCGCC
GTGTTCCGGCTGTCAGCGCAGGGGCGCCCGTTCTTTTTGTCAAGACCGACCTGTCCGG

TGCCCTGAATGAACTGCAAGACGAGGCAGCGCGGCTATCGTGGCTGGCCACGACGGGCG
TTCCTTGCGCAGCTGTGCTCGACGTTGTCACTGAAGCGGGAAGGACTGGCTGCTATTG
GGCGAAGTGCCGGGGCAGGATCTCCTGTCATCTCACCTTGCTCCTGCCGAGAAAGTATC
CATCATGGCTGATGCAATGCGGCGGCTGCATACGCTTGATCCGGCTACCTGCCATTTCG
ACCACCAAGCGAAACATCGCATCGAGCGAGCACGTACTIONCGGATGGAAGCCGGTCTTGTC
GATCAGGATGATCTGGACGAAGAGCATCAGGGGCTCGCGCCAGCCGAACTGTTCCGCCAG
GCTCAAGGCGAGCATGCCCCGACGGCGAGGATCTCGTCGTGACCCATGGCGATGCCTGCT
TGCCGAATATCATGGTGGAAAATGGCCGCTTTTCTGGATTTCATCGACTGTGGCCGGCTG
GGTGTGGCGGACCCTATCAGGACATAGCGTTGGCTACCCGTGATATTGCTGAAGAGCT
TGGCGGCGAATGGGCTGACCGCTTCTCGTGCTTTACGGTATCGCCGCTCCCGATTTCGC
AGCGCATCGCCTTCTATCGCCTTCTTGACGAGTTCTTCTGAGCGGGACTCTGGGGTTTCG
AAATGACCGACCAAGCGACGCCAACCTGCCATCACGAGATTTGATTCCACCGCCGCC
TTCTATGAAAGGTTGGGCTTCGGAATCGTTTTCCGGGACGCCGGCTGGATGATCCTCCA
GCGCGGGGATCTCATGCTGGAGTTCTTCCGCCACCCTAGGGGGAGGCTAACTGAAACAC
GGAAGGAGACAATACCGGAAGGAACCCGCGCTATGACGGCAATAAAAAGACAGAATAAA
ACGCACGGTGTGGGGTCGTTTGTTCATAAACGCGGGGTTTCGGTCCCAGGGCTGGCACTC
TGTCGATACCCACCGAGACCCCATTTGGGGCCAATACGCCCGCGTTTTCTTCTTTTCCC
CACCCACCCCAAGTTCCGGTGAAGGCCAGGGCTCGCAGCCAACGTCGGGGCGGCA
GGCCCTGCCATAGCCTCAGGTTACTCATATATACTTTAGATTGATTTAAAACCTTCATTT
TTAATTTAAAAGGATCTAGGTGAAGATCCTTTTTGATAATCTCATGACCAAAATCCCTT
AACGTGAGTTTTTCGTTCCACTGAGCGTCAGACCCCGTAGAAAAGATCAAAGGATCTTCT
TGAGATCCTTTTTTTTCTGCGCGTAATCTGCTGCTTGCAAACAAAAAACACCGCTACC
AGCGGTGGTTTTGTTTGCCGGATCAAGAGCTACCAACTCTTTTTCCGAAGGTAACGGCT
TCAGCAGAGCGCAGATACCAATACTGTCTTCTAGTGTAGCCGTAGTTAGGCCACCAC
TTCAAGAACTCTGTAGCACCGCTACATACTCGCTCTGCTAATCCTGTTACCAGTGGC
TGCTGCCAGTGGCGATAAGTCGTGTCTTACCGGGTTGGACTCAAGACGATAGTTACCGG
ATAAGGCGCAGCGGTCGGGCTGAACGGGGGTTTCGTGCACACAGCCCAGCTTGGAGCGA
ACGACCTACACCGAACTGAGATACCTACAGCGTGAGCTATGAGAAAGCGCCACGCTTCC
CGAAGGGAGAAAGGCGGACAGGTATCCGGTAAGCGGCAGGGTCGGAACAGGAGAGCGCA
CGAGGGAGCTTCCAGGGGGAAACGCCTGGTATCTTTATAGTCTGTCCGGTTTTGCCAC
CTCTGACTTGAGCGTCGATTTTTGTGATGCTCGTCAGGGGGCGGAGCCTATGGAAAAA
CGCCAGCAACGCGCCTTTTTACGGTTCTGGCCTTTTTGCTGGCCTTTTGCTCACATGT
TCTTCTGCGTTATCCCCTGATTCTGTGGATAACCGTATTACCGCCATGCAT

(D) Codon-optimised sequence for cloning superstable quadruple mutant of p53 from pET15b into pET28a

```

atggaagaaccgcaatctgacccgagtggtgaaccgccgctgagccaggaaaccttctct
M E E P Q S D P S V E P P L S Q E T F S      20
gatctgtggaaactgctgcccggaaaacaacgttctgagtcgctgccgtcccaggcaatg
D L W K L L P E N N V L S P L P S Q A M      40
gatgacctgatgctgagcccggatgacattgaacaatggttcaccgaagatccgggtccg
D D L M L S P D D I E Q W F T E D P G P      60
gacgaagctccgcgcatgccggaagcggcaccgccggtcgcaccggctccggcagctccg
D E A P R M P E A A P P V A P A P A A P      80
acgccggcagcaccggcaccggcaccgctcctggccgctgagctctagtgtgccgagccag
T P A A P A P A P S W P L S S S V P S Q     100
aaaacctatcaaggctcttacggttttctgctcgggcttctcctgcatagcggtagcggaaa
K T Y Q G S Y G F R L G F L H S G T A K     120
tcggttacctgcacgtattctccggcactgaataaa[green]ttttgccagctggctaaaacc
S V T C T Y S P A L N K [green] F C Q L A K T     140
tgtccggttcaactgtgggtcgatagcaccgccgcccgggtacgcgtgtccgtgcaatg
C P V Q L W V D S T P P P G T R V R A M     160
gctatttacaaacagttctcaacacatgacggaagtggttcgtcgtgcccgcatcacgaa
A I Y K Q S Q H M T E V V R R C P H H E     180
cgctgtagcgattctgacggtctggccccgccgacacctgatccgcgtggaaggtaac
R C S D S D G L A P P Q H L I R V E G N     200
ctgcgt[green]gaatatctggatgaccgcaatacctttcgtcattcagtcgtggttccgtac
L R [green] E Y L D D R N T F R H S V V V P Y     220
gaaccgccggaagtgggctcggattgtaccacgattcactataactacatgtgc[green]tcc
E P P E V G S D C T T I H Y N Y M C [green] S     240
tcatgtatgggcggtatgaaccgctcgcccgatcctgaccattatcacgctggaagattcg
S C M G G M N R R P I L T I I T L E D S     260
agcggcaacctgctgggtcgc[green]agtttcgaagtcctgtgtgtgcgcacatgtccgggtcgt
S G N L L G R [green] S F E V R V C A C P G R     280
gaccgctgcaccgaagaagaaaacctgcgtaagaaaggcgaaccgcatcacgaactgccg
D R R T E E E N L R K K G E P H H E L P     300
ccggtagcaccaaacgtgcactgccgaacaatacgtctagtctccccgcagccgaagaaa
P G S T K R A L P N N T S S S P Q P K K     320
aaaccgctggatggcgaatatattttaccctgcaaatccgtggtcgcgaacgttttgaaatg
K P L D G E Y F T L Q I R G R E R F E M     340
ttccgcaactgaacgaagcgtggaactgaaagatgcgcaggccggcaagaaccgggc
F R E L N E A L E L K D A Q A G K E P G     360
ggtagtcgtgccattcatcgcacctgaaaagcaagaaggccagagcacgagccgcat
G S R A H S S H L K S K K G Q S T S R H     380
aaaaaactgatgttcaaaacggaaggcccggacagcgactga
K K L M F K T E G P D S D -

```

Codons altered to produce the mutations M133L, V203A, N239Y and N268D are indicated in green.